# WAVE FRONT ANALYSIS IN THE SCATTERING OF A PLANE COMPRESSIONAL PULSE BY A CYLINDRICAL ELASTIC INCLUSION

Thesis by

Jerry Howard Griffin

In Partial Fulfillment of the Requirements

for the Degree of

Doctor of Philosophy

California Institute of Technology

Pasadena, California

1974

(Submitted July 30, 1973)

ACKNOWLEDGEMENTS

The author is greatly indebted to Professor J. Miklowitz for his stimulating suggestions and wise guidance. The author's wife, Linda, is gratefully thanked for her encouragement and for her preparation of the typed manuscript.

ABSTRACT

The plane-strain problem of a stress pulse striking an elastic circular cylindrical inclusion embedded in an infinite elastic medium is treated. The method used determines dominant stress singularities that arise at wave fronts from the focusing of waves refracted into the interior. It is found that a necessary and sufficient condition for the existence of a propagating stress singularity is that the incident pulse has a step discontinuity at its front. The asymptotic wave front behavior of the first few P and SV waves to focus are determined explicitly and it is shown that the contribution from other waves are less important. In the exterior, it is found that in most composite materials the reflected waves have a singularity at their wave front which depends on the angle of reflection. Also the wave front behavior of the first few singular transmitted waves is given explicitly.

The analysis is based on the use of a Watson-type lemma, developed here, and Friedlander's method (see his book Sound Pulses, Cambridge, 1958). The lemma relates the asymptotic behavior of the solution at the wave front to the asymptotic behavior of its Fourier transform on time for large values of the transform parameter. Friedlander's method is used to represent the solution in terms of angularly propagating wave forms. This method employs integral transforms on both time and $\theta$, the circumferential coordinate. The $\theta$ inversion

integral is asymptotically evaluated for large values of the time transform parameter by use of appropriate asymptotics for Bessel and Hankel functions and the method of stationary phase. The Watson-type lemma is then used to determine the behavior of the solution at singular wave fronts.

The Watson-type lemma is generally applicable to problems which involve singular loadings or focusing in which wave front behavior is important. It yields the behavior of singular wave fronts whether or not the singular wave is the first to arrive. This application extends Friedlander's method to an interior region and physically interprets the resulting representation in terms of ray theory.

TABLE OF CONTENTS

TABLE OF CONTENTS (CONT'D)

# LIST OF FIGURES

LIST OF FIGURES (CONT'D)

# DEFINITIONS

## Dimensional Parameters

| | |
|---|---|
| $a$ | radius of inclusion |
| $c_{d1}$ | dilatation wave velocity in inclusion |
| $c_{d2}$ | dilatation wave velocity outside inclusion |
| $c_{s1}$ | shear wave velocity in inclusion |
| $c_{s2}$ | shear wave velocity outside inclusion |
| $\underset{\sim}{r}$ | radial coordinate |
| $\underset{\sim}{t}$ | time |
| $\underset{\sim}{u}$ | radial displacement |
| $\underset{\sim}{v}$ | circumferential displacement |
| $\underset{\sim}{x}$ | cartesian coordinate |
| $\underset{\sim}{y}$ | cartesian coordinate |
| $\lambda_1, \mu_1$ | Lame' elastic constants of material in inclusion |
| $\lambda_2, \mu_2$ | Lame' elastic constants of material outside inclusion |
| $\rho_1$ | density of material in inclusion |
| $\rho_2$ | density of material outside inclusion |
| $\underset{\sim}{\sigma}_{r_1}$ | radial stress in inclusion |
| $\underset{\sim}{\sigma}_{r_2}$ | radial stress outside inclusion |
| $\underset{\sim}{\sigma}_o$ | stress amplitude of incident wave |
| $\underset{\sim}{\tau}_{r\theta_1}$ | shear stress in inclusion |
| $\underset{\sim}{\tau}_{r\theta_2}$ | shear stress outside inclusion |

DEFINITIONS (CONT'D)

Dimensionless Parameters Used in Analysis ($\alpha = 1,2$)

$c = c_{d1}/c_{d2}$

$k = c_{d1}c_{s2}/c_{d2}c_{s1}$

$k_\alpha = c_{d\alpha}/c_{s\alpha}$

$r = \underset{\sim}{r}/a$

$t = \underset{\sim}{t}c_{d2}/a$

$u_\alpha = \underset{\sim}{u}_\alpha/a$

$v_\alpha = \underset{\sim}{v}_\alpha/a$

$\mu = \mu_1/\mu_2$

$\rho = \rho_1/\rho_2$

$\sigma_{r_\alpha} = \underset{\sim}{\sigma}_{r_\alpha}/(\lambda_2+2\mu_2)$

$\sigma_o = \underset{\sim}{\sigma}_o/(\lambda_2+2\mu_2)$

$\tau_{r\theta_\alpha} = \underset{\sim}{\tau}_{r\theta_\alpha}/(\lambda_2+2\mu_2)$

# 1. INTRODUCTION

The purpose of the present investigation is to determine the nature of stress singularities that occur when a stress pulse impinges on an elastic circular cylindrical inclusion embedded in an infinite elastic medium as portrayed in Figure 1. The two dimensional, plane-strain problem is considered in which the incident pulse is the same at all points of any straight line parallel to the axis of the cylinder. The specific incident pulse considered is a plane-fronted dilatation wave whose stress has step function time dependence.

There has been interest in this problem in recent years because its solution provides information about the behavior of individual fibers in a composite material subjected to impact loading. Singular stresses which arise from focusing in fiber-reinforced composites can cause separation at the fiber-matrix interface and subsequent loss of load carrying capabilities in the composite.

Papers written on this problem are of two types. Papers by Ko [1] and by Ting and Lee [2] have analyzed this problem with the goal of determining the scattering effect of the inclusion on the incident wave. Their eventual goal is to determine the dispersive effect of an array of such inclusions on a stress pulse. While these papers briefly mention that focusing occurs, neither attempts to analyze the nature of the resulting singularities. Achenbach, Hemann, and Ziegler [3], however, are predominantly interested in focusing effects and

analyze the first wave front (dilatational) to focus by successive use of wave front analysis, similar to geometric optics, and Poisson's integral representation of the solution to the wave equation.

It is the purpose of this investigation to corroborate and extend the findings of Achenbach, et.al. by use of a more general method of treating stress singularities. In addition to those wave fronts treated by Achenbach, et.al., the wave fronts associated with the following waves are investigated here: the shear waves, the diffracted waves, the Stonely interface wave, reflected exterior waves, transmitted (doubly refracted), exterior waves, and the interior refracted wave after many reflections from the interface.

The method of analysis presented here uses a Watson-type lemma which relates the asymptotic behavior of the solution at the wave front to the asymptotic behavior of its Fourier transform on time for large values of the transform parameter. This lemma provides a generalization of Knopoff and Gilbert's technique [4]. Their method is essentially limited to the first wave front to arrive while the method presented here treats subsequent wave fronts as well. This is especially important in problems involving focusing as it is often the later arriving waves which have focused and are singular. Also in the analysis, Friedlander's technique [5] is used to represent the solution in terms of angularly propagating wave forms. Friedlander's technique has been used in exterior

regions by Miklowitz [6], Peck and Miklowitz [7], Gilbert [8], and Gilbert and Knopoff [9], to solve problems in which wave pulses are scattered by cylindrical holes or rigid inclusions which cannot directly transmit waves. Chen [10] uses a similar representation to Friedlander's to solve a composite problem with an inclusion that transmits waves, but for a periodic excitation of high frequency rather than a transient problem of the type analyzed here. The use of the aforementioned Watson-type lemma, translates the high frequency asymptotics of Chen's type into wave front behavior and is a vehicle for interpreting Friedlander's representation for an interior region.

## 2. METHOD OF ANALYSIS

### 2.1 Statement of Problem

Consider the plane-strain problem shown in Figure 1. A plane dilatation wave, propagating in the exterior region, impinges on a circular inclusion, first striking it at time $t = -1$. Both regions are occupied by homogeneous, isotropic, linearly elastic materials which are perfectly bonded at the interface.

The problem is formulated in terms of the displacement potentials $\varphi_\alpha$ and $\psi_\alpha$, $\alpha = (1,2)$, where the subscripts 1 and 2 refer to the inner and outer solids, respectively. The radial and circumferential displacements are related to $\varphi_\alpha$ and $\psi_\alpha$ by the equations

$$u_\alpha = \frac{\partial \varphi_\alpha}{\partial r} + \frac{1}{r} \frac{\partial \psi_\alpha}{\partial \theta} \tag{2.1a}$$

$$v_\alpha = \frac{1}{r} \frac{\partial \varphi_\alpha}{\partial \theta} - \frac{\partial \psi_\alpha}{\partial r} , \tag{2.1b}$$

where all quantities have been nondimensionalized, their meaning specified on page x. Let $L_x$ be the differential wave operator defined as

$$L_x \equiv \frac{\partial^2}{\partial r^2} + \frac{1}{r} \frac{\partial}{\partial r} + \frac{1}{r^2} \frac{\partial^2}{\partial \theta^2} - \frac{1}{x^2} \frac{\partial^2}{\partial t^2} .$$

In the absence of body forces if the displacement potentials satisfy the wave equations

$$L_c[\varphi_1] = L_{\frac{c}{k_1}}[\psi_1] = 0 \text{ for } r < 1, \text{ and} \tag{2.2a}$$

$$L_1[\varphi_2] = L_{\frac{1}{k_2}}[\psi_2] = 0 \text{ for } r > 1, \tag{2.2b}$$

where the dimensionless speeds of the dilatation and shear waves are c and $c/k_1$ in the inclusion, and 1 and $k_2^{-1}$ in the exterior region. Then the displacements given by equation (2.1) are a solution to the displacement equations of motion. In addition, the stresses are related to the potentials by the relations

$$\sigma_{r_1} = c^2\rho\nabla^2\varphi_1 + \frac{2c^2\rho}{k_1^2}\left(-\frac{1}{r}\frac{\partial\varphi_1}{\partial r} - \frac{1}{r^2}\frac{\partial^2\varphi_1}{\partial\theta^2} - \frac{1}{r^2}\frac{\partial\psi_1}{\partial\theta} + \frac{1}{r}\frac{\partial^2\psi_1}{\partial r\partial\theta}\right),$$

$$\tau_{r\theta_1} = \frac{c^2\rho}{k_1^2}\left(\frac{2}{r}\frac{\partial^2\varphi_1}{\partial r\partial\theta} - \frac{2}{r^2}\frac{\partial\varphi_1}{\partial\theta} + \frac{1}{r^2}\frac{\partial^2\psi_1}{\partial\theta^2} - \frac{\partial^2\psi_1}{\partial r^2} + \frac{1}{r}\frac{\partial\psi_1}{\partial r}\right), \tag{2.3}$$

$$\sigma_{r_2} = \nabla^2\varphi_2 + \frac{2}{k_2^2}\left(-\frac{1}{r}\frac{\partial\varphi_2}{\partial r} - \frac{1}{r^2}\frac{\partial^2\varphi_2}{\partial\theta^2} - \frac{1}{r^2}\frac{\partial\psi_2}{\partial\theta} + \frac{1}{r}\frac{\partial^2\psi_2}{\partial r\partial\theta}\right),$$

$$\tau_{r\theta_2} = \frac{1}{k_2^2}\left(\frac{2}{r}\frac{\partial^2\varphi_2}{\partial r\partial\theta} - \frac{2}{r^2}\frac{\partial\varphi_2}{\partial\theta} + \frac{1}{r^2}\frac{\partial^2\psi_2}{\partial\theta^2} - \frac{\partial^2\psi_2}{\partial r^2} + \frac{1}{r}\frac{\partial\psi_2}{\partial r}\right).$$

In the external region, the solution is separated into scattered and incident parts, denoted by the subscripts sc and inc, respectively. The incident part is specified to be the step stress dilatation wave

$$\varphi_{inc} = \frac{\sigma_o}{2}(t + r\cos\theta)^2 H(t + r\cos\theta) \tag{2.4}$$

where H is the Heaviside step function.

Perfect bonding takes place at the interface between the two solids, hence at r = 1

$$u_1 - u_{sc} = u_{inc} \quad , \qquad v_1 - v_{sc} = v_{inc} \quad ,$$
$$\sigma_{r_1} - \sigma_{r_{sc}} = \sigma_{r_{inc}} \quad , \qquad \tau_{r\theta_1} - \tau_{r\theta_{sc}} = \tau_{r\theta_{inc}} \quad . \tag{2.5}$$

The initial conditions are, $\alpha = 1,2$,

$$\varphi_{sc} = \frac{\partial \varphi_{sc}}{\partial t} = \psi_\alpha = \frac{\partial \psi_\alpha}{\partial t} = \varphi_1 = \frac{\partial \varphi_1}{\partial t} = 0 \text{ at } t = -1. \tag{2.6}$$

In the exterior domain the scattered waves are outgoing as $r \to \infty$, and in the interior the solution is bounded as $r \to 0$. Lastly, the solution is of period $2\pi$ in $\theta$, the angular dimension.

## 2.2 Types of Waves Generated

The waves that are generated when the pulse strikes the inclusion are of three types: diffracted, reflected and refracted. Essentially, the diffracted wave fronts circle the inclusion and propagate around the interface with some characteristic velocity, e.g. the dilatation wave speed in the exterior region. The reflected waves are waves that are generated in the exterior region when the incident dilatation wave strikes the interface. The reflected P ray is depicted in Figure 2. The refracted waves occur when a wave from one media strikes the interface and generates waves in the second media. The system of refracted dilatation waves that are generated when the incident P ray strikes the interface is also illustrated in Figure 2. The refracted wave bounces

around the interior, and each time it strikes the interface it spews refracted P and SV waves into the exterior and generates a reflected interior SV wave. The geometry and the analytical nature of these waves will be discussed in detail in later chapters.

## 2.3 Friedlander's Representation of the Solution

The following discussion parallels that of Miklowitz [6] and Peck and Miklowitz [7] who solved the problem of a stress pulse striking a circular cavity. It differs from their discussion in that Friedlander's representation [5] has been extended to an interior region with the accompanying complications that result from refraction. This representation may be obtained by various means. The most direct method is the application of Poisson's summation formula, which may be stated

$$\sum_{n=-\infty}^{\infty} g(n) = \sum_{m=-\infty}^{\infty} \int_{-\infty}^{\infty} g(\xi) e^{2m\pi\xi i} d\xi \ .$$

Applied to the Fourier series representation of a typical response function $f(r,\theta,t)$ this gives

$$f(r,\theta,t) = \sum_{n=-\infty}^{\infty} F(r,n,t) e^{in\theta}$$

$$= \sum_{m=-\infty}^{\infty} f^*(r,\theta+2m\pi,t) \qquad (2.7)$$

where $f^*(r,\theta,t) \equiv \int_{-\infty}^{\infty} F(r,\xi,t) e^{i\xi\theta} d\xi$. (2.8)

$f^*$ is called the "wave form" of f, and the sum on m in equation (2.7) is called the "wave sum."

The wave form of the response, f*, has a physical interpretation. This response corresponds to the disturbance propagating outward in $\theta$. As discussed in the previous section these disturbances are of two types; diffracted and refracted waves. Both propagate along $\theta$. For $\theta$'s beyond the wave front, f* is identically zero, therefore for finite t, the sum on m is finite. Thus, f* overlaps itself as it propagates in $\theta$ and the wave sum is simply the sum of the overlapping responses. Both the total solution f and the wave form f* are defined on $-\infty < \theta < \infty$, but f* is not periodic in $\theta$ while f is of period $2\pi$, hence satisfying that physical requirement.

The present problem can be cast in the wave sum form by first finding the Fourier series representation of the solution and then applying the above formulas; however, a more direct method is as follows. Because the only given function in this problem is the incident potential, once its expression in the wave sum form is found, one can simply require that each term of the wave sum for $\varphi_{sc}$, $\psi_\alpha$ and $\varphi_1$ satisfy the wave equations

$$L_1\varphi^*_{sc} = \frac{L_1}{k_2}\psi^*_2 = 0 \text{ for } r > 1,\ -\infty < \theta < \infty\ ,$$
$$L_c\varphi^*_2 = \frac{L_c}{k_1}\psi^*_1 = 0 \text{ for } r < 1,\ -\infty < \theta < \infty\ , \tag{2.9}$$

and that the boundary conditions are also satisfied term-by-term

$$u_1^* - u_{sc}^* = u_{inc}^* \quad , \qquad v_1^* - v_{sc}^* = v_{inc}^* \quad ,$$
$$\sigma_{r_1}^* - \sigma_{r_{sc}}^* = \sigma_{r_{inc}}^* \quad , \qquad \tau_{r\theta_1}^* - \tau_{r\theta_{sc}}^* = \tau_{r\theta_{inc}}^* \tag{2.10}$$

at $r = 1$ and $-\infty < \theta < \infty$. When the quiescent initial conditions are added together with the appropriate conditions as $r \to \infty$ and $r \to 0$, it is clear that the wave sum of the solution to the above problem is the solution to the original problem. To complete the formulation of the problem in wave sum form, the wave form of the incident potential must be obtained. This is done after the application of integral transforms.

## 2.4 Transformed Solution

The Fourier transform on time will be denoted by

$$\bar{f}(r,\theta,\omega) = \int_{-\infty}^{\infty} f(r,\theta,t) e^{i\omega t} dt \tag{2.11a}$$

with the inversion integral

$$f(r,\theta,t) = \frac{1}{2\pi} \int_{-\infty+i\gamma}^{\infty+i\gamma} \bar{f}(r,\theta,\omega) e^{-i\omega t} d\omega \tag{2.11b}$$

where $\gamma > 0$. The subsequent Fourier transform on $\theta$ is denoted by

$$\tilde{\bar{f}}(r,\nu,\omega) = \int_{-\infty}^{\infty} \bar{f}(r,\theta,\omega) e^{-i\nu\theta} d\theta \tag{2.12a}$$

with the inversion integral

$$\bar{f}(r,\theta,\omega) = \frac{1}{2\pi} \int_{-\infty}^{\infty} \tilde{\bar{f}}(r,\nu,\omega) e^{i\nu\theta} d\nu. \tag{2.12b}$$

The double transform of the wave sum form of the incident potential is found by applying the Poisson summation formula to the Fourier series of $\bar{\varphi}_{inc}$. From equation (2.4), $\bar{\varphi}_{inc} = \bar{\varphi}_o(\omega)\exp(-i\omega r\cos\theta)$, where $\bar{\varphi}_o(\omega) = \sigma_o/(-i\omega)^3$. The Fourier

series may be written as

$$\bar{\varphi}_{inc}(r,\theta,\omega) = \sum_{n=-\infty}^{\infty} \bar{\varphi}_o(\omega) e^{-|n|\pi i/2} J_{|n|}(\omega r) e^{in\theta}$$

where the integral definition of $J_n$, the Bessel function of the first kind, has been used. Then, applying equation (2.8) and taking the Fourier transform with respect to $\theta$ yields

$$\tilde{\bar{\varphi}}^*_{inc}(r,\nu,\omega) = \bar{\varphi}_o(\omega) \int_{-\infty}^{\infty} \int_{-\infty}^{\infty} e^{-\frac{1}{2}|\xi|\pi i} J_{|\xi|}(\omega r) e^{i\theta(\xi-\nu)} d\xi d\theta \ .$$

Since $J_{|\nu|}(z)$ approaches zero exponentially as $\nu \to \infty$, the Fourier transform theorem gives

$$\tilde{\bar{\varphi}}^*_{inc}(r,\nu,\omega) = 2\pi \bar{\varphi}_o(\omega) e^{-\frac{1}{2}|\nu|\pi i} J_{|\nu|}(\omega r) \ . \qquad (2.13)$$

Applying the double Fourier transform to equations (2.9) for $\varphi^*_{sc}$, $\psi^*_\alpha$ and $\varphi^*_i$ gives the equations for the Bessel functions. Using only those solutions that are outgoing as $r \to \infty$ and bounded as $r \to 0$, one obtains

$$\begin{aligned}
\tilde{\varphi}^*_i(r,\nu,\omega) &= A(\nu,\omega) J_{|\nu|}(\omega r/c) \\
\tilde{\psi}^*_i(r,\nu,\omega) &= B(\nu,\omega) J_{|\nu|}(\omega r k_1/c) \\
\tilde{\varphi}^*_{sc}(r,\nu,\omega) &= C(\nu,\omega) H^{(1)}_\nu(\omega r) \\
\tilde{\psi}^*_2(r,\nu,\omega) &= D(\nu,\omega) H^{(1)}_\nu(\omega r k_2)
\end{aligned} \qquad (2.14)$$

where $H^{(1)}_\nu(z)$ is the Hankel function of the first kind of order $\nu$.

The transformed continuity conditions of equation (2.10) are applied to determine A, B, C and D. To do this

the following transformed relations are used

$$\tilde{u}^*_\alpha = \frac{d}{dr}\tilde{\varphi}^*_\alpha + \frac{i\nu}{r}\tilde{\psi}^*_\alpha \quad , \tag{2.15a}$$

$$\tilde{v}^*_\alpha = \frac{i\nu}{r}\tilde{\varphi}^*_\alpha - \frac{d}{dr}\tilde{\psi}^*_\alpha \quad , \tag{2.15b}$$

$$\tilde{\sigma}^*_{r_1} = \frac{\rho c^2}{r^2 k_1^2}\left[(2\nu^2 - \frac{k_1^2 r^2 \omega^2}{c^2})\tilde{\varphi}^*_1 - 2r\frac{d}{dr}\tilde{\varphi}^*_1 - 2i\nu(\tilde{\psi}^*_1 - r\frac{d}{dr}\tilde{\psi}^*_1)\right], \tag{2.15c}$$

$$\tilde{\tau}^*_{r\theta_1} = \frac{\rho c^2}{r^2 k_1^2}\left[2i\nu(r\frac{d}{dr}\tilde{\varphi}^*_1 - \tilde{\varphi}^*_1) + (\frac{\omega^2 r^2 k_1^2}{c^2} - 2\nu^2)\tilde{\psi}^*_1 + 2r\frac{d}{dr}\tilde{\psi}^*_1\right], \tag{2.15d}$$

$$\tilde{\sigma}^*_{r_2} = \frac{1}{r^2 k_2^2}\left[(2\nu^2 - \omega^2 r^2 k_2^2)\tilde{\varphi}^*_2 - 2r\frac{d}{dr}\tilde{\varphi}^*_2 - 2i\nu(\tilde{\psi}^*_2 - r\frac{d}{dr}\tilde{\psi}^*_2)\right], \tag{2.15e}$$

$$\tilde{\tau}^*_{r\theta_2} = \frac{1}{r^2 k_2^2}\left[2i\nu(r\frac{d}{dr}\tilde{\varphi}^*_2 - \tilde{\varphi}^*_2) + (\omega^2 r^2 k_2^2 - 2\nu^2)\tilde{\psi}^*_2 + 2r\frac{d}{dr}\tilde{\psi}^*_2\right]. \tag{2.15f}$$

Hence $\underline{x} = [A, B, C, D]^T$ satisfies the matrix equation

$$[E]\underline{x} = 2\pi\bar{\varphi}_o(\omega)\exp\left(\frac{-|\nu|\pi i}{2}\right)\underline{Y} \tag{2.16}$$

where $[E] = [\underline{e}_1, \underline{e}_2, \underline{e}_3, \underline{e}_4]$

$$\underline{e}_1 = \begin{vmatrix} \frac{\omega}{c}J'_{|\nu|}(\frac{\omega}{c}) \\ i\nu J_{|\nu|}(\frac{\omega}{c}) \\ \mu[(2\nu^2 - \frac{k_1^2\omega^2}{c^2})J_{|\nu|}(\frac{\omega}{c}) - \frac{2\omega}{c}J'_{|\nu|}(\frac{\omega}{c}) \\ 2i\nu\mu[\frac{\omega}{c}J'_{|\nu|}(\frac{\omega}{c}) - J_{|\nu|}(\frac{\omega}{c})] \end{vmatrix}$$

$$\underline{e}_2 = \begin{vmatrix} i\nu J_{|\nu|}(\frac{\omega k_1}{c}) \\ -\frac{\omega k_1}{c}J'_{|\nu|}(\frac{\omega k_1}{c}) \\ -2i\nu\mu[J_{|\nu|}(\frac{\omega k_1}{c}) - \frac{\omega k_1}{c}J'_{|\nu|}(\frac{\omega k_1}{c})] \\ -\mu[(2\nu^2 - \frac{k_1^2\omega^2}{c^2})J_{|\nu|}(\frac{\omega k_1}{c}) - \frac{2\omega k_1}{c}J'_{|\nu|}(\frac{\omega k_1}{c})] \end{vmatrix}$$

$$\underline{e}_3 = -\begin{vmatrix} \omega H_\nu^{(1)\prime}(\omega) \\ i\nu H_\nu^{(1)}(\omega) \\ (2\nu^2-\omega^2k_2^2)H_\nu^{(1)}(\omega)-2\omega H_\nu^{(1)\prime}(\omega) \\ 2i\nu[\omega H_\nu^{(1)\prime}(\omega)-H_\nu^{(1)}(\omega)] \end{vmatrix}$$

$$\underline{e}_4 = \begin{vmatrix} -i\nu H_\nu^{(1)}(\omega k_2) \\ \omega k_2 H_\nu^{(1)\prime}(\omega k_2) \\ 2i\nu[H_\nu^{(1)}(\omega k_2) - \omega k_2 H_\nu^{(1)\prime}(\omega k_2)] \\ (2\nu^2-\omega^2k_2^2)H_\nu^{(1)}(\omega k_2) - 2\omega k_2 H_\nu^{(1)\prime}(\omega k_2) \end{vmatrix}$$

$$\underline{Y} = \begin{vmatrix} \omega J'_{|\nu|}(\omega) \\ i\nu J_{|\nu|}(\omega) \\ (2\nu^2-\omega^2k_2^2)J_{|\nu|}(\omega)-2\omega J'_{|\nu|}(\omega) \\ 2i\nu[\omega J'_{|\nu|}(\omega) - J_{|\nu|}(\omega)] \end{vmatrix}$$

which uniquely determines $\underline{x}$. From symmetry, $u_\alpha^*$, $\alpha = 1,2$, must be even functions of $\theta$ and $v_\alpha^*$ must be odd functions of $\theta$ which implies $\tilde{u}_\alpha^*$ are even functions of $\nu$ and $\tilde{v}_\alpha^*$ odd. Hence, the absolute value signs in the above equations are dropped and, instead of (2.12b), the half range inversion integrals

$$\bar{u}_\alpha^*(r,\theta,\omega) = \frac{1}{\pi}\int_0^\infty \tilde{u}_\alpha^*(r,\nu,\omega)\cos(\nu\theta)d\nu \qquad (2.17a)$$

$$\bar{v}_\alpha^*(r,\theta,\omega) = \frac{i}{\pi}\int_0^\infty \tilde{v}_\alpha^*(r,\nu,\omega)\sin(\nu\theta)d\nu \quad , \qquad (2.17b)$$

$\alpha = 1,2$ are used where $\tilde{u}_\alpha^*$ and $\tilde{v}_\alpha^*$ are given in equations (2.15a) and (2.15b).

## 2.5 A Watson-Type Lemma for the Fourier Transform

Since the governing equations of dynamic elasticity are hyperbolic, any non-stationary discontinuity must occur at wave fronts. In order for singularities from focusing to occur the wave front must be converging. Often the first wave to arrive at a point is not singular while a later wave caused, for example, by a reflection from a concave interface will have converged and hence is singular when it arrives at the point.

In this section a method is prescribed for determining the wave front behavior of later arriving singular waves from the integral expressions for the solution without completely evaluating the integrals in closed form.

The solution near the wave fronts is obtained by applying a Watson-type lemma to its Fourier time transform. Essentially, the lemma states that if $\bar{f}(\omega,\underline{x})$ is the Fourier transform of $f(t,\underline{x})$, $\underline{x}$ a position vector, and $f(t,\underline{x})$ is the sum of several types of singular functions that commonly occur in focusing, then the Fourier transform of the most singular one will dominate asymptotically as $\omega \to \infty$. Furthermore, this result holds independent of the time of arrival of the various singular waves that compose $f(t,\underline{x})$. This is not true for Watson's lemma as it is normally stated for the Laplace transform of a function, which is why it is not in

general applicable to focusing problems.[1] Preliminary analysis using stationary phase approximations to find the high frequency behavior of the solution helped suggest the types of singularities that are considered in the following lemma. Formally, Lemma: Let the Fourier transform of the function $f(t,\underline{x})$ be defined as

$$\bar{f}(\omega,\underline{x}) = \int_{-\infty}^{\infty} e^{i\omega t} f(t,\underline{x})\,dt.$$

Suppose $f(t,\underline{x}) = \sum_{n=0}^{4} f_n(t,\underline{x})$ where

$$f_0(t,\underline{x}) = a_0(\underline{x})\,(t-t_0(\underline{x}))^{-b} H(t-t_0(\underline{x})),\quad b \in (0,1)$$

$$f_1(t,\underline{x}) = a_1(\underline{x})\,(t_1(\underline{x})-t)^{-d} H(t_1(\underline{x})-t),\quad d \in (0,1)$$

$$f_2(t,\underline{x}) = \begin{cases} a_2(\underline{x}) \ln|t-t_2(\underline{x})| & \text{for } |t-t_2(\underline{x})| < 1 \\ 0, & \text{for } |t-t_2(\underline{x})| > 1 \end{cases}$$

$$f_3(t,\underline{x}) = a_3(\underline{x}) H(t-t_3(\underline{x}))$$

$$f_4(t,\underline{x}) = h(t,\underline{x}) H(t-t_4(\underline{x})),\ f_4 \text{ continuous and } \left|\frac{\partial f_4}{\partial t}\right| < M_1 \text{ for } t < T \text{ and } |h| < M_2 t^n, \text{ for } t > T, \text{ where } M_2 \text{ is independent of } \underline{x} \text{ and } t, \text{ and } n = (0,1,2,\ldots).$$

Then

$$\bar{f}(\omega,\underline{x}) = \frac{a_0(\underline{x})\Gamma(1-b)\,e^{i\omega t_0(\underline{x})}}{(-i\omega)^{1-b}} + \frac{a_1(\underline{x})\Gamma(1-d)\,e^{i\omega t_1(\underline{x})}}{(i\omega)^{1-d}} + \frac{\pi a_2(\underline{x})\,e^{i\omega t_2(\underline{x})}}{-\omega} + \frac{a_3(\underline{x})\,e^{i\omega t_3(\underline{x})}}{-i\omega} + o(\omega^{-1}) \text{ as } \omega\to\infty.$$

To prove this the transforms of $f_0$, $f_1$, $f_2$ and $f_3$ are directly calculated. To show that $\bar{f}_4(\omega)$ is $o(\omega^{-1})$, the

---

(1) If $\tilde{f}(p,\underline{x})$ is the Laplace transform of $f(t,\underline{x})$, where f is as above, then the transform of the first wave to arrive always dominates asymptotically as $p \to \infty$ independent of how smooth or singular it may be.

transform of $f_4$ is integrated once by parts and the Reimann-Lebesque lemma applied to the resulting integral for $Im\{\omega\}>0$. The result holds by analytic continuation as $Im\{\omega\}\to 0$ and $\omega \to +\infty$.

To use the above lemma it is assumed that the only singularities present are of the type stated. Hence, if it is found, for example, that $\bar{f}(\omega,r,\theta) \sim \frac{m(r,\theta)e^{i\omega t_o(r,\theta)}}{\omega}$ as $\omega\to\infty$, the above lemma implies $f(t,r,\theta) \sim \frac{-m(r,\theta)}{\pi} \ln|t-t_o(r,\theta)|$ as $t \to t_o$. This lemma is applied in the next chapter to the focusing of refracted waves in the following manner. The Fourier inversion integral on $\theta$ of equation (2.12b) is used to give an integral representation of the Fourier (time) transform of the solution. This integral is then approximated asymptotically for large values of the parameter $\omega$ using the method of stationary phase, and the lemma applied to the resulting expressions.

## 3. REFRACTED AND REFLECTED WAVES

### 3.1 Introduction

When the stress pulse strikes the inclusion, the discontinuity in material properties at the interface and the shape of the inclusion cause the refracted rays to intersect either on their first pass across the inclusion or on their second pass following a reflection from the interface. Whether the first or the latter event occurs depends on the order of wave speeds of the two materials. While there are

six possible wave speed orders only two will be analyzed. They are:

$$\text{(i)} \quad c > c/k_1 > 1 > 1/k_2 \quad \Leftrightarrow \quad c > k_1$$

$$\text{(ii)} \quad 1 > 1/k_2 > c > c/k_1 \quad \Leftrightarrow \quad c < k_2^{-1} \ .$$

Case (i) is of major interest in composite materials since it is usual for the fiber to be stiffer than the matrix material and hence have faster wave speeds. Other wave speed orders can be analyzed using the methods devised here for these two cases. Case (ii) is especially instructive since the wave speeds are ordered completely different from (i) and represent the opposite physical case of a soft inclusion.

A caustic is an envelope of converging rays. When a ray touches a caustic, focusing or unfocusing can occur. When focusing occurs singular stresses are found at the wave front after it has passed through the caustic. Since the balance of momentum at the wave front yields

$$n_j[\sigma_{ij}] = -\rho s\left[\frac{\partial u_i}{\partial t}\right] ,$$

where jumps in field quantities are indicated by the usual brackets, and where $n_j$ is the jth component of the unit vector normal to the surface of discontinuity and s is the speed of the wave, the nature of the stress discontinuities may be disclosed by simply calculating the discontinuities in the velocity vector.

## 3.2 The Focusing of a Refracted Dilatation Wave for c<1

Consider the directly refracted interior P wave when c is less than one. If $\alpha$ is the angle of incidence of the exterior P wave which strikes the interface, the angle of refraction of the generated P wave is $\beta$, where $\alpha$ and $\beta$ are related by Snell's law, i.e.

$$c\sin\alpha = \sin\beta \tag{3.1}$$

Using simple geometry, the envelope of converging refracted P rays is depicted in Figure 3, where, in addition to this caustic, three of its generating incident and refracted ray pairs are shown.

Consider how the solution varies along a refracted ray that touches the caustic. Let $d_{1p}$ be the distance traveled along the ray from the interface where it was generated to a point $(r,\theta)$ and $h_{1p}$ be the distance along the ray to this caustic. From Figure 3, it is clear that there are three regions in which $(r,\theta)$ might lie:

(1) $d_{1p} < h_{1p}$ and there is only one ray per point,

(2) $d_{1p} \sim h_{1p}$, a region that includes the caustic as well as a transition zone where there are two rays per point,

(3) $d_{1p} > h_{1p}$ and only one ray per point.

Call the collections of all such points for all the directly refracted dilatation rays $R_1$, $R_2$ and $R_3$, respectively. These regions are portrayed for $\theta > 0$ and $c = 1/2$ in Figure 4. When a ray touches this caustic it picks up a singularity

which propagates along its wave front. Thus points in $R_2$ and $R_3$ see singular stresses from these refracted rays. Consider the following mathematical analysis that verifies the above discussion and reveals the orders of these singularities.

Let the part of the radial velocity, $\dot{u}_1^*$, that propagates with the dilatation speed c be denoted as $\dot{u}_1^*(\text{dil})$. From the elementary properties of the wave equation, contributions from $\varphi_1^*$ propagate with this velocity while contributions from $\psi_1^*$ propagate with the shear velocity $c/k_1$, thus equations (2.15a) and (2.14) imply

$$\tilde{\dot{u}}_{1(\text{dil})}^*(r,\nu,\omega) = -\frac{i\omega^2}{c}A(\nu,\omega)J_\nu'(\tfrac{\omega r}{c}) \quad . \tag{3.2}$$

Equation (2.17a) implies

$$\bar{\dot{u}}_{1(\text{dil})}^*(r,\theta,\omega) = \frac{1}{\pi}\int_0^\infty \tilde{\dot{u}}_{1(\text{dil})}^*(r,\nu,\omega)\cos\nu\theta\, d\nu \quad .$$

The asymptotic behavior of this quantity for large $\omega$ is of interest. Once it is known, the lemma of section 2.5 will be used. For $\omega = \omega_1 + i\omega_2$, $\omega_2 > 0$ and $\omega_1$ large, the change of variable $\nu = s\omega$ yields

$$\bar{\dot{u}}_{1(\text{dil})}^*(r,\theta,\omega) = \frac{1}{2\pi}\int_{C_s} \omega\tilde{\dot{u}}_{1(\text{dil})}^*(r,s\omega,\omega)[e^{i\omega s\theta} + e^{-is\omega\theta}]ds, \tag{3.3}$$

where $C_s$ is a line from the origin to $\infty$ inclined at an angle of $-\tan^{-1}\frac{\omega_2}{\omega_1}$. Consider the contribution from the term $e^{i\omega s\theta}$ in (3.3), which will be called $\bar{\dot{u}}_{1(\text{dil})}^{*+}$, i.e.

$$\bar{\dot{u}}_{1(\text{dil})}^{*+}(r,\theta,\omega) = \frac{1}{2\pi}\int_{C_s} \omega\tilde{\dot{u}}_{1(\text{dil})}^*(r,s\omega,\omega)e^{is\omega\theta}ds. \tag{3.4}$$

As $\omega_1 \to \infty$, $C_s$ is equivalent to a path along the real s-axis which is indented below any poles of the integrand that might lie on the real s-axis. With this understanding, equation (3.4) is written

$$\bar{\dot{u}}_{1(dil)}^{*+}(r,\theta,\omega) = \frac{1}{2\pi}\int_0^\infty \omega \bar{\tilde{u}}_{1(dil)}^{*}(r,s\omega,\omega)e^{is\omega\theta}ds \ . \tag{3.5}$$

In the following discussion this integral is evaluated asymptotically for large $\omega$ in a manner similar to that used by Chen [10]. For $\omega$ large, (A.5) and (A.8) of Appendix A imply that for $s\in[0,\min(1,1/c))$, i.e., $0 \le s < \min(1,1/c) \equiv$ smaller of either 1 or $1/c$, $A(s\omega,\omega)$ may be expanded in a geometric series, each term of which corresponds to a different refracted ray. It is found, for $s\in[0,\min(1,1/c))$, that

$$A(s\omega,\omega) \sim A_o(s,\omega)[1-\delta_{11}(s)M_{1/c}(s) + \Gamma_1] \tag{3.6}$$

where

$$A_o(s,\omega) = \frac{2\pi\sigma_o(m_{1/c}(s)m_1(s))^{\frac{1}{2}}\, a_o(s)\exp[i\omega(\frac{-s\pi}{2}+\psi_{1/c}(s)-\psi_1(s))]}{-i\omega^3\delta_{1o}(s)}$$

$$a_o(s) = 4e_2s^2(m_{\frac{k_1}{c}}+m_{k_2})-8s^4(m_{k_2}+\mu m_{\frac{k_1}{c}})-2e_2(m_{\frac{k_1}{c}}e_2-m_{k_2}\mu e_1)$$
$$+ 4\mu s^2(m_{\frac{k_1}{c}}e_2-m_{k_2}e_1) \ ,$$

$$\delta_{1o}(s) = (m_1m_{\frac{k_1}{c}}+s^2)(e_2^2+4s^2m_1m_{k_2})+\mu[-2s^2(2m_1m_{\frac{k_1}{c}}+e_1)(2m_1m_{k_2}+e_2)$$
$$+\left(\frac{k_1k_2}{c}\right)^2(m_1m_{k_2}+m_1m_{\frac{k_1}{c}})]+\mu^2(e_1^2+4s^2m_1m_{\frac{k_1}{c}})(m_1m_{k_2}+s^2) \ ,$$

$$\delta_{11}\,\delta_{1o} = (-m_1m_{\frac{k_1}{c}}+s^2)(e_2^2+4s^2m_1m_{k_2})+\mu[2s^2(2m_1m_{\frac{k_1}{c}}+e_1)(2m_1m_{k_2}+e_2)$$
$$+\left(\frac{k_1k_2}{c}\right)^2(m_1m_{\frac{k_1}{c}}-m_1m_{k_2})]+\mu^2(e_1^2-4s^2m_1m_{\frac{k_1}{c}})(m_1m_{k_2}+s^2) \ ,$$

$$\psi_x(s) = m_x(s) - s\cos^{-1}(s/x) ,$$

$$M_x(s) = -i\exp(2i\omega\psi_x(s)) ,$$

$$m_x(s) = \sqrt{|x^2-s^2|} , \quad e_1 = (2s^2-\tfrac{k_1^2}{c^2}) , \quad e_2 = (2s^2-k_2^2) .$$

It will be shown that in equation (3.6), $A_o$ corresponds to the directly refracted dilatation wave before it reflects for the first time from the interface. $-A_o\delta_{11}M_{\frac{1}{c}}$ corresponds to the same wave after one reflection but before the second reflection, and $\Gamma_1$ corresponds to other refracted waves. In anticipation of this physical meaning, let $\dot{u}^*_{1p}$ be the contribution to the velocity from $A_o$ where p refers to dilatation. Using the asymptotic forms for the Bessel functions given in Appendix A gives,

$$\bar{\dot{u}}^*_{1p}(r,\theta,\omega) \sim \int_o^{\min(\frac{r}{c},1)} \frac{H_{1p}(s,r)e^{i\pi/4}}{\sqrt{\omega}}[e^{i\omega f_{d1}} - ie^{i\omega f_{d2}}]ds \tag{3.7}$$

where

$$H_{1p}(s;r) = \frac{\sigma_o a_o(s)}{r\delta_{1o}(s)}\left(\frac{m_1/c\, m_1 m_r/c}{2\pi}\right)^{\frac{1}{2}} ,$$

$$f_{d1}(s;r,\theta) = -\frac{s\pi}{2} + s\theta + \psi_{\frac{1}{c}}(s) - \psi_1(s) + \psi_{\frac{r}{c}}(s) ,$$

$$f_{d2}(s;r,\theta) = -\frac{s\pi}{2} + s\theta + \psi_{\frac{1}{c}}(s) - \psi_1(s) - \psi_{\frac{r}{c}}(s) .$$

Consider the contribution from the second term in the above integrand. A point of stationary phase, $s_o$, exists provided $f'_{d2}(s_o;r,\theta) = 0$, i.e.

$$-\gamma + \beta - \alpha + \theta = 0 \tag{3.8a}$$

where

$$\alpha = \sin^{-1}s_o , \quad \beta = \sin^{-1}s_o c , \quad \gamma = \sin^{-1}\frac{s_o c}{r} . \tag{3.8b}$$

Equation (3.8a) is satisfied if $\theta \geq 0$ and when $s_o$ is such that $\alpha$, $\beta$ and $\gamma$ have the geometric relationship shown in Figure 5. Note that $\alpha$ and $\beta$ satisfy Snell's law, equation (3.1). Furthermore,

$$f_{d2}(s_o;r,\theta) = \frac{d_{1p}}{c} + d_1 - 1 = t_{1p}(r,\theta) \quad , \tag{3.9}$$

where $d_1$ is the distance the incident ray travels from time $t = -1$ until it strikes the interface, $d_{1p}$ is the distance from the interface to the point $(r,\theta)$ and hence $t_{1p}$ is the time of arrival of the refracted P wave at the point $(r,\theta)$, thus justifying the nomenclature that has been used. The mathematical restriction that $0 \leq s_o < \min(\frac{r}{c},1)$ physically restricts the incident ray to the positive illuminated zone $0 \leq \alpha < \pi/2$, and restricts the refracted ray so that $d_{1p} < \cos\beta$. Since

$$f''_{d2}(s_o;r,\theta) = -\frac{c}{r\cos\gamma} + \frac{c}{\cos\beta} - \frac{1}{\cos\alpha} < 0, \text{ for } c < 1 \ , \tag{3.10}$$

the method of stationary phase implies the contribution from this term is

$$\frac{-iH_{1p}(s_o;r)}{\omega}\sqrt{\frac{2\pi}{-f''_{d2}(s_o;r,\theta)}}\ e^{i\omega t_{1p}(r,\theta)} \tag{3.11}$$

for $d_{1p} < \cos\beta$ and $\theta > 0$.

The first term in the integrand of equation (3.4) has a point of stationary phase, $s_o$, provided $f'_{d1}(s_o;r,\theta) = 0$, i.e.

$$\gamma' - \pi + \beta - \alpha + \theta = 0 \tag{3.12a}$$

where $\alpha$ and $\beta$ are as in equation (3.5b), $\theta \geq 0$ and

$$\gamma' = \sin^{-1}(s_o c/r) \ . \tag{3.12b}$$

The restriction that $s_o < r/c$ implies $d_{1p} > \cos\beta$. The angles $\alpha$ and $\beta$ have the same physical interpretation as before and $\gamma'$ is the supplement of $\gamma$ as illustrated in Figure 6. Again

$$f_{d_1}(s_o;r,\theta) = \frac{d_{1p}}{c} + d_1 - 1 = t_{1p}(r,\theta) \ , \tag{3.12c}$$

however,

$$f''_{d_1}(s_o;r,\theta) = -(d_{1p}-h_{1p})/\lambda_{1p} \tag{3.12d}$$

where

$$h_{1p} = \cos^2\beta/(\cos\beta - c\cos\alpha) > \cos\beta,$$

$$\lambda_{1p} = r\cos\alpha\cos\gamma\cos\beta/(\cos\beta - c\cos\alpha) > 0, \text{ for } c < 1.$$

Summarizing for $\theta > 0$,

$$\bar{\dot{u}}^*_{1p}(r,\theta,\omega) \sim \begin{cases} \dfrac{-iH_{1p}(s_o;r)}{\omega} \sqrt{\dfrac{2\pi}{-f''_{d_2}(s_o;r,\theta)}}\, e^{i\omega t_{1p}(r,\theta)}, & \text{if } d_{1p} < \cos\beta \\ \dfrac{e^{i\pi/4}}{\sqrt{\omega}} \displaystyle\int_o^{\min(\frac{r}{c},1)} H_{1p}(s;r)\, e^{i\omega f_{d_1}(s;r,\theta)}\, ds, & \text{if } d_{1p} > \cos\beta. \end{cases} \tag{3.13}$$

Consider the solution for $d_{1p} > \cos\beta$. If the point $(r,\theta)$ is restricted to lie on a particular refracted ray specified by the angle of incidence $\alpha_o = \sin^{-1}s_o$, $s_o \epsilon (0,1)$, then on this ray, as $d_{1p}$ increases, five cases will be considered and discussed in terms of the physical description given at the beginning of this section. The cases are:

(i) $(r,\theta)\epsilon R_1$, $d_{1p} < h_{1p}$. $s_o$ is the only zero of $f'_{d_1}(s;r,\theta)$ on $(0,\min(\frac{r}{c},1))$.

(ii) $(r,\theta)\ \epsilon R_2$, $d_{1p}<h_{1p}$ and two zeros exist $s_1$ and $s_o$, $s_1> s_o$, where $f''_{d_1}(s_1;r,\theta) < 0$.

(iii) $d_{1p} = h_{1p}$, $f''_{d_1}(s_o;r,\theta) = 0$, $f'''_{d_1}(s_o,r,\theta) < 0$.

(iv) $(r,\theta)\ \epsilon R_2$, $d_{1p}>h_{1p}$ and two zeros exist $s_o$ and $s_2$, $s_o>s_2$, $f''_{d_1}(s;r,\theta) > 0$.

(v) $(r,\theta)\ \epsilon R_3$, $d_{1p}>h_{1p}$. $s_o$ only zero.

For each of these cases $f''_{d_1}(s_o;r,\theta)$ is given by equation (3.12d). The behavior of $f_{d_1}(s;r,\theta)$ is depicted in Figure 7. It is assumed that $s_o$, $s_1$ and $s_2$ are sufficiently distinct that the method of stationary phase can be separately applied to the three points. Hence, the solutions found for cases (ii) and (iii) do not apply as $d_{1p} \to h_{1p}$, which is why case (iii) must be considered separately. Thus, for all the cases except (iii), the method of stationary phase is applied and the following asymptotics are found for $\bar{u}^*_{1p}(r,\theta,\omega)$:

$$\frac{H_{1p}(s_o;r)}{-i\omega}\sqrt{\frac{2\pi}{|f''_{d_1}(s_o;r,\theta)|}}\,e^{i\omega t_{1p}}\ ,\ \text{for (i)},$$

$$\frac{H_{1p}(s_o,r)}{-i\omega}\sqrt{\frac{2\pi}{|f''_{d_1}(s_o;r,\theta)|}}\,e^{i\omega t_{1p}} + \frac{H_{1p}(s_1;r)}{\omega}\sqrt{\frac{2\pi}{|f''_{d_1}(s_1;r,\theta)|}}\,e^{i\omega f_{d_1}(s_1;r,\theta)},\ \text{for (ii)}$$

$$\frac{H_{1p}(s_o;r)}{\omega}\sqrt{\frac{2\pi}{|f''_{d_1}(s_o;r,\theta)|}}\,e^{i\omega t_{1p}} + \frac{H_{1p}(s_2;r)}{-i\omega}\sqrt{\frac{2\pi}{|f''_{d_1}(s_2;r,\theta)|}}\,e^{i\omega f_{d_1}(s_2;r,\theta)},\ \text{for (iv)},$$

and

$$\frac{H_{1p}(s_o;r)}{\omega}\sqrt{\frac{2\pi}{|f''_{d_1}(s_o;r,\theta)|}}\,e^{i\omega t_{1p}},\ \text{for (v)},\ \text{as } \omega\to\infty,\ d_{1p}>\cos\beta,\ \theta>0. \tag{3.14}$$

For case (iii), $d_{1p} = h_{1p}$, $f_{d_1}$ is approximated near the point of stationary phase as

$$f_{d_1}(s;h_{1p}) \sim t_{1p} + \frac{f'''_{d_1}}{6}(s_o;h_{1p})(s-s_o)^3 .$$

Since $f'''_{d_1}(s_o;h_{1p}) = -3c^3 h_{1p}/[\cos^2\beta(h_{1p}-\cos\beta)^2] < 0$, the contribution from near $s_o$ is, for $\epsilon$ small and $> 0$,

$$\bar{u}^*_{1p}(h_{1p},\omega) \sim \frac{e^{i\omega t_{1p}} H_{1p}(s_o;r) e^{i\pi/4}}{\sqrt{\omega}} \int_{s_o-\epsilon}^{s_o+\epsilon} e^{-i\omega |f'''_{d_1}(s_o;h_{1p})|(s-s_o)^3/6} ds.$$

Using the change of variable $v = \sqrt[3]{\frac{|f'''_{d_1}(s_o;h_{1p})|\omega}{6}}(s-s_o)$, the above becomes

$$\bar{u}^*_{1p}(h_{1p},\omega) \sim \frac{e^{i\omega t_{1p}} H_{1p}(s_o;r) e^{i\pi/4}}{\omega^{5/6} \sqrt[3]{\frac{|f'''_{d_1}(s_o;h_{1p})|}{6}}} \int_{-\infty}^{\infty} \cos v^3 dv \text{ as } \omega \to +\infty ,$$

where only the even part of the integrand has been kept. From integral tables [11]

$$\bar{u}^*_{1p}(h_{1p},\omega) \sim \frac{H_{1p}(s_o;r) e^{i\omega t_{1p} + i\pi/4}}{\omega^{5/6} \sqrt[3]{\frac{|f'''_{d_1}(s_o;h_{1p})|}{6}}} \frac{2\pi}{3\Gamma(2/3)} \text{ as } \omega \to +\infty. \tag{3.15}$$

Equations (3.13), (3.14) and (3.15) together with the lemma of section 2.5 imply for $\theta > 0$

$$\bar{u}^*_{1p}(r,\theta,t) \sim -H_{1p}(s_o;r)\sqrt{\frac{2\pi}{|f'''_{d_2}(s_o;r,\theta)|}} H(t-t_{1p}) \text{ as } t \to t_{1p} , \tag{3.16a}$$

$d_{1p} < \cos\beta$. And for $d_{1p} > \cos\beta$

$$\dot{u}^{*}_{1p} \sim \begin{cases} H_{1p}(s_o;r)\left(\frac{2\pi\lambda_{1p}}{h_{1p}-d_{1p}}\right)^{\frac{1}{2}} H(t-t_{1p}), & d_{1p} \in R_1 , \\ H_{1p}(s_o;r)\left(\frac{2\pi\lambda_{1p}}{h_{1p}-d_{1p}}\right)^{\frac{1}{2}} H(t-t_{1p}) - H_{1p}(s_1;r)\left(\frac{-2}{\pi f''_{d1}(s_1;r,\theta)}\right)^{\frac{1}{2}} \ln|t-f_{d1}(s_1;r,\theta)|, \\ \qquad \text{for } d_{1p} \in R_2,\ d_{1p} < h_{1p}, \\ \frac{2\pi H_{1p}(s_o;r)}{3\Gamma(2/3)\Gamma(5/6)}\left(\frac{6}{|f'''_{d1}(s_o;h_{1p})|}\right)^{\frac{1}{3}} [(t_{1p}-t)^{-1/6} H(t_{1p}-t) + \sqrt{3}(t-t_{1p})^{-1/6} H(t-t_{1p})], \\ \qquad \text{for } d_{1p} = h_{1p}, \\ H_{1p}(s_2;r)\left(\frac{2\pi}{f''_{d1}(s_2;r,\theta)}\right)^{\frac{1}{2}} H(t-f_{d1}(s_2;r,\theta)) - H_{1p}(s_o;r)\left(\frac{2\lambda_{1p}}{\pi(d_{1p}-h_{1p})}\right)^{\frac{1}{2}} \ln|t-t_{1p}| \\ \qquad \text{for } d_{1p} \in R_2,\ d_{1p} > h_{1p}, \\ -H_{1p}(s_o;r)\left(\frac{2\lambda_{1p}}{\pi(d_{1p}-h_{1p})}\right)^{\frac{1}{2}} \ln|t-t_{1p}|, \quad d_{1p} \in R_3, \\ \qquad \text{where } \frac{df_{d1}}{ds}\Big|_{s=s_o,s_1,s_2} = 0, \quad s_1 > s_o > s_2 . \end{cases}$$

The physics of this solution is clear. For $d_{1p} < \cos\beta$ the solution along the ray given by $\alpha$ (angle of incidence) = $\sin^{-1}s_o$ is a nonsingular step function. As $d_{1p}$ increases the ray reaches the region $R_2$, see Figures 3 and 4, in which there are two rays per point. The second ray, specified by $\alpha' = \sin^{-1}s_1$ has already touched the caustic and propagates a logarithmic singularity at its wave front which arrives at the point $(r,\theta)$ at time $t = f_{d1}(s_1;r,\theta)$. $d_{1p}$ continues to increase until it is at the caustic, $d_{1p} = h_{1p}$, where a singularity of order $(t-t_{1p})^{-1/6}$ is calculated. After touching the caustic, the ray is again in a region where there are two rays per point; however, this time it is the ray $\alpha = \sin^{-1}s_o$ that has

touched the caustic and propagates a logarithmic singularity. Lastly, the ray continues into $R_3$, another region in which there is only one ray per point and since it has touched the caustic it has a logarithmic singularity at it's wave front. This logarithmic singularity at the wave front agrees with that found in reference [3] where methods (Poisson's integral representation of the solution to the wave equation) analogous to those used in Friedlander's book [5] were used to investigate the singular nature of the solution. However, in that paper it was incorrectly concluded, as one might from case (ii) by taking an improper limit, that the discontinuity increases beyond bounds like $(h_{1p}-d_{1p})^{-\frac{1}{2}}$ as $d_{1p} \to h_{1p}$.

The right hand side of (3.15b) is written symbolically as

$$\Omega\left(H_{1p}, s_o, \frac{d_{1p}-h_{1p}}{\lambda_{1p}}, t_{1p}\right)$$

where $H_{1p}$ is a refraction coefficient,

$s_o$ specifies the refracted ray since

$\alpha$(angle of incidence of external ray) = $\sin^{-1} s_o$,

$\beta$(angle of refraction of internal ray) = $\sin^{-1} s_o c$,

$d_{1p}$ is the distance along the refracted ray from where it was generated at the interface to the point $(r,\theta)$,

$h_{1p}$ is the distance along the refracted ray to the caustic, and

$t_{1p}$ is the time of arrival of the wave front traveling along that ray.

Thus for $\theta > 0$,

$$\dot{u}^*_{1p}(r,\theta,t) \sim \begin{cases} -H_{1p}(s_o,r)\sqrt{\dfrac{2\pi}{|f''_{d_2}(s_o;r,\theta)|}}\, H(t-t_{1p}), \text{for } d_{1p}<\cos\beta, \\ \Omega(H_{1p}, s_o, \dfrac{d_{1p}-h_{1p}}{\lambda_{1p}}, t_{1p}), \text{ for } d_{1p} > \cos\beta. \end{cases} \tag{3.17}$$

Recall that (3.17) is the contribution from the term $e^{i\omega s\theta}$ in (3.3). The role of the neglected term $e^{-i\omega s\theta}$ in (3.3) is now clear. Since points of stationary phase existed only for $\theta \geq 0$ for $e^{i\omega s\theta}$, $e^{-i\omega s\theta}$ will have stationary phase points only if $\theta \leq 0$. Thus the solution for negative $\theta$ comes from this second term $e^{-i\omega s\theta}$ and it is clear from (3.3) that

$$\dot{u}^*_{1\,(dil)}(r,\theta,t) = \dot{u}^*_{1\,(dil)}(r,-\theta,t) \ . \tag{3.18}$$

When $\theta = 0$, both terms $e^{i\omega s\theta}$ and $e^{-i\omega s\theta}$ contribute to the solution. However, since $s_o$, the point of stationary phase, is zero, an end point of the interval $[0,r/c)$, each term contributes only half as much. Thus the result is the same as in (3.17) for $\theta = 0$.

Do all refracted dilatation rays touch the caustic? According to the above analysis, a ray touches the caustic provided the maximum of $d_{1p}$ is greater than or equal to $h_{1p}$ i.e. if

$$2\cos\beta \geq \cos^2\beta/(\cos\beta - c\cos\alpha) \ . \tag{3.19a}$$

Equation (3.19a) is satisfied if either

$$c \leq \tfrac{1}{2} \quad \text{or} \quad s_o = \sin\alpha \geq \left(\frac{4c^2-1}{3c^2}\right)^{\frac{1}{2}} , \tag{3.19b}$$

where $\alpha$ is the angle of incidence of the incoming P wave. That is, all refracted dilatation rays touch a caustic on their first pass across the cylinder if $c \leq \frac{1}{2}$. However, if $c > \frac{1}{2}$, then only those rays such that $\sin\alpha \geq \left(\frac{4c^2-1}{3c^2}\right)^{\frac{1}{2}}$ touch the caustic on their first pass.

## 3.3 Summary of Results for $c < k_2^{-1}$

The following notation is adopted with regards to refracted and reflected waves. The subscript 1 or 2 implies that the solution applies to the inner or the exterior region, respectively. Subsequent subscripts of p and/or s yield the "ray history" of the wave and its type, P or SV (shear vertical wave) in the following manner. When the incident exterior P ray strikes the interface it generates refracted interior P and SV waves which will have the subscripts 1p and 1s, and the reflected exterior P and SV rays with subscripts 2p and 2s. When the 1p ray strikes the interface after transversing the inclusion it generates rays in the interior denoted by the subscripts 1pp (reflected P wave) and 1ps (reflected SV wave) and in the exterior denoted by 2pp (refracted P wave) and 2ps (refracted SV wave). In turn, the 1pp ray strikes the interface and similarly generates rays denoted by subscripts 1ppp, 1pps, 2ppp and 2pps. Analogous to the 1p ray striking the interface, the 1s SV ray strikes the interface and generates rays with the subscripts 1sp (interior P wave), 1ss (interior SV wave), 2sp (exterior P wave) and 2ss (exterior SV wave). All reflected and refracted rays may be denoted

in this manner. Some refracted and reflected rays are depicted and labeled using this notation in Figure 8. In addition, the above subscripts will be used to denote quantities that are associated with a particular ray. d, h and t when subscripted have the following meanings:

d is the distance along the ray of interest from the interface where it was generated to the point $(r,\theta)$. (Exception: $d_1$ is the distance the incident wave travels from time $t = -1$ until it strikes the interface.)

h, when positive, is the distance along the ray to the caustic, i.e. $(r,\theta)$ is on caustic when $d = h$.

t, when subscripted, is the time of arrival of the wave front propagating along the ray.

H, when subscripted, has the role of a wave amplitude, usually the product of several refraction or reflection coefficients.

$\lambda$ is a positive definite quantity.

Examples of these are $d_{1p}$, $h_{1p}$, $t_{1p}$, $H_{1p}$ and $\lambda_{1p}$ of the previous section.

Using the above notation the following representative interior waves will be considered in this section: $\dot{v}^*_{1p}$, $\dot{u}^*_{1s}$, $\dot{v}^*_{1s}$, $\dot{u}^*_{1ps}$ and $\dot{v}^*_{1ps}$.

In the exterior region there are three types of waves that can be analyzed by stationary phase: the incident

wave,* the reflected waves and waves refracted into the exterior from internally refracted waves. The first two types, for $c < k_2^{-1}$, are nonsingular. However, the third type can be singular and is examined here as represented by $\dot{u}^*_{2pp}$, $\dot{v}^*_{2pp}$, $\dot{u}^*_{2ps}$ and $\dot{v}^*_{2ps}$. In this section it is assumed that $\theta > 0$. The fact that $\dot{u}^*$ is an even function of $\theta$ and $\dot{v}^*$ an odd function of $\theta$ determines their behavior for $\theta < 0$.

The geometry of the rays for the directly refracted P wave $\dot{v}^*_{1p}$ is identical to that of $\dot{u}^*_{1p}$ of the previous section, thus as $t \to t_{1p}$

$$\dot{v}^*_{1p}(r,\theta,t) \sim \begin{cases} \tan\gamma H_{1p}(s_o;r)\left(\dfrac{-2\pi}{f''_{d2}(s_o;r,\theta)}\right)^{\frac{1}{2}} H(t-t_{1p}), \text{ for } d_{1p} < \cos\beta, \\ \Omega(\tan\gamma' H_{1p}, s_o, \dfrac{d_{1p}-h_{1p}}{\lambda_{1p}}, t_{1p}), \text{ for } d_{1p} > \cos\beta. \end{cases} \tag{3.20}$$

The analysis for the directly refracted SV waves $\dot{u}^*_{1s}$ and $\dot{v}^*_{1s}$ is analogous to that of $\dot{u}^*_{1p}$ and $\dot{v}^*_{1p}$. Thus, it is found that as $t \to t_{1s}$

$$\begin{bmatrix} \dot{u}^*_{1s} \\ \dot{v}^*_{1s} \end{bmatrix} \sim H_{1s}(s_o;r)\begin{bmatrix} 1 \\ -\cot\chi \end{bmatrix}\left(\frac{-2\pi}{f''_{s2}(s_o;r,\theta)}\right)^{\frac{1}{2}} H(t-t_{1s}), \text{for } d_{1s} < \cos\zeta, \tag{3.21a}$$

$$\begin{bmatrix} \dot{u}^*_{1s} \\ \dot{v}^*_{1s} \end{bmatrix} \sim \begin{bmatrix} \Omega(H_{1s}, s_o, \dfrac{d_{1s}-h_{1s}}{\lambda_{1s}}, t_{1s}) \\ \Omega(H_{1s}\cot\chi', s_o, \dfrac{d_{1s}-h_{1s}}{\lambda_{1s}}, t_{1s}) \end{bmatrix}, \text{ for } d_{1s} > \cos\zeta \tag{3.21b}$$

*The external potential $\tilde{\varphi}^*_{\ell}$ has a stationary phase point that corresponds to the incident wave only if $(r,\theta)$ is in the illuminated region, $|\theta| \le \pi/2$ or if $\pi > |\theta| > \pi/2$ and $r > |1/\sin\theta|$.

where $s_o$ is such that if

$$\alpha = \sin^{-1}s_o\ ,\quad \zeta = \sin^{-1}(s_o c/k_1),\quad \chi = \chi' = \sin^{-1}(s_o c/rk_1) \tag{3.21c}$$

then

$$\zeta - \chi - \alpha + \theta = 0, \text{for } d_{1s} < \cos\zeta, \tag{3.21d}$$

$$\zeta - \pi + \chi' - \alpha + \theta = 0,\ \text{for } d_{1s} > \cos\zeta \tag{3.21e}$$

Equations (3.21d) and (3.21e) are analogous to equations (3.8a) and (3.12a) and have ray interpretations similar to those shown in Figures 5 and 6. Furthermore,

$$H_{1s}(s;r) = -\frac{\sigma_o s b_o(s)}{r\delta_{1o}(s)}\left(\frac{m_1 m_{k_{1/c}}}{2\pi m_{k_1} r/c}\right)^{\frac{1}{2}}, \tag{3.21f}$$

where

$$b_o(s) = -4se_2(m_{1/c}m_{k_{1/c}} - s^2) + 4s^3(2m_{1/c}m_{k_2} - \mu e_1)$$
$$-2se_2(e_2 - 2m_{1/c}m_{k_2}) + 2\mu s(e_1 e_2 - 4s^2 m_{1/c}m_{k_{1/c}}),$$

and $\delta_{1o}$, $e_\alpha$ and $m_x$ are given in equation (3.6). Also,

$$f''_{s1}(s_o;r,\theta) = -\frac{c}{rk_1\cos\zeta} + \frac{c}{k_1\cos\chi} - \frac{1}{\cos\alpha} < 0, \tag{3.21g}$$

$$f''_{s2}(s_o;r,\theta) = -(d_{1s} - h_{1s})/\lambda_{1s}\ , \tag{3.21h}$$

where

$$d_{1s} = \cos\zeta + r\cos\chi'\ ,\quad h_{1s} = \cos^2\chi'/(\cos\zeta - \frac{c}{k_1}\cos\alpha),$$
$$\lambda_{1s} = r\cos\zeta\cos\chi'\cos\alpha/(\cos\zeta - \frac{c}{k_1}\cos\alpha) > 0,$$
$$t_{1s} = \frac{d_{1s}k_1}{c} + d_1 - 1\ . \tag{3.21i}$$

It may be noted that for the restriction $c < k_2^{-1}$, all directly refracted SV waves touch the caustic on their first pass across the inclusion.

The last interior waves to be considered for $c < k_2^{-1}$ are the SV waves $\dot{u}^*_{1ps}$ and $\dot{v}^*_{1ps}$ which are generated when the

refracted dilatation wave strikes the interface for the first time. The ray geometry is depicted in Figure 9. If the condition of equation (3.19b) is met, then the refracted P wave has a logarithmic singularity at its wave front when it strikes the interface and generates the waves

$$\begin{bmatrix} \dot{u}^*_{1ps} \\ \dot{v}^*_{1ps} \end{bmatrix} \sim -H_1 s(s_o) \begin{bmatrix} 1 \\ \cot\chi \end{bmatrix} \frac{(b_1(s_o) - \delta_{11}(s_o))}{\pi} \left| \frac{-2\pi}{f''_{s(d)}(s_o;r,\theta)} \right|^{\frac{1}{2}} \ln|t-t_{1ps}| \tag{3.22a}$$

as $t \to t_{1ps}$, for $d_{1ps} < \cos\zeta$. Where $s_o$ is such that

$$-\chi + \zeta - \alpha + \theta + 2\beta - \pi = 0 , \tag{3.22b}$$

$\alpha$, $\beta$, $\chi$, $\zeta$ given in equations (3.5b) and (3.21c). And

$$b_1(s) = \left\{ 4se_2(m_{1/c} m_{k_{1/c}} + s^2) - 4s^3(2m_{1/c} m_{k_2} + \mu e_1) - 2se_2(e_2 + 2m_{1/c} m_{k_2}) + 2\mu s(e_1 e_2 + 4s^2 m_{1/c} m_{k_2}) \right\} / b_o \tag{3.22c}$$

where $b_o$, $e_\alpha$ and $m_\chi$ are given in equations (3.6) and (3.21),

$$f''_{s(d)}(s_o;r,\theta) = -\frac{c}{k_1} \frac{d_{1ps}}{r\cos\zeta\cos\chi} + \frac{(2c\cos\alpha - \cos\beta)}{\cos\alpha\cos\beta} , \tag{3.22d}$$

$$d_{1ps} = \cos\zeta - r\cos\chi , \tag{3.22e}$$

$$t_{1ps(d)} = \frac{k_1 d_{1ps}}{c} + \frac{2\cos\beta}{c} + d_1 - 1 . \tag{3.22f}$$

Lastly, $H_{1s}$ is given in (3.21f) and $\delta_{11}$ in (3.6).

If the conditions of equation (3.19b) are not met, then the generating refracted P wave ($_1$p) is nonsingular when it strikes the interface but has a converging wave front. The generated SV wave has a converging wave front and focusing takes place. The solution is given by

$$\begin{bmatrix} \dot{u}^*_{1ps} \\ \dot{v}^*_{1ps} \end{bmatrix} \sim \begin{bmatrix} \Omega(H_{1s}\cdot(b_1-\delta_{11}), s_o, \frac{d_{1ps}-h_{1ps}}{\lambda_{1ps}}, t_{1ps}) \\ \Omega(H_{1s}\cdot(-\cot\chi)\cdot(\delta_{11}-b_1), s_o, \frac{d_{1ps}-h_{1ps}}{\lambda_{1ps}}, t_{1ps}) \end{bmatrix}, \tag{3.23}$$

as $t\to t_{1ps}$, for $d_{1ps} < \cos\zeta$, where

$$h_{1ps} = (2c\cos\alpha-\cos\beta)\cos^2\zeta/(\tfrac{c}{k_1}\cos\alpha\cos\beta+\cos\zeta) < \cos\zeta$$

is the distance from the interface to the caustic along the generated (1ps) ray, and $\lambda_{1ps} = r\cos\chi\cos\alpha\cos\beta\cos\zeta/(\frac{c}{k_1}\cos\alpha\cos\beta + \cos\zeta) > 0$.

The analysis of the waves generated in the exterior when the refracted interior dilatation wave reflects from the interface for the first time is very similar to that performed for $\dot{u}^*_{1ps}$ and $\dot{v}^*_{1ps}$. The geometry of the generated P ray (2pp) is depicted in Figure 10. The geometry of the generated SV ray (2ps) is similar. Again, if the condition of equation (3.19b) is satisfied, then the interior dilatation wave has a logarithmic singularity at its wave front when it strikes the interface, thus, analogous to equation (3.22a) it is found that

$$\begin{bmatrix} \dot{u}^*_{2pp} \\ \dot{v}^*_{2pp} \end{bmatrix} \sim -H_{2pp}\cdot(s_o;r) \begin{bmatrix} 1 \\ \tan\delta \end{bmatrix} \ln|t-t_{2pp}| \sqrt{\frac{2\lambda_{2pp}}{\pi(d_{2pp}-h_{2pp})}} \text{ as } t\to t_{2pp} \tag{3.24a}$$

and

$$\begin{bmatrix} \dot{u}^*_{2ps} \\ \dot{v}^*_{2ps} \end{bmatrix} \sim -H_{2ps}\cdot(s_o;r) \begin{bmatrix} \tan\epsilon \\ -1 \end{bmatrix} \ln|t-t_{2ps}| \sqrt{\frac{2\lambda_{2ps}}{\pi(d_{2ps}-h_{2ps})}} \text{ as } t\to t_{2ps}. \tag{3.24b}$$

And if equation (3.19b) is not satisfied then analogous to equation (3.23) it is found that

$$\begin{bmatrix} \dot{u}^*_{2pp} \\ \dot{v}^*_{2pp} \end{bmatrix} \sim \begin{bmatrix} \Omega(H_{2pp}, s_o, (d_{2pp}-h_{2pp})/\lambda_{2pp}, t_{2pp}) \\ \Omega(H_{2pp}\cdot\tan\delta,\ s_o\ ,\ \ (d_{2pp}-h_{2pp})/\lambda_{2pp},\ t_{2pp}) \end{bmatrix} \tag{3.24c}$$

as $t \to t_{2pp}$, and

$$\begin{bmatrix} \dot{u}^*_{2ps} \\ \dot{v}^*_{2ps} \end{bmatrix} \sim \begin{bmatrix} \Omega(H_{2ps}\cdot\tan\epsilon, s_o,\ (d_{2ps}-h_{2ps})/\lambda_{2ps}, t_{2ps}) \\ \Omega(-H_{2ps},\ s_o,\ (d_{2ps}-h_{2ps})/\lambda_{2ps},\ t_{2ps}) \end{bmatrix} \tag{3.24d}$$

as $t \to t_{2ps}$. In equations (3.24a) and (3.24c) $s_o$ is such that

$$-2\alpha + \delta + \theta + 2\beta - \pi = 0,$$

and in equations (3.24b) and (3.24d) $s_o$ is such that

$$-\alpha - \varkappa + \epsilon + \theta + 2\beta - \pi = 0,$$

where

$$\alpha = \sin^{-1}s_o\ ,\ \beta = \sin^{-1}s_oc\ ,\ \delta = \sin^{-1}s_o/r\ ,$$
$$\varkappa = \sin^{-1}(s_o/k_2),\ \epsilon = \sin^{-1}(s_o/rk_2). \tag{3.24e}$$

In addition,

$$H_{2pp}(s,r) = \frac{\sigma_o}{r\delta_{o1}}\left(\frac{m_r}{2\pi}\right)^{\frac{1}{2}}(c_{31} - \delta_{11}c_{11}),$$
$$H_{2ps}(s,r) = \frac{\sigma_o}{r}\left(\frac{m_1 m_{k_2} m_{rk_2}}{2\pi}\right)^{\frac{1}{2}}(g_{o2} - \delta_{11}\, g_{o1}),$$

where

$$c_{11}(s) = (m_1\overline{m}_{k_1} + s^2)(e_2^2 - 4s^2 m_1 m_{k_2}) - 2s^2\mu(2m_1\overline{m}_{k_1} + e_1)(e_2 - 2m_1 m_{k_2})$$
$$+ \frac{\mu k_1^2 k_2^2}{c^2}(m_1\overline{m}_{k_2} - m_{k_1}\overline{m}_1) - \mu^2(e_1^2 + 4s^2 m_1 m_{k_2})(m_1 m_{k_2} - s^2)\ , \tag{3.24f}$$

$$c_{31}(s) = (s^2-\frac{m_1}{c}\frac{m_{k_1}}{c})(e_2^2-4s^2m_1m_{k_2})+2s^2\mu(2\frac{m_1}{c}\frac{m_{k_1}}{c}-e_1)(e_2-2m_1m_{k_2})$$
$$-\frac{\mu k_1^2k_2^2}{c^2}(\frac{m_1}{c}m_{k_2}+\frac{m_{k_1}}{c}m_1)-\mu^2(e_1^2-4s^2m_1m_{k_2})(m_1m_{k_2}-s^2), \quad (3.24g)$$

$$g_{o1}(s) = -(\frac{m_1}{c}\frac{m_{k_1}}{c}+s^2)4se_2+\mu s(4s^2+2e_1)(2\frac{m_1}{c}\frac{m_{k_1}}{c}+e_1)$$
$$-\mu^2 2s(e_1^2+4s^2\frac{m_1}{c}\frac{m_{k_1}}{c}), \quad (3.24h)$$

$$g_{o2}(s) = (\frac{m_1}{c}\frac{m_{k_1}}{c}-s^2)4se_2-\mu s(4s^2+2e_1)(2\frac{m_1}{c}\frac{m_{k_1}}{c}-e_1)$$
$$-2s\mu^2(e_1^2-4s^2\frac{m_1}{c}\frac{m_{k_1}}{c}), \quad (3.24i)$$

and $m_x$, $e_\alpha$, $\delta_{11}$, $\delta_{10}$ are given in equation (3.6). The distances $d_{2pp}$ and $d_{2ps}$ are

$$d_{2pp} = r\cos\delta - \cos\alpha,$$

$$d_{2ps} = r\cos\varepsilon - \cos\varkappa.$$

Also, the caustics are given by $d_{2pp} = h_{2pp}$ and $d_{2ps} = h_{2ps}$, where

$$h_{2pp} = (2c\cos\alpha - \cos\beta)/2(\cos\beta - c\cos\alpha)$$

and

$$h_{2ps} = \cos^2\varkappa(2c\cos\alpha-\cos\beta)/[k_2^{-1}\cos\alpha\cos\beta-\cos\varkappa(2c\cos\alpha-\cos\beta)].$$

The times of arrival are

$$t_{2pp} = d_{2pp} + d_1 + 2\cos\beta/c - 1, \quad t_{2ps} = d_{2ps}k_2 + d_1 + 2\cos\beta/c.$$

Lastly,

$$\lambda_{2pp} = \cos\alpha\cos\beta r\cos\delta/(2\cos\beta - c\cos\alpha)$$

and $\lambda_{2ps} = r\cos\varepsilon\cos\varkappa\cos\alpha\cos\beta/[k_2^{-1}\cos\alpha\cos\beta-\cos\varkappa(2c\cos\alpha-\cos\beta)]$ are greater than zero.

Thus it has been found that when $c < k_2^{-1}$, dilatation and shear waves refracted into the interior have converging wave fronts on their first pass across the inclusion. If $c < \frac{1}{2}$, then all interior refracted rays touch a caustic and have a logarithmic singularity at their wave fronts when they strike the interface for the first time. The generated reflected and externally refracted waves propagate this singularity. If $\frac{1}{2} < c < 1$ then the interior refracted P rays whose angles of refraction, $\beta$, are less than $\sin^{-1}\sqrt{(4c^2-1)/3}$, while converging, do not touch a caustic before striking the interface. However, the refracted and reflected waves that are generated at the interface continue to focus and eventually form caustics. This is illustrated in Figure 11 where the dilatation caustics are shown for $c = .75$.

## 3.4 Analysis for $c > k_1$

In this instance the directly refracted P rays diverge on their first pass across the inclusion. However, when they strike the interface for the first time the reflected P and SV rays that are generated converge and form caustics. The following discussion of the generated P rays and their focusing parallels that given in section 3.2 for the case $c < k_2^{-1}$.

Using the fact that when a P ray reflects from an interface the angle of reflection equals the angle of incidence, and Snell's law which relates the angle of incidence of the exterior P ray, $\alpha$, to the angle of refraction of the interior P ray, $\beta$, the envelope on converging reflected P rays is

depicted in Figure 12 where, in addition to this caustic, several generating refracted/reflected P ray pairs are shown.

Consider how the solution varies along a reflected ray. $d_{1pp}$ is the distance traveled along the reflected P ray from the interface where it was generated to the point $(r,\theta)$ and $h_{1pp}$ is the distance along this ray to the caustic. From Figure 12 it is clear that for $\theta > 0$ there are two regions where $(r,\theta)$ might lie:

(1) $d_{1pp}$ such that $\theta \leq \pi$. In this region there are two rays per point, one that has touched the caustic and one that has not. Call the collection of all such points for all once reflected P rays $R_2^*$.

(2) $d_{1pp}$ sufficiently large so that $\theta > \pi$, then there is only one ray per point and it has touched the caustic. Call the collection of all such points $R_3^*$.

$R_2^*$ and $R_3^*$ are portrayed for $\theta > 0$ and $c = 1.5$ in Figure 13. $R_2^*$ and $R_3^*$ are analogous to $R_2$ and $R_3$ discussed in section 3.2 and shown in Figure 4. Points contained in $R_2^*$ and $R_3^*$ experience logarithmic singularities in stresses associated with the arrival of wave fronts that propagate along rays that have touched the caustic. Hence, from Figure 13, it is clear that the interface, $r = 1$, experiences logarithmic singularities for $\sin^{-1}(1/c) < \theta < 2\pi$ from positively propagating reflected P waves and for $-2\pi < \theta < -\sin^{-1}(1/c)$ from negatively propagating waves. Thus, every point of the physical interface experiences a logarithmic singularity from waves that have reflected once.

$\dot{u}^*_{1pp}$ and $\dot{v}^*_{1pp}$ are the contributions to the radial and angular velocity from this once reflected P ray. These reflected dilatation waves are analogous to the reflected SV waves discussed in section 3.3, $\dot{u}^*_{1ps}$ and $\dot{v}^*_{1ps}$. Thus, similar to the result of equation (3.23), it is found that for $d_{1pp} < \cos\beta$

$$\begin{bmatrix} \dot{u}^*_{1pp}(r,\theta,t) \\ \dot{v}^*_{1pp}(r,\theta,t) \end{bmatrix} \sim \begin{bmatrix} \Omega(H_{1p}\cdot\delta_{11},\ s_o,\ (d_{1pp}-h_{1pp})/\lambda_{1pp},\ t_{1pp}) \\ \Omega(-\tan\gamma H_{1p}\cdot\delta_{11},\ s_o,\ (d_{1pp}-h_{1pp})/\lambda_{1pp},\ t_{1pp}) \end{bmatrix} \tag{3.25a}$$

as $t \to t_{1pp}$. $H_{1p}$ and $\delta_{11}$ are given in (3.7) and (3.6). $s_o$ is such that

$$\theta - \gamma + 3\beta - \alpha - \pi = 0, \tag{3.25b}$$

where $\alpha$, $\beta$ and $\gamma$ are given in (3.8b). The geometric significance of (3.25b) is shown in Figure 14. $d_{1pp}$, the distance from the interface where the reflected P ray is generated to the point $(r,\theta)$, equals $\cos\beta - r\cos\gamma$ and $h_{1pp}$, the distance to the caustic, is equal to $\cos\beta(2c\cos\alpha - \cos\beta)/(3c\cos\alpha - \cos\beta)$, is always less than $\cos\beta$, and, hence, focusing occurs for all rays. In addition,

$$\lambda_{1pp} = r\cos\gamma\cos\alpha\cos\beta/(3c\cos\alpha - \cos\beta) > 0$$

and $t_{1pp} = \frac{d_{1pp}}{c} + \frac{2\cos\beta}{c} + d_1 - 1$, is the time of arrival of the wave front.

For $d_{1pp} > \cos\beta$, all of the reflected P rays have focused and have a logarithmic singularity at the wave front, i.e. for $d_{1pp} > \cos\beta$

$$\begin{bmatrix} \dot{u}^*_{1pp} \\ \dot{v}^*_{1pp} \end{bmatrix} \sim \begin{bmatrix} 1 \\ \tan\gamma' \end{bmatrix} H_{1p}\cdot(s_o)\,\delta_{11}(s_o)\sqrt{\frac{2\lambda_{1pp}}{\pi(d_{1pp}-h_{1pp})}}\ln|t-t_{1pp}| \text{ as } t\to t_{1pp}. \tag{3.26}$$

$\gamma' = \sin^{-1}(s_o c/r)$ is the supplement of $\gamma$.

The first singular shear waves to reach an interior point are the reflected SV waves $\dot{u}^*_{1ps}$ and $\dot{v}^*_{1ps}$ which are generated when the refracted dilatation wave strikes the boundary for the first time. These waves were discussed in section 3.3 for the case $c < k_2^{-1}$. In section 3.3 two cases were considered. In the first case the generating P ray was singular at its wave front. In the second case the generating P ray was not singular and the reflected shear waves focused. The second case is identical to the present situation of $c > k_1^{-1}$ and the solution given in equation (3.23) is also the solution for $c > k_1^{-1}$.

In the exterior region two types of waves can be singular when $c > k_1$: reflected waves, and waves refracted into the exterior by internally refracted waves.

When $\alpha$, the angle of incidence of the exterior P ray, equals $\sin^{-1}(1/c)$, Snell's law, (3.1), implies that $\beta$, the angle of refraction of the interior P ray, is $90^\circ$ and hence this ray is critically refracted. This situation, in a simpler physical context, is discussed briefly for acoustic waves in Friedlander's book [5]. As is noted there, the reflected waves experience a logarithmic singularity at their wave fronts when $\alpha > \sin^{-1}(1/c)$. Mathematically, the treatment of these waves is analogous to those of previous sections

with the difference that $s_o$, the point of stationary phase, is greater than $1/c$. As in all the previous cases, $s_o = \sin^{-1}\alpha$ and since for critical refraction $\sin\alpha > 1/c$, asymptotics other than those of Appendix A must be used. These asymptotics are given in Appendix B and are used there to determine the asymptotic behavior of $\tilde{\dot{u}}^*_{sc(dil)}(r,s\omega,\omega)$ and $\tilde{\dot{v}}^*_{sc(dil)}(r,s\omega,\omega)$, the double Fourier transform of the radial and angular components of the scattered wave form dilatational velocities, for $s\epsilon[1/c,1)$. $\dot{u}^*_{2p}$ and $\dot{v}^*_{2p}$ are the parts of the scattered dilatation velocities that are directly reflected from the interface. When $\alpha > \sin^{-1}(1/c)$, the asymptotics (B.5) and (B.6a) and the method of stationary phase implies

$$\begin{bmatrix} \bar{\dot{u}}^*_{2p}(r,\theta,\omega) \\ \bar{\dot{v}}^*_{2p}(r,\theta,\omega) \end{bmatrix} \sim \frac{\sigma_o H_{2p}(s_o) e^{i\omega t_{2p}}}{-i\omega} \sqrt{\frac{\cos\alpha}{2d_{2p}+\cos\alpha}} \begin{bmatrix} \cos\delta \\ \sin\delta \end{bmatrix} \text{ as } \omega\to\infty\,, \tag{3.27a}$$

where

$$H_{2p} = H^R_{2p} + iH^I_{2p} \tag{3.27b}$$

$$H^R_{2p} = (C_{OR}C_{1R} + C_{OI}C_{1I})/(C^2_{1R} + C^2_{1I}) \tag{3.27c}$$

$$H^I_{2p} = (C_{OI}C_{1R} - C_{OR}C_{1I})/(C^2_{1R} + C^2_{1I}) \tag{3.27d}$$

where for $s\epsilon[1/c,k_{1/c}]$

$$C_{OR}(s) = s^2(e_2^2-4s^2m_1m_{k_2})-2\mu e_1 s^2(e_2^2-2m_1m_{k_2})-\mu\left(\frac{k_1k_2}{c}\right)^2 m_1 m_{\frac{k_1}{c}} - \mu^2 e_1^2(m_1m_{k_2}-s^2), \tag{3.28a}$$

$$C_{OI}(s) = m_1 \left[ m_{\frac{k_1}{c}} (e_2^2 - 4s^2 m_1 m_{k_2}) - 4\mu m_{\frac{k_1}{c}} s^2 (e_2 - 2m_1 m_{k_2}) + \mu m_{k_2} \frac{k_1^2 k_2^2}{c^2} \right.$$

$$\left. -4s^2 \mu^2 m_{\frac{k_1}{c}} (m_1 m_{k_2} - s^2) \right] , \qquad (3.28b)$$

and

$$C_{1R}(s) = s^2 (e_2^2 + 4s^2 m_1 m_{k_2}) - 2\mu e_1 s^2 (e_2 + 2m_{k_2} m_1) + \mu \frac{k_1^2 k_2^2}{c^2} m_1 m_{\frac{k_1}{c}}$$

$$+\mu^2 e_1^2 (m_1 m_{k_2} + s^2) , \qquad (3.28c)$$

$$C_{1I}(s) = m_1 \left[ m_{\frac{k_1}{c}} (e_2^2 + 4s^2 m_1 m_{k_2}) - 4\mu s^2 m_{\frac{k_1}{c}} (e_2 + 2m_1 m_{k_2}) \right.$$

$$\left. +\mu m_{k_2} \left(\frac{k_1 k_2}{c}\right)^2 + \mu^2 4s^2 m_{\frac{k_1}{c}} (m_1 m_{k_2} + s^2) \right] . \qquad (3.28d)$$

However, for $s \in [k_1/c, 1)$

$$C_{OR}(s) = (s^2 - m_1 m_{\frac{k_1}{c}}) (e_2^2 - 4s^2 m_1 m_{k_2}) + 2s^2 \mu (e_1 - 2m_1 m_{\frac{k_1}{c}}) (e_2 - 2m_1 m_{k_2})$$

$$+\mu^2 (4s^2 m_1 m_{\frac{k_1}{c}} - e_1^2) (m_1 m_{k_2} - s^2), \qquad (3.29a)$$

$$C_{OI}(s) = \mu \left(\frac{k_1 k_2}{c}\right)^2 (m_{k_2} m_1 - m_1 m_{\frac{k_1}{c}}) , \qquad (3.29b)$$

and

$$C_{1R}(s) = (s^2 - m_1 m_{\frac{k_1}{c}}) (e_2^2 + 4s^2 m_1 m_{k_2}) - 2s^2 \mu (e_1 - 2m_1 m_{\frac{k_1}{c}}) (e_2 + 2m_1 m_{k_2})$$

$$+\mu^2 (e_1^2 - 4s^2 m_1 m_{\frac{k_1}{c}}) (m_1 m_{k_2} + s^2), \qquad (3.29c)$$

$$C_{1I}(s) = \mu \left(\frac{k_1 k_2}{c}\right)^2 (m_{k_2} m_1 + m_1 m_{\frac{k_1}{c}}) . \qquad (3.29d)$$

$m_x$, $e_1$ and $e_2$ are given in (3.6). In addition, $s_o$ is such that

$$-2\alpha + \delta + \theta = 0 \qquad (3.30a)$$

where

$$\alpha = \sin^{-1}s_o, \quad \delta = \sin^{-1}(s_o/r), \; s_o > \sin(1/c) \; . \qquad (3.30b)$$

(3.30a) has the simple ray interpretation of Figure 15. $d_{2p}$ is equal to $r\cos\delta-\cos\alpha$ and is the distance along the reflected P ray from the interface where it was generated to the point $(r,\theta)$ and $t_{2p}$ equals $d_{2p}+d_1-1$ and is the time of arrival of a wave front along this ray.

The lemma of section 2.5 and (3.27) implies that

$$\begin{bmatrix}\dot{u}^*_{2p}(r,\theta,t)\\ \dot{v}^*_{2p}(r,\theta,t)\end{bmatrix} \sim \sigma_o\sqrt{\frac{\cos\alpha}{2d_{2p}+\cos\alpha}}\begin{bmatrix}\cos\delta\\ \sin\delta\end{bmatrix}\Big\{H^R_{2p}(s_o)H(t-t_{2p}) + H^I_{2p}(s_o)\frac{\ln|t-t_{2p}|}{\pi}\Big\}, \text{ as } t\to t_{2p}, \qquad (3.31)$$

for $\alpha > \sin^{-1}(1/c)$. For $\alpha$ and $\theta$ negative the evenness and oddness of $\dot{u}^*_{2p}$ and $\dot{v}^*_{2p}$ is invoked. The asymptotic behavior of the reflected shear velocities $\dot{u}^*_{2s}$ and $\dot{v}^*_{2s}$ are similarly calculated and are

$$\begin{bmatrix}\dot{u}^*_{2s}(r,\theta,t)\\ \dot{v}^*_{2s}(r,\theta,t)\end{bmatrix} \sim \frac{\sigma_o k_2\cos\alpha\cos\varkappa}{\sqrt{\frac{d_{2s}}{k_2}(\cos\alpha+k_2\cos\varkappa)+\cos^2\varkappa}}\begin{bmatrix}\sin\epsilon\\ \cos\epsilon\end{bmatrix}\Big\{H^R_{2s}(s_o)H(t-t_{2s}) + H^I_{2s}(s_o)\frac{\ln|t-t_{2s}|}{\pi}\Big\} \text{ as } t\to t_{2s}, \qquad (3.32)$$

for $\alpha > \sin^{-1}(1/c)$. Where $s_o$ is such that

$$\epsilon + \theta - \alpha - \varkappa = 0,$$

$$\alpha = \sin^{-1}s_o, \; \varkappa = \sin^{-1}(s_o/k_2) \text{ and } \epsilon = \sin^{-1}(s_o/rk_2).$$

Also,

$$H^R_{2s}(s) = (g_{OR}C_{1R}+g_{IR}C_{1I})/(C^2_{1R}+C^2_{1I})$$

and

$$H^I_{2s}(s) = (g_{OR}C_{1R}-g_{OR}C_{1I})/(C^2_{1R}+C^2_{1I}).$$

If $s_o \in [1/c, k_1/c]$ then

$$g_{OR}(s) = -2s(2s^2e_2-\mu e_1(2s^2+e_2)+\mu^2e_1^2),$$

$$g_{OI}(s) = -4sm_1m_{\frac{k_1}{c}}[e_2-2s^2(1+\mu)](1-\mu),$$

and

$C_{1R}$ and $C_{1I}$ are given by (3.28). If $s_o \in [\frac{k_1}{c},1)$, then

$$g_{OR}(s) = 4se_2(m_1m_{\frac{k_1}{c}}-s^2)-4s\mu(2m_1m_{\frac{k_1}{c}}-e_1)(2s^2+e_2)$$

$$+2\mu^2s(4s^2m_1m_{\frac{k_1}{c}}-e_1^2),$$

$$g_{OI}(s) = 0,$$

and $C_{1R}$ and $C_{1I}$ are given by (3.29). $m_x$, $e_1$ and $e_2$ are given in (3.6). Physically this is analogous to the reflected P ray of Figure 15, where $\varkappa$ is the angle of reflection of the SV ray and $\epsilon$ is the angle between r, the vector to the point of interest, and the reflected SV ray. $d_{2s}$ is the distance traveled along the reflected ray and $t_{2s}$ is the time of arrival of the reflected SV wave front, i.e.

$$d_{2s} = r\cos\epsilon - \cos\varkappa,$$

$$t_{2s} = k_2d_{2s} + d_1 - 1.$$

The above applies for $\alpha > \sin^{-1}(1/c)$. A fact that will be of importance in section 3.5 is that for $s_o = 1/c$ or $k_1/c$ transitional asymptotics for the Bessel function and its derivative, which also are found in reference [12], yields

the same results as those given above in (3.31) and (3.32). Hence, (3.31) actually holds for $\sin^{-1}(1/c) \le \alpha \le \sin^{-1}(k_1/c)$ and (3.32) holds for $\sin^{-1}(k_1/c) \le \alpha < \pi/2$. Furthermore, since $H^I_{2s}$ and $H^I_{2d}$ are zero for $s_o = 1/c$, the solutions on the reflected rays for $\alpha = \sin^{-1}(1/c)$ are not singular. This result holds as $r \to 1$.

Lastly, as representative of singular waves that are refracted into the exterior by internally refracted waves, the contributions of $\dot{u}^*_{2ppp}$, $\dot{v}^*_{2ppp}$, $\dot{u}^*_{2pps}$ and $\dot{v}^*_{2pps}$, the dilatation and shear waves generated when the refracted P ray strikes the interface for the second time, are given. Recall that the interior P wave focuses after striking the interface for the first time and has a logarithmic singularity at its wave front the second time it strikes the interface (see (3.26)). Thus, the asymptotics of Appendix A, the method of stationary phase, and the lemma of section 2.5 imply the following singular behavior

$$\begin{bmatrix} \dot{u}^*_{2ppp}(r,\theta,t) \\ \dot{v}^*_{2ppp}(r,\theta,t) \end{bmatrix} \sim \frac{\sigma_o H_{2ppp}(s_o)}{\pi} \begin{bmatrix} \cos\delta \\ \sin\delta \end{bmatrix} \ln|t-t_{2ppp}| \text{ as } t \to t_{2ppp}, \tag{3.33a}$$

and

$$\begin{bmatrix} \dot{u}^*_{2pps}(r,\theta,t) \\ \dot{v}^*_{2pps}(r,\theta,t) \end{bmatrix} \sim \frac{\sigma_o H_{2pps}(s_o)}{\pi} \begin{bmatrix} -\sin\epsilon \\ \cos\epsilon \end{bmatrix} \ln|t-t_{2pps}| \text{ as } t \to t_{2pps}. \tag{3.33b}$$

In (3.33a), $s_o$ is such that

$$-2\alpha + \delta + \theta + 4\beta = 2\pi$$

and in (3.33b), $s_o$ is such that

$$-\alpha - \varkappa + \epsilon + \theta + 4\beta = 2\pi$$

where $\alpha$, $\beta$, $\delta$, $\epsilon$ and $\varkappa$ are given in (3.24e). In addition,

$$H_{2ppp}\big|_{s=s_o} = \left[\frac{\cos\beta}{2d_{2ppp}\left(2c-\frac{\cos\beta}{\cos\alpha}\right)+4c\cos\alpha-\cos\beta}\right]^{\frac{1}{2}} \cdot \frac{\delta_{11}}{\delta_{10}}\left(c_{31}-c_{11}\delta_{11}\right)\Big|_{s=s_o}$$

and

$$H_{2pps}\big|_{s=s_o} = \frac{k_2\cos\alpha\cos\varkappa}{\left[\cos\varkappa\left(d_{2pps}+\cos\varkappa\right)\left(4c\frac{\cos\alpha}{\cos\beta}-1\right)-d_{2pps}\frac{\cos\alpha}{k_2}\right]^{\frac{1}{2}}} \cdot \frac{\delta_{11}}{\delta_{10}}\left(g_{o1}-g_{o2}\right)\Big|_{s=s_o}$$

where $\delta_{10}$ and $\delta_{11}$ are given in (3.6), and $c_{11}$, $c_{31}$, $g_{o1}$ and $g_{o2}$ are given in (3.24). Also,

$$d_{2ppp} = r\cos\delta - \cos\alpha$$

$$d_{2pps} = r\cos\epsilon - \cos\varkappa$$

$$t_{2ppp} = d_{2ppp} + \frac{4\cos\beta}{c} + d_1 - 1$$

$$t_{2pps} = \frac{d_{2pps}}{k_2} + \frac{4\cos\beta}{c} + d_1 - 1,$$

where these distances and times have the usual physical meaning.

## 3.5 The Interior Dilatation Wave Front After n Reflections for n Large

From the previous discussion it is clear that the reflection of refracted interior waves is an important physical mechanism in this problem. To further understand this phenomenon consider

$$\dot{u}^*_{1p(n)}(r,\theta,t) \equiv \dot{u}^*_{\underbrace{pppp\ldots p}_{n\ p's}}(r,\theta,t), \tag{3.34}$$

where, by the notation of section 3.3, $\dot{u}^*_{1p(n)}$ is the interior radial component of velocity after n reflections from the interface.

By looking at the stationary phase points associated with various terms in the asymptotic expansions of $\frac{\omega}{2\pi}\tilde{\dot{u}}^*_1(dil)(r,s\omega,\omega)$ for large $\omega$ in (A.9) of Appendix A the term that contributes to $\dot{u}^*_{1p(n)}$ is picked out as

$$\frac{(i)^{n+1}\sigma_o a_o(s)}{r\delta_{1o}(s)}\left(\frac{m_1 m_{1/c}\, m_{r/c}}{2\pi\omega}\right)^{\frac{1}{2}} e^{i\omega(-s\pi/2+\psi_{1/c}-\psi_1)}\left[e^{i\omega\psi_{r/c}-i\pi/4}\right.$$

$$\left.-e^{-i\omega\psi_{r/c}+i\pi/4}\right][\delta_{11}(s)]^n e^{i2n\omega\psi_{1/c}},$$

where $a_o$, $\delta_{1o}$, $\delta_{11}$, $m_x$ and $\psi_x$ are given in (3.6). Using procedures analogous to those of section 3.2, it is found for $\theta > 0$ that

$$\tilde{\dot{u}}^*_{1p(n)}(r,\theta,\omega) \sim \int_o^{\min(r/c,1)} \frac{(i)^n H_{1p(n)}(s;r)e^{i\pi/4}}{\sqrt{\omega}} \cdot\left[e^{i\omega j_n(s;r,\theta)} - ie^{i\omega f_n(s;r,\theta)}\right]ds \tag{3.35}$$

where $H_{1p(n)} = \sigma_o\left(\frac{m_1 m_{1/c} m_{r/c}}{2\pi}\right)^{\frac{1}{2}} \frac{a_o(\delta_{11})^n}{r\delta_{1o}}$,

$$j_n = \psi_{r/c} - \frac{s\pi}{2} + \psi_{1/c}\cdot(1+2n) - \psi_1 + s\theta \ ,$$

and

$$f_n = j_n - 2\psi_{r/c} \ .$$

Note that for n = 0 (3.35) yields (3.7). As in the n = 0 case, discussed in section 3.2, the second term, $e^{i\omega f_n}$, has a point of stationary phase if $d_{1p(n)}$, the distance along the ray from the interface where the last, i.e. nth, reflection took place to the point of interest $(r,\theta)$, is less than $\cos\beta$, and the first term, $e^{i\omega j_n}$, has a point of stationary phase if $d_{1p(n)}$ is greater than $\cos\beta$. To see this consider the contribution from the second term. A point of stationary phase, $s_o$, exists if $df_n(s_o;r,\theta)/ds = 0 \Leftrightarrow$

$$-\gamma + (1+2n)\beta - n\pi + \theta - \alpha = 0, \qquad (3.36)$$

where

$$\alpha = \sin^{-1}s_o, \ \beta = \sin^{-1}s_o c \text{ and } \gamma = \sin^{-1}s_o c/r.$$

Equation (3.36) has the ray interpretation illustrated in Figure 16. The restriction that $s_o < r/c$ implies $\gamma<\pi/2$ which implies $d_{1p(n)} <\cos\beta$, as was asserted. Consider $\frac{d^2f_n}{ds^2}(s_o;r,\theta)$. Equation (3.35) implies

$$\frac{d^2f_n}{ds^2}(s_o;r,\theta) = \frac{-d_{1p(n)}+h_{1p(n)}}{\lambda_{1p(n)}}$$

where

$$h_{1p(n)} = \cos\beta(2nc\cos\alpha-\cos\beta)/[(2n+1)c\cos\alpha-\cos\beta]$$

and

$$\lambda_{1p(n)} = r\cos\gamma\cos\beta\cos\alpha/[(2n+1)c\cos\alpha-\cos\beta] \ .$$

For n large

$$h_{1p(n)} \to \cos\beta \text{ and } \lambda_{1p(n)} \to r\cos\gamma\cos\beta/2nc \ .$$

Thus for $d_{1p(n)} < \cos\beta$, $\frac{d^2 f_n}{ds^2}(s_o;r,\theta) > 0$ and the method of stationary phase implies that the contribution from $s_o$ is

$$\frac{\sigma_o}{c\omega}(i)^n \cos\gamma\cos\beta \sqrt{\frac{\cos\alpha}{2nc(\cos\beta - d_{1p(n)})}} \frac{a_o(\delta_{11})^n}{\delta_{1o}}\Big|_{s=s_o} e^{i\omega t_{1p(n)}} \tag{3.37}$$

as n and $\omega \to \infty$, where $d_{1p(n)} < \cos\beta$, $\theta > 0$ and

$$t_{1p(n)} = \frac{d_{1p(n)}}{c} + \frac{n(2\cos\beta)}{c} + d_1 - 1$$

is the time of arrival of the wave front.

Similarly, from the first term, $e^{i\omega j_n}$, in (3.35), the contribution from $s_o$ for $d_{1p(n)} > \cos\beta$ and $\theta > 0$ is

$$\frac{\sigma_o}{c\omega}(i)^{n+1} \cos\gamma'\cos\beta \sqrt{\frac{\cos\alpha}{2nc(d_{1p(n)} - \cos\beta)}} \frac{a_o(\delta_{11})^n}{\delta_{1o}}\Big|_{s=s_o} e^{i\omega t_{1p(n)}}, \tag{3.38}$$

as n and $\omega \to \infty$, where $\gamma'$ is the supplement of $\gamma$.

Using the lemma of section 2.5, the asymptotics (3.37) and (3.38) imply that if n is odd, say $n = 2j+1$, j a large positive integer, then

$$\dot{u}^*_{1p(2j+1)}(r,\theta,t) \sim \frac{\sigma_o(-1)^j \cos\gamma\cos\beta}{c} \sqrt{\frac{\cos\alpha}{2nc|\cos\beta - d_{1p(2j+1)}|}}$$

$$\cdot \frac{a_o(\delta_{11})^{2j+1}}{\delta_{1o}}\Big|_{s=s_o} \begin{cases} H(t - t_{1p(2j+1)}), & \text{if } d_{1p(n)} < \cos\beta \\ -\frac{1}{\pi}\ln|t - t_{1p(2j+1)}|, & \text{if } d_{1p(n)} > \cos\beta \end{cases} \tag{3.39a}$$

as $t \to t_{1p(2j+1)}$. However, if n is even, say $n = 2j+2$, j as above, then

$$\dot{u}^{*}_{1p(2j+2)}(r,\theta,t) \sim \sigma_o(-1)^{j+1}\cos\gamma\cos\beta\sqrt{\frac{\cos\alpha}{2nc\,|\cos\beta-d_{1p(2j+2)}|}}$$

$$\cdot\ \frac{a_o(\delta_{11})^{2j+2}}{\delta_{1o}}\Big|_{s=s_o}\begin{cases}-\frac{1}{\pi}\ln|t-t_{1p(2j+2)}|, & \text{if } d_{1p(n)}<\cos\beta\\ -H(t-t_{1p(2j+2)}), & \text{if } d_{1p(n)}>\cos\beta\end{cases} \tag{3.39b}$$

as $t \to t_{1p(2j+2)}$.

From these asymptotics it is clear that for n large $\dot{u}^{*}_{1p(n)}$ alternately focuses after an odd number of reflections and unfocuses after an even number of reflections as the wave propagates in $\theta$. Such behavior is to be expected after one considers the case of three dimensional focusing that Friedlander discusses in his book [5]. Since he considers three dimensional focusing, his converging wave front (initially a Heaviside step function) has two radii of curvature and hence two focal points. After passing through the first focal point he observes a logarithmic singularity which after passing through the next focal point again becomes a Heaviside function, i.e. the wave focuses and unfocuses as in (3.39a) and (3.39b). Physically, it is clear that each time the P wave reflects from the interface it looses energy into the outside media and hence the amplitude should decrease. From (3.39), the amplitude is proportional to

$$[\delta_{11}(s_o)]^n. \tag{3.40}$$

Since $\delta_{11} = (X^2-Y^2)/(X^2+Y^2)$ where from (3.6)

$$X^2 = s^2[e_2-\mu e_1]^2+m_1m_{k_2}[2s^2-\mu e_1]^2+\mu\left(\frac{k_1k_2}{c}\right)^2 m_1 m_{\frac{k_1}{c}} > 0\ ,$$

$$Y^2 = m_1 m_{k_1} [2s^2\mu - e_2]^2 + 4s^2 m_1 m_{k_2} m_{k_1} (1-\mu)^2 + \mu \left(\frac{k_1 k_2}{c}\right)^2 m_1 m_{k_2} > 0$$

for $s_o < \min(1, 1/c)$, then $|\delta_{11}(s_o)| < 1$. Hence $|\delta_{11}(s_o)| = e^{-b}$ where $b > 0$ and $|\delta_{11}(s_o)|^n = e^{-bn}$. Thus, (3.40) implies that the amplitude decreases exponentially as n increases.

Lastly, note that since $h_{1p(n)} \to \cos\beta$ as $n \to \infty$ and the length of the ray between two interface reflection points is $2\cos\beta$, the caustic tends towards the midpoint of the ray for n large, which is as far as possible from the interface.

Thus, it may be concluded that the wave alternately focuses and unfocuses as it propagates in $\theta$, that its amplitude decreases exponentially in n as n, the number of times it reflects from the interface, increases and the focal point moves as far as possible from the interface as n increases. It is clear, then, that the effects of later arriving waves which result from large numbers of reflections are not as important as the effects of waves that have reflected only a few times such as those calculated in sections 3.2 through 3.4.

One final point of interest that is associated with multiple reflections is the shape of the caustics. Let $C_n$ be the nth caustic, n = 1,2,3,.... Then for c = 1.5 the first three interior dilatation caustics are portrayed in Figure 17. Note that these first three caustics (it can be shown that this is true for all $C_n$) start at the point r=1, $\theta = \sin^{-1}(1/c)$.

Since this point is on the interface it is important to know just how singular are the stresses there. Recall from the analysis of 3.4 that the method of stationary phase did not apply for interior waves when the stationary phase point, $s_o$, equaled $\sin^{-1}(1/c)$ and hence the conclusions reached about the order of the singularity at the caustic being $(t-t_o)^{-1/6}$ do not apply at this point on the boundary. Recall the comments from section 3.4 that followed equation (3.32). It was found that in the exterior region there was only one reflected dilatation and shear wave pair associated with the stationary phase point $s_o=\sin^{-1}(1/c)$ and that for $\theta=\sin^{-1}(1/c)$, $r \to 1$ they were nonsingular. Since the incident wave is not singular, the perfect bonding boundary condition insures that the point $r = 1$, $\theta=\sin^{-1}(1/c)$ does not, in fact, experience logarithmically singular stresses, let alone singularities of the same order as the interior caustics. Hence this point is not, as it appeared at first glance, an interface failure mechanism.

## 3.6 A Necessary Condition for the Existence of a Propagating Stress Singularity

It has been shown in the previous sections that if the incident stress pulse has a step discontinuity then logarithmic stress singularities will propagate at the wave front after focusing. Suppose, instead, that the incident stress wave had

been continuous, as given by the incident potential

$$\varphi_{inc_2} = \frac{\sigma_o \Gamma(b)\,(t+r\cos\theta)^{2+b}}{b(b+1)(b+2)}\, H(t+r\cos\theta), b > 0.$$

The Fourier transform of this function is

$$\bar{\varphi}_{inc_2}(r,\theta,\omega) = \frac{\sigma_o}{(-i\omega)^3} \exp(-i\omega r\cos\theta) \frac{\Gamma(b)}{(-i\omega)^b} .$$

By comparing $\bar{\varphi}_{inc_2}$ with $\bar{\varphi}_{inc}$ and considering the method of analysis used, it is clear that the Fourier transform with respect to time of the solution is unchanged except that it is multiplied by the factor $\Gamma(b)/(-i\omega)^b$. From the convolution theorem, the solution for $\varphi_{inc_2}$ is the convolution of $t^{b-1}\,H(t)$ (which has the transform $\Gamma(b)/(-i\omega)^b$) and the solution for $\varphi_{inc}$. Consider the propagating logarithmic singularity of (3.16b) that arrives at time $t_{1p}$. When it is convoluted with the function $f(t) = t^{b-1}H(t)$, it contributes at time $t = t_{1p}$ an amount proportional to the integral

$$\int_{t_{1p-1}}^{t_{1p}} (t_{1p}-u)^{b-1} \ln(t_{1p}-u)\,du.$$

Let $u = t_{1p}-v$. Then the above equals

$$\int_0^1 v^{b-1} \ln v\,dv = -\frac{1}{b^2} , \text{ for } b > 0.$$

Hence, the convoluted solution no longer has a singularity at its wave front after touching a caustic.

It is known from the previous section that the internal refracted waves alternately focus and unfocus as they bounce

around the interior. The stresses at the wave fronts were found to go from step discontinuities to logarithmic singularities and back to step discontinuities. If the incident stress pulse is continuous, all of these logarithmic singularities would become bounded functions as above. Thus, a necessary condition for the existence of a propagating infinite discontinuity in stress is that the incident stress pulse have at least a step discontinuity at its wave front.

Ting and Lee [2] suggested that even if the first focusing did not cause infinite singularities in stress at the wave front, subsequent ones might. As is clear from the above discussion, this is, in fact, not possible.

# 4. THE CONTRIBUTIONS OF THE DIFFRACTED WAVES AND THE STONELY WAVE TO THE INTERFACE SOLUTION

## 4.1 Introduction and Derivation of a Residue Representation of the Solution

The nature of the stresses at the interface are of primary interest since bond failure is a major weakness in fiber reinforced composites when they are subjected to impact loading. It was found in the previous chapter that the refracted waves focus and produce singular stresses at the interface. It is the purpose of this chapter to show that wave fronts associated with the diffracted P and SV waves, and the Stonely (Rayleigh-like) interface wave are not singular and hence are negligible near their wave arrival times. Since these effects are negligible the following analysis is intentionally brief.

Let $\dot{u}_I^*(\theta,t)$ be the radial component of velocity of a point on the interface, i.e.

$$\dot{u}_I^*(\theta,t) = \dot{u}_1^*(r,\theta,t)\Big|_{r=1} = \dot{u}_2^*(r,\theta,t)\Big|_{r=1} . \qquad (4.1)$$

From (2.14) and (2.15)

$$\tilde{\dot{u}}_I^*(\nu,\omega) = -i\omega[A(\nu,\omega)\tfrac{\omega}{c}J_\nu'(\tfrac{\omega}{c}) + i\nu B(\nu,\omega)J_\nu(\tfrac{\omega k_1}{c})] . \qquad (4.2)$$

Taking the inverse Fourier transform with respect to $\nu$ yields

$$\bar{\dot{u}}_I^*(\theta,\omega) = \frac{1}{\pi}\int_0^\infty \tilde{\dot{u}}^*(\nu,\omega)\cos\nu\theta\, d\nu .$$

Change of variable: $\nu=s\omega$, since $\omega=\omega_1+i\omega_2$, $\omega_2>0$, this yields

$$\bar{\tilde{u}}_I^*(\theta,\omega) = \frac{1}{\pi}\int_{C_s} \omega \tilde{\tilde{u}}_I^*(s\omega,\omega)\cos s\omega\theta ds \ , \qquad (4.3)$$

$C_s$ is portrayed in Figure 18b. Using another change of variable $\bar{\tilde{u}}_I^*$ may be written

$$\bar{\tilde{u}}_I^*(\theta,\omega) = I_1(\theta,\omega) + I_2(\theta,\omega) \qquad (4.4)$$

where

$$I_1(\theta,\omega) = \frac{1}{2\pi}\int_{C_s} \omega \tilde{\tilde{u}}_I^*(s\omega,\omega) e^{i\omega s\theta} ds \ ,$$

$$I_2(\theta,\omega) = \frac{1}{2\pi}\int_{C_s'} \omega \tilde{\tilde{u}}_I^*(-s\omega,\omega) e^{i\omega s\theta} ds \ .$$

$C_s'$ is the line inclined at an angle of $-\tan^{-1}\frac{\omega_2}{\omega_1}$ from $-\infty e^{-i\tan^{-1}\frac{\omega_2}{\omega_1}}$ to the origin and is depicted in Figure 18a.

Consider the poles in the complex s-plane of the integrand which are the zeros of the function $\Delta(\nu,\omega)\big|_{\nu=s\omega}$, where

$$\Delta(\nu,\omega) = \det[E] \ ,$$

where [E] is given in (2.16). For $\omega = \omega_1 + i\omega_2$, $\omega_1$ large, the zeros of $\Delta(s\omega,\omega)$ are of five types. On the positive real s axis there are an infinite set of zeros associated with the interior dilatation waves, an infinite set of zeros associated with the interior SV waves and a zero associated with the Stonely wave.

In the first and third quadrants of the complex s plane there are two infinite sets of zeros associated with the exterior P and SV waves. Using this information, the location of the poles of $\tilde{\tilde{u}}_I^*(-s\omega,\omega)$ for $\omega$ large are portrayed in Figure 18a. For $\theta > 0$, consider $I_2$. By completing the closed

contour in the upper half s plane, also shown in Figure 18a, and letting $R \to \infty$ while using Jordan's lemma and asymptotics to prove $\int_{C_R'} \to 0$, one has from residue theory

$$I_2(\theta,\omega) + \int_o^\infty \frac{\omega \tilde{\dot{u}}_I^*(-s\omega,\omega)e^{i\omega\theta s}ds}{2\pi} = 2\pi i\left\{\sum_{n=0}^{\infty}(R_n^{(2p)}+R_n^{(2s)})\right\} \tag{4.5}$$

where $R_n^{(2p)}$ is the nth residue of $\omega\tilde{\dot{u}}_I^*(-s\omega,\omega)e^{i\omega s\theta}/(2\pi)$ associated with exterior dilatation waves and $R_n^{(2s)}$ is the nth residue of the same function associated with the exterior SV waves.

Secondly, consider $I_1$; again for $\theta > 0$ and $\omega$ large, a similar procedure using the contour of Figure 18b yields

$$I_1(\theta,\omega) - \int_o^\infty \frac{\omega \tilde{\dot{u}}_I^*(s\omega,\omega)e^{i\omega\theta s}ds}{2\pi} = \pi i\left\{\sum_{n=0}^{\infty}(R_n^{(1p)}+R_n^{(1s)})\right\} + \pi i R_{ST} \tag{4.6}$$

where $R_n^{(1p)}$ is the nth residue of $\omega\tilde{\dot{u}}_I^*(s\omega,\omega)e^{i\omega\theta s}/(2\pi)$ associated with the interior dilatation waves, $R_n^{(1s)}$ is the nth residue associated with the interior SV waves and $R_{ST}$ is the residue from the Stonely pole. Since all these poles are on the real s axis two things occur: the residues in (4.6) are multiplied by $\pi i$ rather than $2\pi i$ and $\int_o^\infty$ in (4.6) is a Cauchy principal value integral in reference to the interior P and SV poles as well as the Stonely pole which lie on the path of integration.

Thus, (4.5) and (4.6) imply that (4.4) may be written:

$$\bar{\dot{u}}_I^*(\theta,\omega) = \frac{1}{2\pi}\int_0^\infty \omega e^{i\omega s\theta}[\tilde{\dot{u}}_I^*(s\omega,\omega)-\tilde{\dot{u}}_I^*(-s\omega,\omega)]ds$$

$$+ \pi i\left\{\sum_{n=0}^{\infty}[2R_n^{(2p)}+2R_n^{(2s)}+R_n^{(1p)}+R_n^{(1s)}] + R_{ST}\right\} \tag{4.7}$$

Hence, by the procedures outlined in this section the line integral representation of $\bar{\dot{u}}_I^*(\theta,\omega)$ in equation (4.4) has been exchanged for the principal value integral (principal value is for $\tilde{\dot{u}}_I^*(s\omega,\omega)$ part of the integral) and the residues of (4.7).

In a similar problem, one investigator [10], while seeking the contribution from diffracted waves, overlooked the existence of a principal value integral which was analogous to the one in (4.7). To understand this error consider the source of the integral in (4.7). In equations (2.14) the doubly transformed interior solutions are given as Bessel functions of order absolute value of $\nu$. The $|\nu|$ was necessary so that the solution would be bounded as $r \to 0$, however, its use destroyed the analyticity of the doubly transformed solution with respect to $\nu$. To restore analyticity, the Fourier inversion integrals were rewritten in half range form in (2.17) and the absolute value signs dropped. The integrands in (2.17), or for that matter in (4.3), were now analytic and hence complex variable theory could be used to derive (4.7). However, when the absolute value signs were dropped the evenness of $\tilde{\dot{u}}_\alpha^*$ and $\tilde{\dot{u}}_I^*$ with respect to $\nu$ was destroyed and thus

$\tilde{\dot{u}}_I^*(-s\omega,\omega) \neq \tilde{\dot{u}}_I^*(s\omega,\omega)$. Hence, the integral of (4.7) contributes to the solution. Actually, the author of [10] failed to realize the need for the absolute value signs from the beginning and his error followed from that oversight.

4.2 Contribution from P and SV Residues

Consider the contribution to the solution from the residues $R_n^{(2p)}$ and $R_n^{(2s)}$. For high frequency, $\omega$ large, these residues are associated with the zeros of $H_{s\omega}^{(1)}(\omega)$ and $H_{s\omega}^{(1)}(\omega k_2)$, which are located in the first and third quadrants of the complex s plane. The asymptotic evaluation of these residues is done using the asymptotic expansions for the Bessel and Hankel functions given in Olver's paper [13]. This evaluation is analogous to that of Gilbert and Knopoff's [9] where they evaluated the wave front behavior of an elastic wave diffracted by a rigid cylinder. It is found that the nature of these residues, which are associated with externally diffracted waves, is essentially unchanged when the rigid cylinder is replaced by a linearly elastic one. $R_n^{(2p)}$ and $R_n^{(2s)}$ are exponentially small as $\omega \to \infty$ and hence as one would expect from the lemma of section 2.5, Gilbert and Knopoff show that they contribute velocities which are infinitely continuous at the wave front. By continuity at the interface, any waves refracted into the interior also have an infinitely continuous wave front. As shown in section 3.6, a necessary condition for a wave front to propagate an infinite stress discontinuity after focusing is

that it must have at least a simple jump discontinuity in velocity beforehand. Hence any externally diffracted/internally refracted waves are nonsingular even after focusing.

Consider the contribution to the solution from the residues $R_n^{(1p)}$ and $R_n^{(1s)}$. The asymptotics of appendices A and B together with the following transitional asymptotics from reference [12] may be used to evaluate the asymptotic behavior of these residues for large $\omega$, when $c > k_1$.

For $\nu = s\omega$, $s = 1/c - (z\omega^{-2/3})/c^{1/3}$, then

$$J_{s\omega}(\tfrac{\omega}{c}) \sim 2^{1/3} (\tfrac{c}{\omega})^{1/3} Ai(-2^{1/3}z)$$

$$J'_{s\omega}(\tfrac{\omega}{c}) \sim -2^{2/3} (\tfrac{c}{\omega})^{2/3} Ai'(-2^{1/3}z)$$

as $\omega \to \infty$. $Ai(x)$ is the Airy function which satisfies

$$Ai''(x) - xAi(x) = 0,\ Ai(o) = \frac{3^{-2/3}}{\Gamma(2/3)}, Ai'(o) = \frac{-3^{-1/3}}{\Gamma(1/3)}.$$

Let $a_j$ be the jth zero of the Airy function. The $a_j$'s are tabulated in reference [12] and are real and negative. The asymptotic behavior of the residue $R_j^{(1p)}$ as $\omega \to +\infty$ is proportional to $(-i\omega)^{-3/2} \exp[i\omega t_o + i a_j (\omega/2c)^{1/3}\lambda]$, where $t_o$ is the time of arrival of the diffracted wave front and $\lambda$ is the diffracted path length. Since this term is of order $\omega^{-3/2}$ as $\omega \to \infty$ the lemma of section 2.5 suggests that it corresponds to a function of time with the behavior $(t-t_o)^{\frac{1}{2}}$ as $t \to t_o$. The function of time that has the above transform is complicated but can be expressed as an integral by use of the inversion

integral (2.11b) and the convolution theorem. Using this representation it is possible to verify that the wave front behavior is, in fact, continuous. Hence, as with the diffracted exterior wave, no propagating singular stresses can be generated by focusing.

## 4.3 Contribution from Stonely Interface Wave

The Stonely pole exists if certain requirements are satisfied by the material constants of the two materials. These requirements are quite involved and are explored in detail in Cagniard's book [14]. If these requirements are satisfied, he shows that the Stonely pole, $s = k_{ST}$, exists and that $k_{ST} = c_{d_1}/c_{st} > \max(k_1/c, k_2)$, i.e. the dimensionless Stonely slowness, $k_{ST}$, is larger than the dimensionless shear wave slowness in either material. As a result, the appropriate asymptotics for evaluating the large $\omega$ behavior of the contribution from the Stonely wave are those of Appendix B for the Bessel function and its derivative and for the Hankel functions again from reference [12], for $s > x$

$$H_{s\omega}^{(1)}(\omega x) \sim -i\sqrt{\frac{2}{\pi\omega m_x(s)}}\, e^{\omega\Omega_s(s)}$$

and

$$xH_{s\omega}^{(1)\prime}(\omega x) \sim -m_x(s)H_{s\omega}^{(1)}(\omega x)$$

where

$$m_x(s) = \sqrt{|s^2-x^2|}$$

and

$$\Omega_x(s) = s\cosh^{-1}\left(\frac{s}{x}\right) - m_x(s) \ .$$

Let $\dot{u}^*_{I(ST)_1}$ be the contribution to $\dot{u}^*_I$ from the Stonely residue term $\pi i R_{ST}$ in (4.7) and $\dot{u}^*_{I(ST)_2}$ be the contribution from the principal value integral near the Stonely pole. Using the aforementioned asymptotics, it is found that

$$\bar{\dot{u}}^*_{I(ST)_1}(\theta,\omega) \sim i\sqrt{\frac{\pi}{2}}\ \frac{F(k_{ST})e^{ik_{ST}\omega(\theta-\pi/2)-\omega\Omega_1(k_{ST})}}{\omega^{\frac{1}{2}}\Delta'(k_{ST})} \tag{4.8}$$

where

$$F(s) = \sigma_o m_1^{\frac{1}{2}} \cdot\Big[s^2(m_1 m_{k_1}+s^2)4e_2-4\mu s^4(2m_1 m_{k_1}-e_1)$$

$$-2[e_2(m_1 m_{k_1}-s^2)-\mu m_1 m_{k_2}(\tfrac{k_1}{c})^2]e_2+2\mu s^2[e_1(m_1 m_{k_2}-e_2)$$

$$-2m_1 m_{k_1} k_2^2]\Big],$$

$$\Delta(s) = (s^2-m_1 m_{k_1})(4s^2 m_1 m_{k_2}-e_1^2)+2s^2\mu(2m_1 m_{k_1}-e_1)(2m_1 m_{k_2}-e_2)$$

$$+\mu(\tfrac{k_1 k_2}{c})^2(m_1 m_{k_2}+m_1 m_{k_1})+\mu^2(4s^2 m_1 m_{k_1}-e_1^2)(s^2-m_1 m_{k_2}),$$

$$e_1 = 2s^2-k_1^2/c^2, \quad e_2 = 2s^2-k_2^2.$$

As it would be expected from the transform integral (2.11a), $\bar{\dot{u}}^*_{I(ST)_1}(\theta,\omega)$ is the complex conjugate of $\dot{u}^*_{I(ST)_1}(\theta,-\omega)$. Hence, using the inversion integral (2.11b) to find the function of time whose transform is the right hand side of (4.8) yields

$$\dot{u}^*_{I(ST)_1}(\theta,T) \sim \frac{1}{\pi}\int_o^\infty \frac{\sin(T\omega)}{\sqrt{\omega}}\ e^{-\omega\Omega_1(k_{ST})}d\omega\ \frac{F(k_{ST})}{\Delta'(k_{ST})}\sqrt{\frac{\pi}{2}}$$

as $t \to 0$, where $T = t-k_{ST}(\theta-\pi/2)$. Integral transform tables yield

$$\dot{u}^{*}_{I(ST)_1}(\theta,T) \sim \frac{F(k_{ST})}{2\Delta'(k_{ST})} \frac{[(\Omega_1^2(k_{ST})+T^2)^{\frac{1}{2}}-\Omega_1(k_{ST})]}{[\Omega_1^2(k_{ST})+T^2]^{\frac{1}{2}}}, \tag{4.9}$$

as $T \to 0$.

Secondly, consider $\bar{\dot{u}}^{*}_{I(ST)_2}$. The contribution from the principal value integral from near the Stonely pole is approximately

$$\int_{k_{ST}-\epsilon}^{k_{ST}+\epsilon} \frac{F(s)e^{i\omega s(\theta-\pi/2)-\omega\Omega_1(s)}}{\sqrt{2\pi\omega}\,\Delta(s)}\,ds .$$

Since the role of $\Delta(s) \to 0$ as $s \to k_{ST}$ is of interest, the integral is approximated as

$$\frac{F(k_{ST})e^{-\omega\Omega_1(k_{ST})}}{\sqrt{2\pi\omega}\,\Delta'(k_{ST})} \int_{k_{ST}-\epsilon}^{k_{ST}+\epsilon} \frac{e^{i\omega s(\theta-\pi/2)}}{(s-k_{ST})}\,ds .$$

Keeping only the even part of the integrand, a change of variable yields,

$$\bar{\dot{u}}^{*}_{I(ST)_2}(\theta,\omega) \sim \frac{2F(k_{ST})e^{-\omega\Omega_1(k_{ST})+i\omega k_{ST}(\theta-\pi/2)}}{\sqrt{2\pi\omega}\,\Delta'(k_{ST})} \int_0^{\epsilon\omega(\theta-\pi/2)} \frac{\sin v}{v}\,dv$$

$$\sim \sqrt{\frac{\pi}{2\omega}}\,\frac{F(k_{ST})e^{-\omega\Omega_1(k_{ST})+i\omega(\theta-\pi/2)k_{ST}}}{\Delta'(k_{ST})}$$

as $\omega \to \infty$. Analogous to $\bar{\dot{u}}^{*}_{I(ST)_1}$, the inversion integral is applied and it is found that as $T \to 0$

$$\dot{u}^{*}_{I(ST)_2}(\theta,T) \sim \frac{F(k_{ST})}{2\Delta'(k_{ST})} \frac{[(\Omega_1^2(k_{ST})+T^2)^{\frac{1}{2}}+\Omega_1(k_{ST})]^{\frac{1}{2}}}{(\Omega_1^2(k_{ST})+T^2)^{\frac{1}{2}}} . \tag{4.10}$$

Note the following:

(i) Both $\bar{\dot{u}}^{*}_{I(ST)_1}$ and $\bar{\dot{u}}^{*}_{I(ST)_2}$ are of the same order as $\omega \to \infty$.

(ii) Both are exponentially decaying as $\omega \to \infty$ and, as one would expect from the lemma of section 2.5, their corresponding functions of time are infinitely continuous for all T.

(iii) $\dot{u}^*_{I(ST)_1} \to 0$ as $T \to 0$ while $\dot{u}^*_{I(ST)_2}$ does not. In fact, $\dot{u}^*_{I(ST)_2}$ is a pulse which is maximum at $T = 0$.

With regards to (iii), if $\dot{v}^*_{I(ST)_1}$ and $\dot{v}^*_{I(ST)_2}$ were computed the opposite result would be observed, i.e. the main contribution to $\dot{v}^*_{I(ST)}$ comes from the residue and not the principal value integral. Hence, both residues and principal value integrals are equally important.

Lastly, note that Miklowitz [ 6 ] obtained results essentially analogous to those of this section for the Rayleigh wave while investigating the problem of a stress pulse striking a cylindrical cavity.

4.4 Contribution from the Principal Value Integral from Near the P and SV Poles

As was the case for the Stonely wave, the principal value integrals from near the P and SV poles yield contributions to the solution of the same order in $\omega$ as their residue counterparts. Hence, as was shown in section 4.2 for the residues, they do not contribute to singular stresses.

In summary, neither diffracted waves nor the Stonely interface wave cause singular stresses in the composite. However, if their wave front behavior is to be ascertained, then contributions from the principal value integral and the residues are equally important.

## 5. CONCLUSIONS

In the present analysis a Watson-type lemma for use with the Fourier transform was constructed and used to determine the asymptotic behavior at singular wave fronts of the solution of a stress pulse striking an elastic inclusion embedded in an infinite elastic solid. This lemma is generally applicable to problems which involve singular loadings or focusing in which wave front behavior is important. Furthermore, unlike some methods, it yields the behavior of singular wave fronts whether or not the singular wave is the first to arrive.

Secondly, Friedlander's technique, which formulates the solution in terms of wave forms associated with propagation in $\theta$, has been extended to an interior region, the inclusion. With no inclusion, i.e. a circular cylindrical hole, Miklowitz [6] and Peck and Miklowitz [7] found that Friedlander's representation yielded reflected waves, and angularly propagating diffracted and Rayleigh surface waves. It was found here that when the hole is filled with an elastic inclusion that, in addition to waves analogous to the above (substitute Stonely interface wave for Rayleigh wave), there are refracted interior waves that also propagate in $\theta$. Such waves bounce around the interior by reflecting from the interface.

These techniques applied to the problem of a stress pulse striking a circular cylindrical elastic inclusion yield the following results. Dominant stress singularities arise from the focusing of waves refracted into the interior. In order

for any refracted stress pulse to propagate an infinite singularity at its wave front after focusing, the incident stress wave that strikes the inclusion must have at least a simple step discontinuity at its wave front. If this condition is met then the interior refracted wave bounces around the interior, alternately focusing and unfocusing after each reflection from the interface, i.e. the corresponding stress at the wave front going from a step discontinuity to a logarithmic singularity and back to a step discontinuity. As the number of reflections from the interface increases, the magnitude of a coefficient which multiplies the step discontinuity/logarithmic singularity in stress decreases exponentially and the focal point becomes as far as possible from the interface. Thus, the contributions from the first few reflections are the most important as far as failure at the fiber-matrix interface is concerned and, hence, are given in detail in sections 3.2, 3.3 and 3.4. In addition, this analysis revealed that some of the reflected exterior waves are also infinitely singular at their wave fronts if the dilatation wave speed in the inclusion is greater than the dilatation wave speed in the exterior matrix material (which is the case for most composite materials). Lastly, it was shown that the contributions from the diffracted waves and the Stonely interface wave are not singular.

As was pointed out above, unless the incident stress pulse has a step discontinuity the focused waves do not have an infinite singularity at their wave fronts. A physical

stress pulse is always continuous, thus, the results found here are to be interpreted as a limiting case as the rise time of a continuous incident pulse becomes small. In fact, it is for this reason that the coefficients which multiply the logarithmic singularities are important. As the rise time of the incident stress pulse becomes small, the focused response in the neighborhood of the wave fronts, while still finite, are proportional to these coefficients and, hence, they determine relative stress levels. A related use for the solution found here is that the asymptotic behavior of the wave front response to a continuous incident stress pulse may be determined from it by use of the convolution theorem.

## 6. REFERENCES

[1] W. L. Ko, "Scattering of Stress Waves by a Circular Elastic Cylinder Embedded in an Elastic Medium", J.Appl. Mech., pp.345-355,June 1970.

[2] T. C. T. Ting and E. H. Lee, "Wave-Front Analysis in Composite Materials", J.Appl.Mech., pp. 497-504, September 1969.

[3] J. D. Achenbach, J. H. Hemann, F. Ziegler, "Separation at the Interface of a Circular Inclusion and the Surrounding Medium Under an Incident Compressive Wave", J.Appl. Mech., pp. 298-304, June 1970.

[4] L. Knopoff and F. Gilbert, "First Motion Methods in Theoretical Seismology", J.Acoust.Soc.Amer.,Vol. 31, No. 9, pp. 1161-1168, September 1959.

[5] F. G. Friedlander, Sound Pulses, Cambridge University Press, 1958.

[6] J. Miklowitz, "Scattering of a plane elastic compressional pulse by a cylindrical cavity", Proceedings of the Eleventh International Congress of Applied Mechanics, Munich, Germany, pp.469-483, 1964.

[7] J. C. Peck and J. Miklowitz, "Shadow-Zone Response in the Diffraction of a Plane Compressional Pulse by a Circular Cavity", Int.J.Solids Structures, Vol.5, pp.437-454,1969.

[8] F. Gilbert, "Scattering of Impulsive Elastic Waves by a Smooth Convex Cylinder", J.Acoust.Soc.Amer.,Vol.32,No.7, pp.841-857, July 1960.

[9] F. Gilbert and L. Knopoff, "Scattering of Impulsive Elastic Waves by a Rigid Cylinder", J.Acoust.Soc.Amer., Vol.31,No.9, pp.1169-1175, September 1959.

[10] Y. M. Chen, "Diffraction by a Smooth Transparent Object", J.Mathematical Physics,Vol.5, No.6,pp.820-832,June 1964.

[11] I. S. Gradshteyn and I. M. Ryzhik, Table of Integrals, Series, and Products, Academic Press, New York, 1965.

[12] M. Abramowitz and I. A. Stegun, editors, Handbook of Mathematical Functions, Nat.Bur.Stds.,App.Math.Series 55, 1968.

[13] F. W. J. Olver, "The Asymptotic Expansion of Bessel Functions of Large Order", Phil.Trans.Roy.Soc.A,Vol. 247, pp.328-369, 1955.

[14] L. Cagniard, Reflection and Refraction of Progressive Seismic Waves, McGraw-Hill, London, 1962.

## APPENDIX A. THE ASYMPTOTIC BEHAVIOR OF $\frac{\omega}{2\pi}\tilde{\dot{u}}_1^*(\text{dil})(r,s\omega,\omega)$ AS $\omega\to\infty$ FOR $s\in[0,\min(1,r/c))$.

From equation (3.2)

$$\tilde{\dot{u}}_{1\,(\text{dil})}^{*}(r,s\omega,\omega) = -\frac{i\omega^2}{c}A(s\omega,\omega)J'_{s\omega}(\tfrac{\omega r}{c}) \tag{A.1}$$

where from equation (2.16) for $\nu = s\omega$

$$A(s\omega,\omega) = \frac{2\pi\sigma_o}{i\omega^3}e^{-s\omega\pi i/2}a(s,\omega)/\Delta(s,\omega)$$

where

$$a(s,\omega) = \det[\underline{y},\ \underline{e}_2,\underline{e}_3,\underline{e}_4]\big|_{\nu=s\omega} \quad \text{and}$$

$$\Delta = \det[E]\big|_{\nu=s\omega}.$$

To find the asymptotic behavior of a, $\Delta$ and then $\tilde{\dot{u}}_{1(\text{dil})}^{*}$ for large $\omega$ the following asymptotic formulas for the Hankel and Bessel functions obtained from those of reference [12] are used. If $\nu = s\omega$ and $s\in[0,x)$, i.e. $0 \le s < x$, (A.2a)

then
$$H_\nu^{(1)}(\omega x) \sim \sqrt{\frac{2}{\pi\omega m_x(s)}}\exp\left\{i\omega\psi_x(s)-i\pi/4\right\} \tag{A.2b}$$

$$xH_\nu^{(1)\prime}(\omega x) \sim i\sqrt{\frac{2m_x(s)}{\pi\omega}}\exp\left\{i\omega\psi_x(s)-i\pi/4\right\} \tag{A.2c}$$

$$J_\nu(\omega x) \sim \frac{\exp[-i\omega\psi_x(s)+i\pi/4]}{\sqrt{2\pi\omega m_x(s)}}[1-i\exp\left\{2i\omega\psi_x(s)\right\}] \tag{A.2d}$$

$$xJ'_\nu(\omega x) \sim -i\sqrt{\frac{m_x(s)}{2\pi\omega}}\exp\left\{-i\omega\psi_x(s)+i\pi/4\right\}[1+i\exp\left\{2i\omega\psi_x(s)\right\}] \tag{A.2e}$$

as $\omega\to\infty$, where

$$m_x(s) = \sqrt{|x^2-s^2|} \quad \text{and}$$

$$\psi_x(s) = m_x(s) - s\cos^{-1}(\tfrac{s}{x}).$$

The determinant for $a(s,\omega)$ given in equation (A.1) is expanded and then simplified by using the fact that the Wronskian, $W\{J_\nu(z), H_\nu^{(1)}(z)\}$, equals $2i/\pi z$. Products of this type occur when elements of the vector $\underline{y}$ are multiplied by elements of the vector $\underline{e}_3$ which have the same argument. Following this simplification, the asymptotics of (A.2) are substituted and result in

$$a(s,\omega) \sim \frac{\omega^4 e^{[\psi_{k_2}-\psi_{k_1/c}]}}{\pi^2 (m_{k_1/c} m_{k_2})^{\frac{1}{2}}} [a_o(s)+a_1(s) i e^{2i\omega\psi_{k_1/c}}] \quad (A.3)$$

where

$$a_o(s) = 4e_2 s^2 (m_{\frac{k_1}{c}}+m_{k_2}) - 8s^4 (m_{k_2}+\mu m_{\frac{k_1}{c}}) - 2e_2 (m_{\frac{k_1}{c}} e_2 - \mu m_{k_2} e_1)$$

$$+4\mu s^2 (m_{\frac{k_1}{c}} e_2 - m_{k_1} e_1) ,$$

$$e_1 = (2s^2 - k_1^2/c^2) , \quad e_2 = (2s^2 - k_2^2).$$

The algebraic form of $a_1$ is similar to that of $a_o$. It's explicit representation will not be needed in this work. The requirement (A.2a) restricts s to the interval $[0, \min(1, k_1/c))$, where

$$\min(1,k_1/c) \equiv \text{minimum of 1 and } k_1/c = \begin{cases} 1 \text{ if } c < k_1 \\ k_1/c \text{ if } c > k_1 \end{cases}.$$

The asymptotic behavior of the determinant for $\Delta(s,\omega)$ given in equation (A.1) is also found by the use of the asymptotics of (A.2). Their substitution implies that for large $\omega$

$$\Delta(s,\omega) \sim \frac{-\delta\omega^4 \exp[i\omega(\psi_1+\psi_{k_2}-\psi_{1/c}-\psi_{k_1/c})]}{\pi^2 (m_1 m_{1/c} m_{k_1/c} m_{k_2})^{\frac{1}{2}}} , \quad (A.4a)$$

where

$$\delta(s,\omega) = \delta_{10}\left\{1-i[\delta_{11}e^{2i\omega\psi_1/c}+\delta_{12}e^{2i\omega\psi_{k_1}/c}+\delta_{13}e^{2i\omega(\psi_{k_1}/c+\psi_1/c)}]\right\}, \tag{A.4b}$$

$$\delta_{10}(s) = (m_1\underset{c}{m}_{k_1}+s^2)(e_2^2+4s^2m_1m_{k_2})+\mu[-2s^2(2m_{k_1}\underset{c}{m}_1+e_1)(2m_1m_{k_2}+e_2) + (\frac{k_1k_2}{c})^2(m_1\underset{c}{m}_{k_2}+m_1\underset{c}{m}_{k_1})]+\mu^2(e_1^2+4s^2\underset{c}{m}_{k_1}\underset{c}{m}_1)(m_1m_{k_2}+s^2), \tag{A.4c}$$

and

$$\delta_{11}(s)\delta_{10}(s) = (-\underset{c}{m}_1\underset{c}{m}_{k_1}+s^2)(e_2^2+4s^2m_1m_{k_2})+\mu[2s^2(2m_{k_1}\underset{c}{m}_1+e_1)\cdot(2m_1m_{k_2}+e_2) + (\frac{k_1k_2}{c})^2(m_1\underset{c}{m}_{k_1}-\underset{c}{m}_1m_{k_2})] +\mu^2(e_1^2-4s^2\underset{c}{m}_1\underset{c}{m}_{k_1})(m_1m_{k_2}+s^2) . \tag{A.4d}$$

Again, explicit representations of $\delta_{12}$ and $\delta_{13}$ will not be needed. Requirement (A.2d) restricts the applicability of (A.4a) to s contained in the interval $[0,\min(1,1/c))$.

The asymptotics (A.3) and (A.4) and equation (A.1) imply

$$\Delta(s\omega,\omega) \sim \frac{2\pi\sigma_o}{-i\omega^3\delta(s,\omega)}(m_1\underset{c}{m}_1)^{\frac{1}{2}}[a_o(s)+ia_1(s)e^{2i\omega\psi_{k_1}/c}]e^{i\omega(\psi_1/c-\psi_1)} \tag{A.5}$$

as $\omega\to\infty$, for $s\in[0,\min(1,1/c))$. Thus, the representation for $\tilde{\dot{u}}_1^*(dil)$ of equation (A.1) and the asymptotic for $xJ_\nu'(\omega x)$ of (A.2e) imply

$$\frac{\omega}{2\pi}\tilde{\dot{u}}_1^*(dil)(r,s\omega,\omega) \sim \frac{i\sigma_o}{r\delta(s,\omega)}\left(\frac{m_1/cm_1}{2\pi\omega}\right)^{\frac{1}{2}}e^{i\omega(-s\pi/2+\psi_1/c-\psi_1)} \cdot[a_o+ia_1e^{2i\omega\psi_{k_1}/c}][e^{i\omega\psi_r/c-i\pi/4}-e^{-i\omega\psi_r/c+i\pi/4}] \tag{A.6}$$

as $\omega\to\infty$, where (A.2a) restricts s to the interval $[0,\min(1,r/c))$.

This term is part of the integrand in equation (3.5). The integral is evaluated asymptotically for large $\omega$ using the method of stationary phase. To do this, all exponential terms of the type $e^{i\omega f(s)}$ must appear in the numerator of the integrand. To achieve this result, $\delta^{-1}(s,\omega)$ is expanded in a geometric series. From equation (A.4b)

$$\delta(s,\omega) = (1+z)\delta_{10} \ , \tag{A.7}$$

where

$$z = -i[\delta_{11}e^{2i\omega\psi_{1/c}} + \delta_{12}e^{2i\omega\psi k_{1/c}} + \delta_{13}e^{2i\omega(\psi_{k_1/c}+\psi_{1/c})}].$$

From Fourier transform theory, $\omega$ is restricted to the half plane $\mathrm{Im}\{\omega\} > 0$. Thus the limiting procedure $\omega = \omega_1 + i\omega_2$ where $\omega_2 > 0$ and $\omega_1 \to +\infty$ can be used and for $\omega_2$ sufficiently large, since $\psi_x(s)$ is positive definite, z is less than one. Thus, expanding $\delta^{-1}$ in a geometric series

$$\delta^{-1} = \delta_{10}^{-1} \sum_{n=0}^{\infty} (-z)^n \ . \tag{A.8}$$

Asymptotic relation (A.6) becomes,

$$\frac{\omega\tilde{\dot{u}}_1^*(\mathrm{dil})}{2\pi}(r,s\omega,\omega) \sim \frac{i\sigma_o}{r\delta_{10}(s)}\left(\frac{m_1 m_{1/c} m_{r/c}}{2\pi\omega}\right)^{\frac{1}{2}} e^{i\omega(-s\pi/2+\psi_{1/c}-\psi_1)}$$
$$\cdot[a_o+ia_1 e^{2i\omega\psi_{k_1/c}}][e^{i\omega\psi_{r/c}-i\pi/4} - e^{-i\omega\psi_{r/c}+i\pi/4}]$$
$$\cdot \sum_{n=o}^{\infty} (i)^n[\delta_{11}e^{2i\omega\psi_{1/c}} + \delta_{12}e^{2i\omega\psi_{k_1/c}} + \delta_{13}e^{2i\omega(\psi_{k_1/c}+\psi_{1/c})}]^n \tag{A.9}$$

as $\omega \to \infty$, for $s\in[0,\min(1,r/c))$.

The meaning of this representation is explained in Chapter 3.

## APPENDIX B. THE ASYMPTOTIC BEHAVIOR OF $\frac{\omega}{2\pi}\tilde{\dot{u}}^*_{sc(dil)}(r,s\omega,\omega)$ AND $\frac{\omega}{2\pi}\tilde{\dot{v}}^*_{sc(dil)}(r,s\omega,\omega)$ AS $\omega\to\infty$ FOR $s\in[1/c,1), c>k_1$

The double Fourier transform of the radial and angular components of the scattered wave form dilatational velocities are $\tilde{\dot{u}}^*_{sc(dil)}$ and $\tilde{\dot{v}}^*_{sc(dil)}$. From equations (2.15a), (2.15b) and (2.14)

$$\tilde{\dot{u}}^*_{sc(dil)}(r,\nu,\omega) = -i\omega^2 C(\nu,\omega)H_\nu^{(1)\prime}(\omega r) \tag{B.1a}$$

and

$$\tilde{\dot{v}}^*_{sc(dil)}(r,\nu,\omega) = \frac{\nu\omega}{r}C(\nu,\omega)H_\nu^{(1)}(\omega r) \tag{B.1b}$$

where from equation (2.16) for $\nu = s\omega$

$$C(s\omega,\omega) = \frac{2\pi\sigma_o}{i\omega^3}e^{-s\omega\pi i/2}c(s,\omega)/\Delta(s,\omega)\ , \tag{B.1c}$$

$$c(s,\omega) = \det[\underline{e}_1,\underline{e}_2,\underline{y},\underline{e}_4]\big|_{\nu=s\omega} \tag{B.1d}$$

and

$$\Delta(s,\omega) = \det[E]\big|_{\nu=s\omega} = \det[\underline{e}_1,\underline{e}_2,\underline{e}_3,\underline{e}_4]\big|_{\nu=s\omega}\ . \tag{B.1e}$$

As will be shown later, for $\nu = s\omega$ and $s\in(1/c,1)$, the asymptotic behavior for $\omega$ large of $c$, $\Delta$ and then the transformed scattered dilatation velocities can be found by using the asymptotic formulas of Appendix A, equations (A.2a) to (A.2d) and the following formulas that were also obtained from those of reference [12]. If $\nu = s\omega$ and $\omega\to\infty$, then for $s > x$

$$J_\nu(\omega x) \sim \frac{e^{-\omega\Omega_x(s)}}{\sqrt{2\pi\omega m_x(s)}} \tag{B.2a}$$

and

$$xJ_\nu'(\omega x) \sim \sqrt{\frac{m_x(s)}{2\pi\omega}}\ e^{-\omega\Omega_x(s)} \tag{B.2b}$$

where

$$m_x(s) = \sqrt{|x^2-s^2|}$$

and

$$\Omega_x(s) = s\cosh^{-1}(\tfrac{s}{x})-m_x(s) \ .$$

There are two subintervals of interest: $s\epsilon(1/c,k_1/c)$, i.e. s contained in the open interval $1/c$ to $k_1/c$; and $s\epsilon(k_1/c, 1)$. For s contained in the first subinterval, $(1/c,k_1/c)$, (B.2a) and (B.2b) are used to approximate $\underline{e}_1$ asymptotically since arguments of the Bessel functions of $\underline{e}_1$ are greater than the order, and (A.2a) through (A.2e) are used to approximate $\underline{e}_2$, $\underline{e}_3$, $\underline{e}_4$ and $\underline{y}$ since the arguments of these functions are less than their orders. If s is contained in the second subinterval, $(k_1/c,1)$, then (B.2a) and (B.2b) are used to approximate both $\underline{e}_1$ and $\underline{e}_2$, while (A.2a) to (A.2e) are used for the remaining vectors. Thus, using the notation of (A.2) and (B.2), it is found that for $s\epsilon(1/c,k_1/c)$

$$c(s,\omega) \sim \frac{\omega^4 e^{\omega[-\Omega_{1/c}+i(\psi_{k_2}-\psi_1-\psi_{k_1/c})]+i\pi/4}}{2\pi^2(m_{1/c}\, m_{k_1/c}\, m_1 m_{k_2})^{\frac{1}{2}}}\left[c_0(s)-ic_1(s)e^{2i\omega\psi_1}\right.$$

$$\left.-ic_2(s)e^{2i\omega\psi_{k_1/c}}-c_3(s)e^{2i\omega(\psi_1+\psi_{k_1/c})}\right] \qquad \text{(B.3a)}$$

and

$$\Delta \sim -\frac{\omega^4 e^{\omega[-\Omega_{1/c}+i(\psi_1+\psi_{k_2}-\psi_{k_1/c})]-i\pi/4}}{\pi^2(m_{1/c}\, m_{k_1/c}\, m_1 m_{k_2})^{\frac{1}{2}}}\,\delta_{20}(1-i\delta_{21}e^{2i\omega\psi_{k_1/c}}) \qquad \text{(B.3b)}$$

as $\omega\to\infty$, where

$$c_\alpha = C_{\alpha R} + iC_{\alpha I} \ , \ \alpha = 0,1,2,3.$$

$C_{\alpha R}$ and $C_{\alpha I}$ are real functions of s. Specifically, for $s\epsilon(1/c, k_1/c)$,

$$C_{OR}(s) = s^2(e_2^2-4s^2m_1m_{k_2})-2\mu e_1 s^2(e_2-2m_1m_{k_2})-\mu\left(\frac{k_1k_2}{c}\right)^2 m_1 m_{\frac{k_1}{c}}$$

$$-\mu^2 e_1^2(m_1m_{k_2}-s^2), \qquad \text{(B.3c)}$$

$$C_{OI}(s) = m_{\frac{1}{c}}m_{\frac{k_1}{c}}(e_2^2-4s^2m_1m_{k_2})-4\mu m_{\frac{1}{c}}m_{\frac{k_1}{c}}s^2(e_2-2m_1m_{k_2})$$

$$+\mu m_{\frac{1}{c}}m_{k_2}\left(\frac{k_1k_2}{c}\right)^2-4s^2\mu^2 m_{\frac{1}{c}}m_{\frac{k_1}{c}}(m_1m_{k_2}-s^2), \qquad \text{(B.3d)}$$

$$C_{1R}(s) = s^2(e_2^2+4s^2m_1m_{k_2})-2\mu e_1 s^2(e_2+2m_{k_2}m_1)+\mu\left(\frac{k_1k_2}{c}\right)^2 m_1 m_{\frac{k_1}{c}}$$

$$+\mu^2 e_1^2(m_1m_{k_2}+s^2), \qquad \text{(B.3e)}$$

and

$$C_{1I}(s) = m_{\frac{1}{c}}m_{\frac{k_1}{c}}(e_2^2+4s^2m_1m_{k_2})-4\mu s^2 m_{\frac{1}{c}}m_{\frac{k_1}{c}}(e_2+2m_1m_{k_2})$$

$$+\mu m_{\frac{1}{c}}m_{k_2}\left(\frac{k_1k_2}{c}\right)^2+\mu^2 4s^2 m_{\frac{1}{c}}m_{\frac{k_1}{c}}(m_1m_{k_2}+s^2) \ . \qquad \text{(B.3f)}$$

Also,

$$\delta_{2O}(s) = c_1(s) \ , \ c_3(s) = c_1(s)\delta_{21}(s). \qquad \text{(B.3g)}$$

Explicit representations of $c_2$ , $c_3$ and $\delta_{21}$ are not needed. Hence, expanding $\Delta^{-1}$ in a geometric series as was done in Appendix A, (B.3), B.1) and (A.2) implies

$$\begin{bmatrix}\tilde{\dot{u}}^*(r,s\omega,\omega)\\ \tilde{\dot{v}}^*(r,s\omega,\omega)\end{bmatrix}_{sc(dil)} \sim -\sqrt{\frac{2m_r}{\pi\omega}}\,\frac{\pi\sigma_o}{\omega r}\begin{bmatrix}1\\ s/m_r\end{bmatrix}\frac{e^{i\omega(-s\pi/2+\psi_r)-i\pi/4}}{\delta_{2O}(s)}$$

$$\cdot\left[c_O(s)e^{-i2\omega\psi_1}-ic_1-ic_2e^{2i\omega(\psi_{k_1/c}-\psi_1)}-c_3e^{2i\omega\psi_{k_1/c}}\right]$$

$$\cdot\sum_{n=o}^{\infty}(i\delta_{21}(s)e^{2i\omega\psi_{k_1/c}})^n, \text{ as } \omega\to\infty \qquad \text{(B.4)}$$

for $s\in(1/c,k_1/c)$. $\psi_x(s)$ and $m_x(s)$ are given in (A.2) and

$\Omega_x(s)$ is given in (B.2). Using (B.3g), (B.4) simplifies to

$$\begin{bmatrix} \tilde{\dot{u}}^*(r,s\omega,\omega) \\ \tilde{\dot{v}}^*(r,s\omega,\omega) \end{bmatrix}_{sc(dil)} \sim \sqrt{\frac{2m_r}{\pi\omega}}\,\frac{\pi\sigma_o}{\omega r}\begin{bmatrix} 1 \\ s/m_r \end{bmatrix} e^{i\omega(-s\pi/2+\psi_r)-i\pi/4}$$

$$\cdot\left\{-i + \frac{c_o}{c_1}\,e^{-i2\omega\psi_1} + \frac{i(c_o\delta_{21}-c_2)}{c_1}\,e^{2i\omega(\psi_{k_1/c}-\psi_1)}\right.$$

$$\left.\cdot\sum_{n=o}^{\infty}(i\delta_{21}e^{2i\omega\psi_{k_1/c}})^n\right\} \qquad (B.5)$$

as $\omega\to\infty$ for $s\in(1/c,k_1/c)$.

In the transitional zones, $s \sim 1/c$ or $s \sim k_1/c$, the fact that for $s \sim x$, $J'_{s\omega}(\omega x) = O(\omega^{-1/3}J_{s\omega}(\omega x))$ as $\omega\to\infty$, may be used to show that (B.5) actually holds even in the half opened interval s contained in $(1/c-\epsilon,k_1/c]$, where $\epsilon > 0$ but small.

For $s\in(k_1/c,1)$, a geometric series expansion of the denominator is not possible. However, a procedure similar to the above (except (B.2) is also used to approximate $\underline{e}_2$), yields

$$\begin{bmatrix} \tilde{\dot{u}}^*(r,s\omega,\omega) \\ \tilde{\dot{v}}^*(r,s\omega,\omega) \end{bmatrix}_{sc(dil)} \sim -\sqrt{\frac{2m_r}{\pi\omega}}\,\frac{\pi\sigma_o}{\omega r}\begin{bmatrix} 1 \\ s/m_r \end{bmatrix} e^{i\omega(-s\pi/2+\psi_r)-i\pi/4} \qquad (B.6a)$$

$$\cdot\left[-i + \frac{c_o(s)}{c_1(s)}\,e^{-i2\omega\psi_1}\right]$$

where, again, $\psi_x$ and $m_x$ are given in (A.2) and

$$c_\alpha = C_{\alpha R} + iC_{\alpha I}\,, \quad \alpha = 0,1. \qquad (B.6b)$$

However, for $s\in(k_1/c,1)$, instead of (B.3c) through (B.3f),

$$C_{OR}(s) = (s^2-m_1\tfrac{m_{k_1}}{c})(e_2^2-4s^2m_1m_{k_2})+2s^2\mu(e_1-2m_1\tfrac{m_{k_1}}{c})(e_2-2m_1m_{k_2})$$

$$+\mu^2(4s^2m_1\tfrac{m_{k_1}}{c}-e_1^2)(m_1m_{k_2}-s^2), \qquad \text{(B.6c)}$$

$$C_{OI}(s) = \mu\left(\frac{k_1k_2}{c}\right)^2(m_{k_2}m_1-m_1\tfrac{m_{k_1}}{c}), \qquad \text{(B.6d)}$$

$$C_{1R}(s) = (s^2-m_1\tfrac{m_{k_1}}{c})(e_2^2+4s^2m_1m_{k_2})-2s^2\mu(e_1-2m_1\tfrac{m_{k_1}}{c})(e_2+2m_1m_{k_2})$$

$$+\mu^2(e_1^2-4s^2m_1\tfrac{m_{k_1}}{c})(m_1m_{k_2}+s^2) \qquad \text{(B.6e)}$$

and

$$C_{1I}(s) = \mu\left(\frac{k_1k_2}{c}\right)^2(m_1\tfrac{m_{k_2}}{c}+m_1\tfrac{m_{k_1}}{c}) \qquad \text{(B.6f)}$$

where

$e_1 = (2s^2-k_1^2/c^2)$, $e_2 = (2s^2-k_2^2)$ and $m_x = \sqrt{|x^2-s^2|}$.

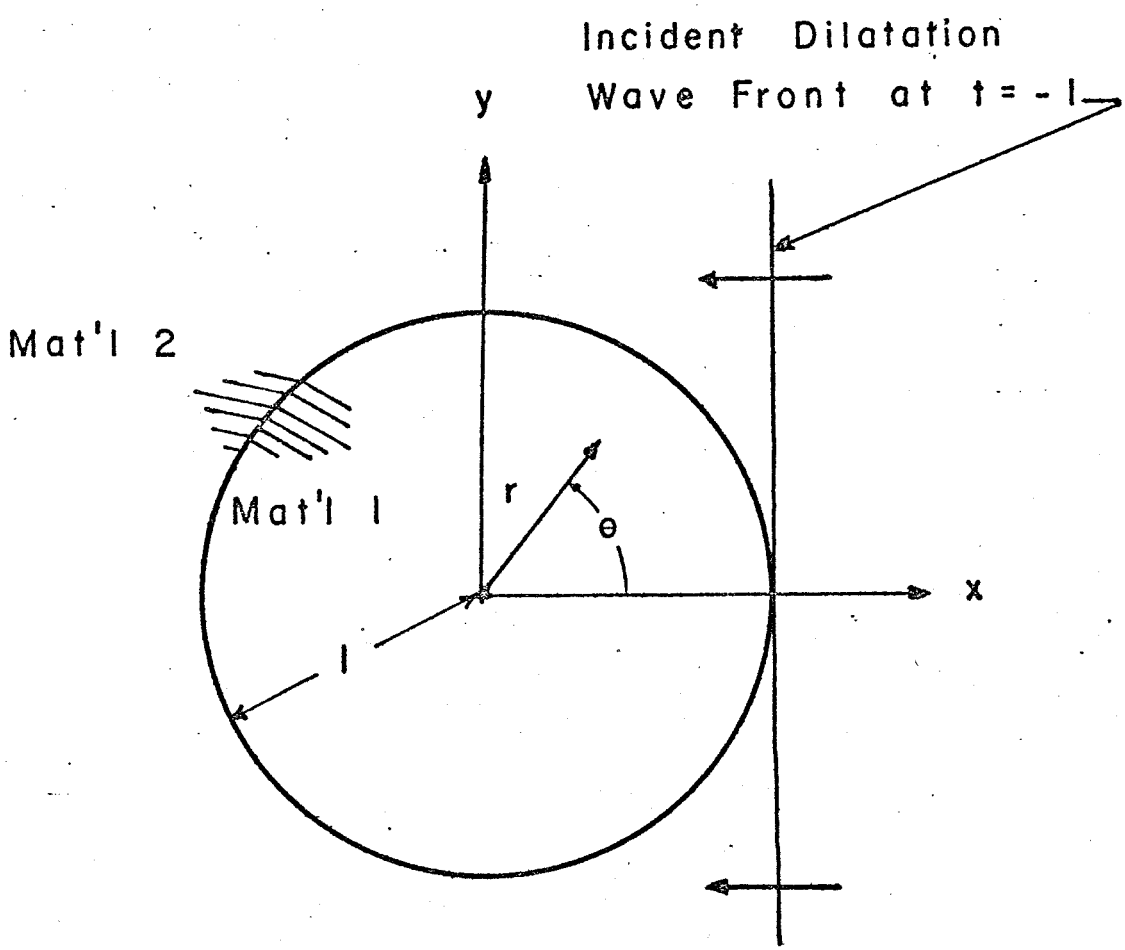


Figure 1. Plane Dilatation Wave Propagating in the Exterior Region Impinges on a Circular Cylindrical Inclusion.

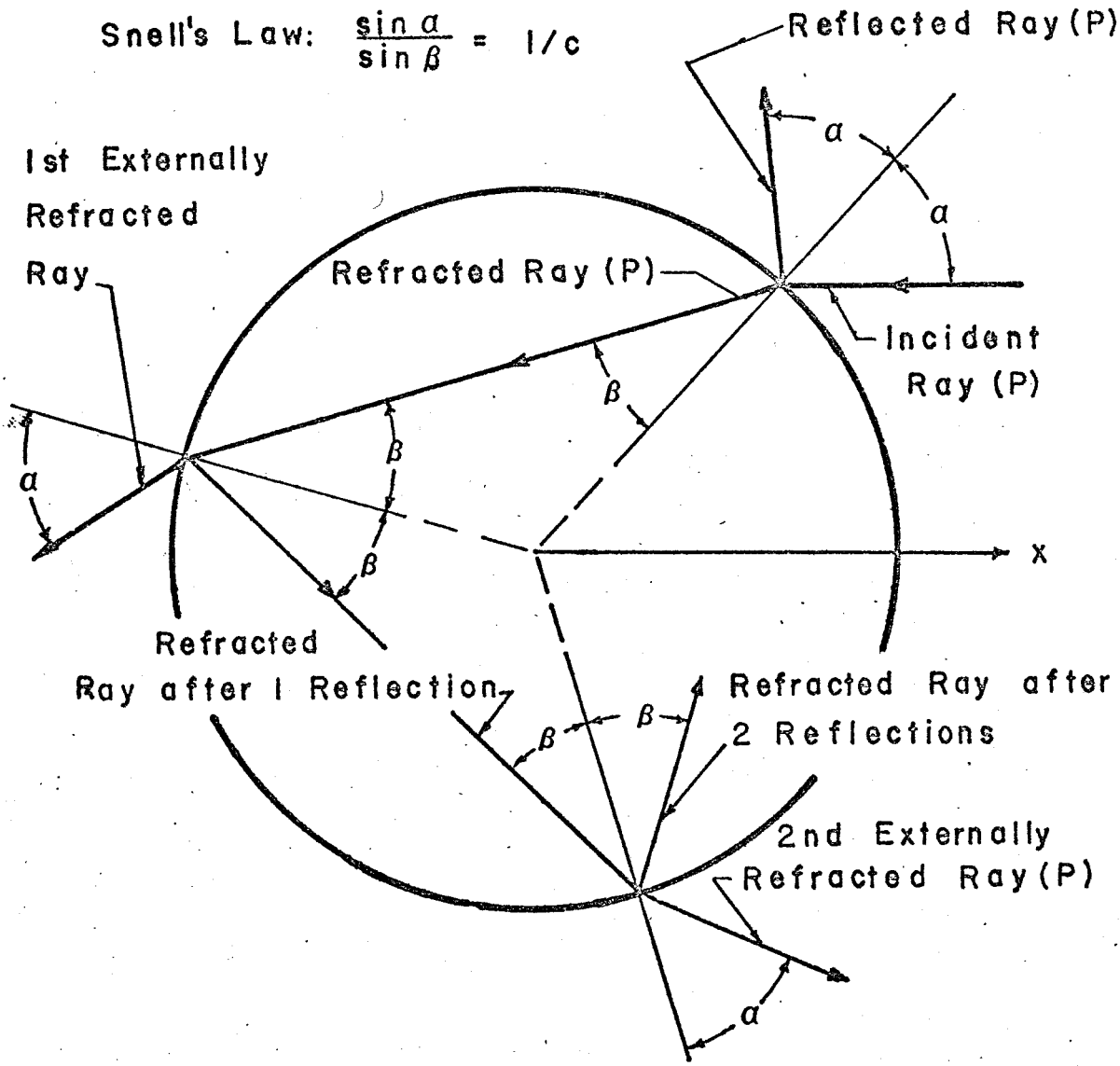


Figure 2. Ray Geometry of the Refracted Dilatation Waves.

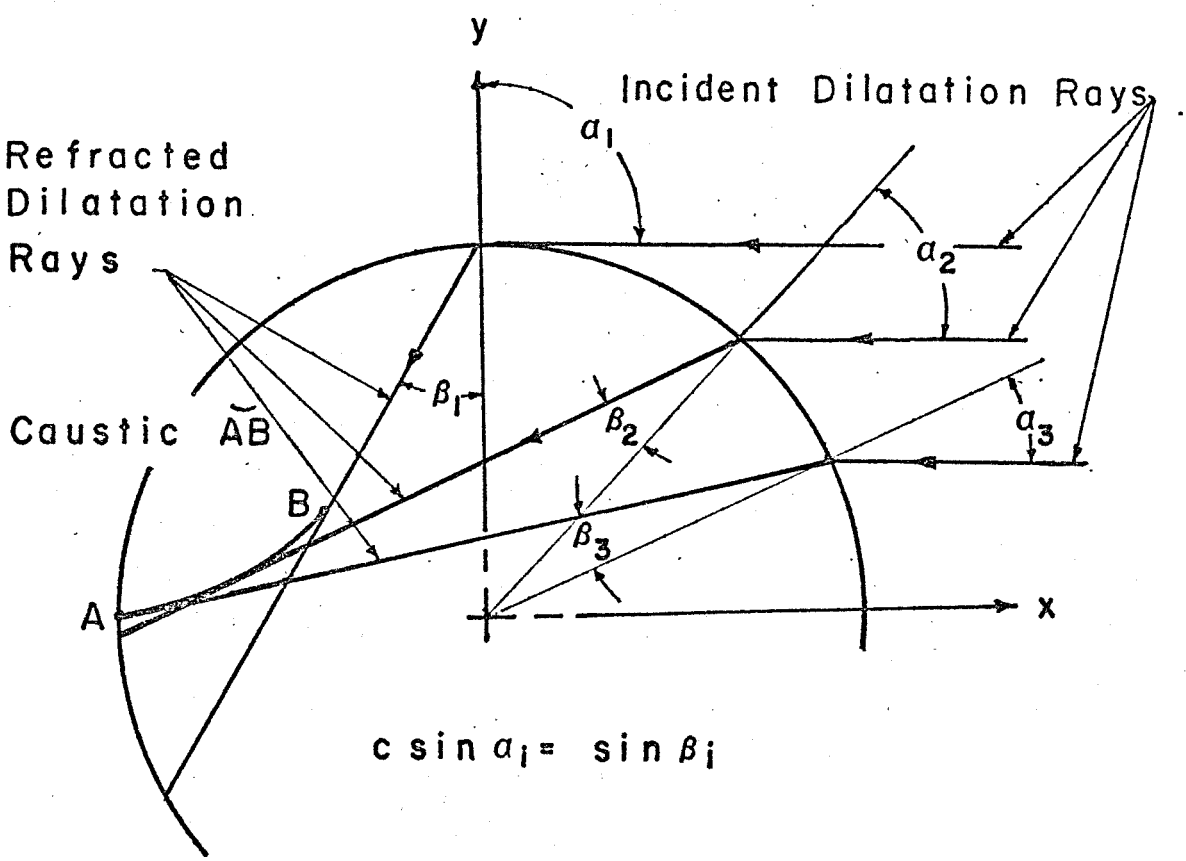


Figure 3. Refracted Dilatation Rays and Caustic For $c = \frac{1}{2}$, $\theta > 0$.

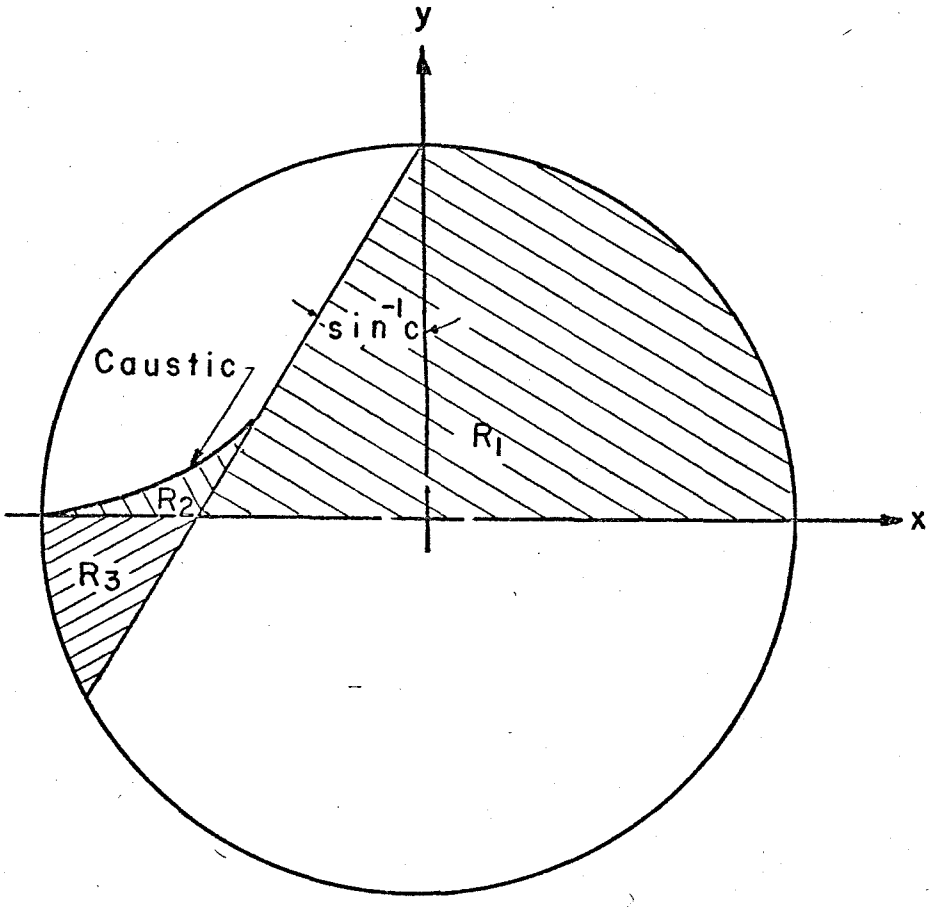


Figure 4. Regions $R_1$, $R_2$ and $R_3$ For $c = \frac{1}{2}$, $\theta > 0$.

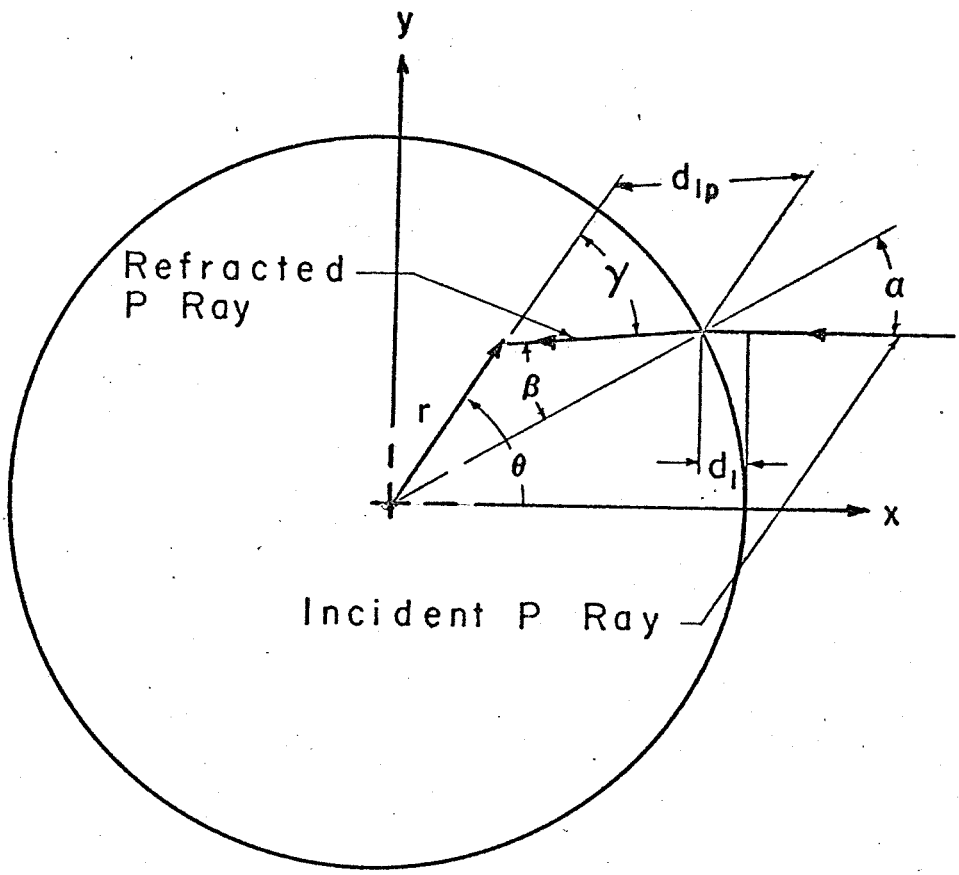


Figure 5. Refracted Dilatation Ray For $c < 1$, $d_{1p} < \cos\beta$.

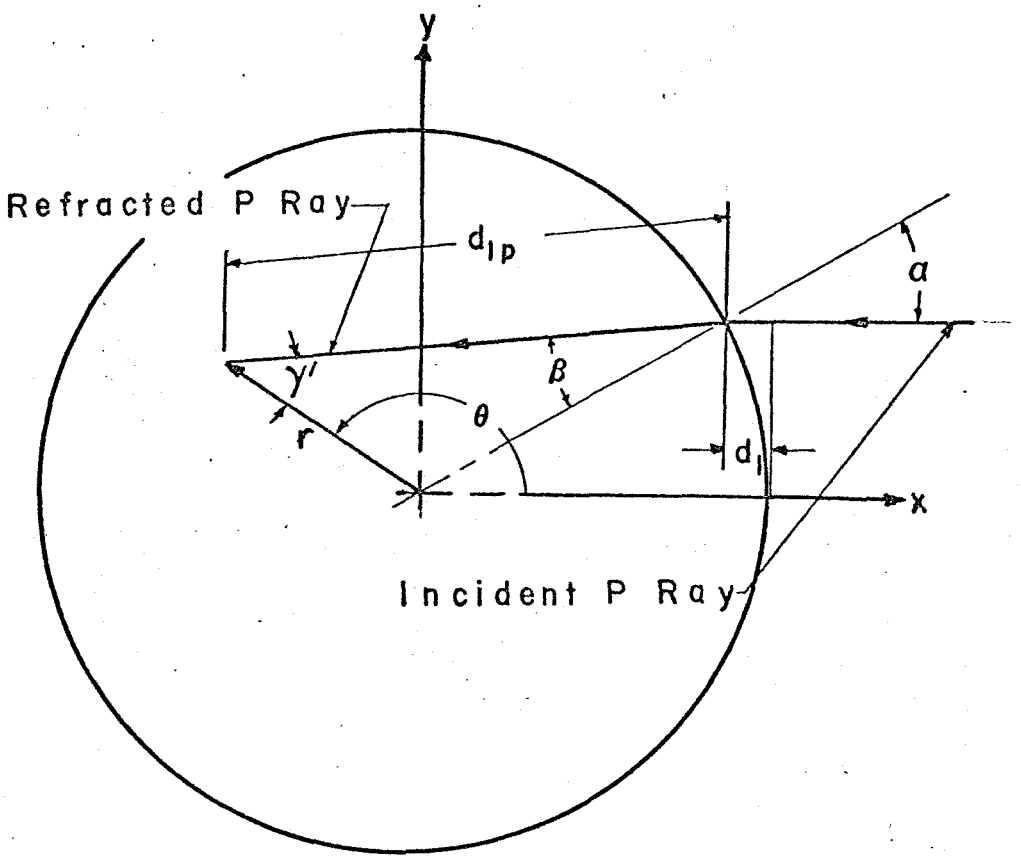


Figure 6. Refracted Dilatation Ray For $c < 1$, $d_{1p} > \cos\beta$.

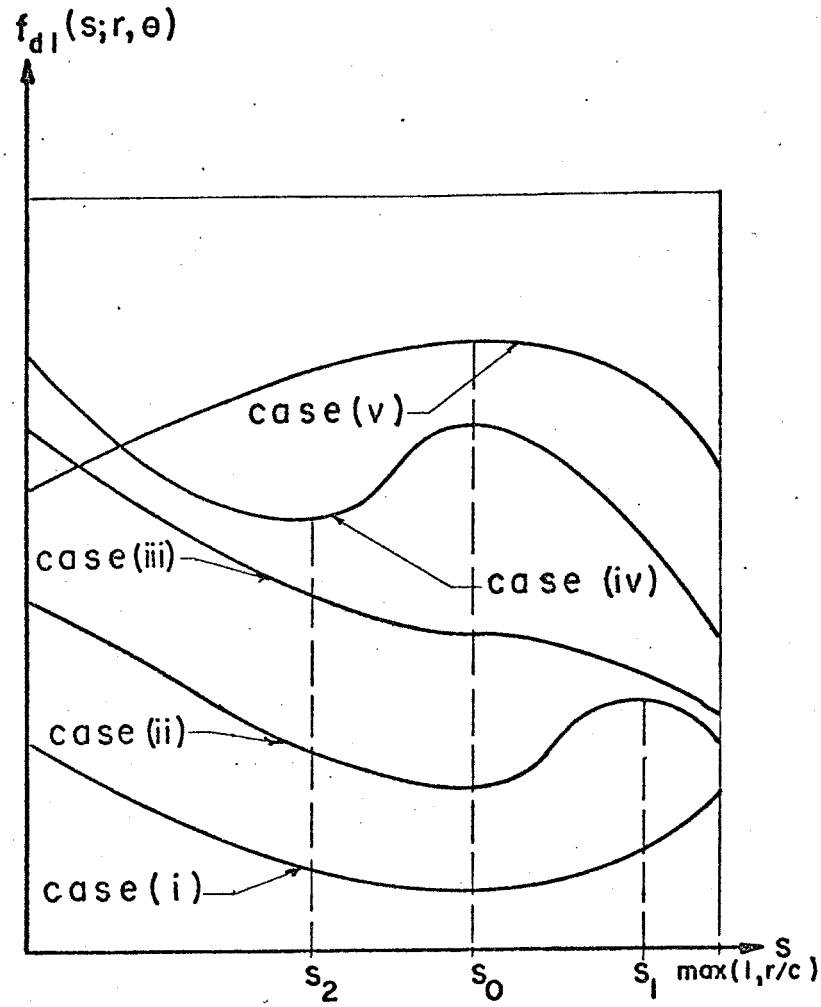


Figure 7. $f_{d1}(s;r,\theta)$ as a Function of s.

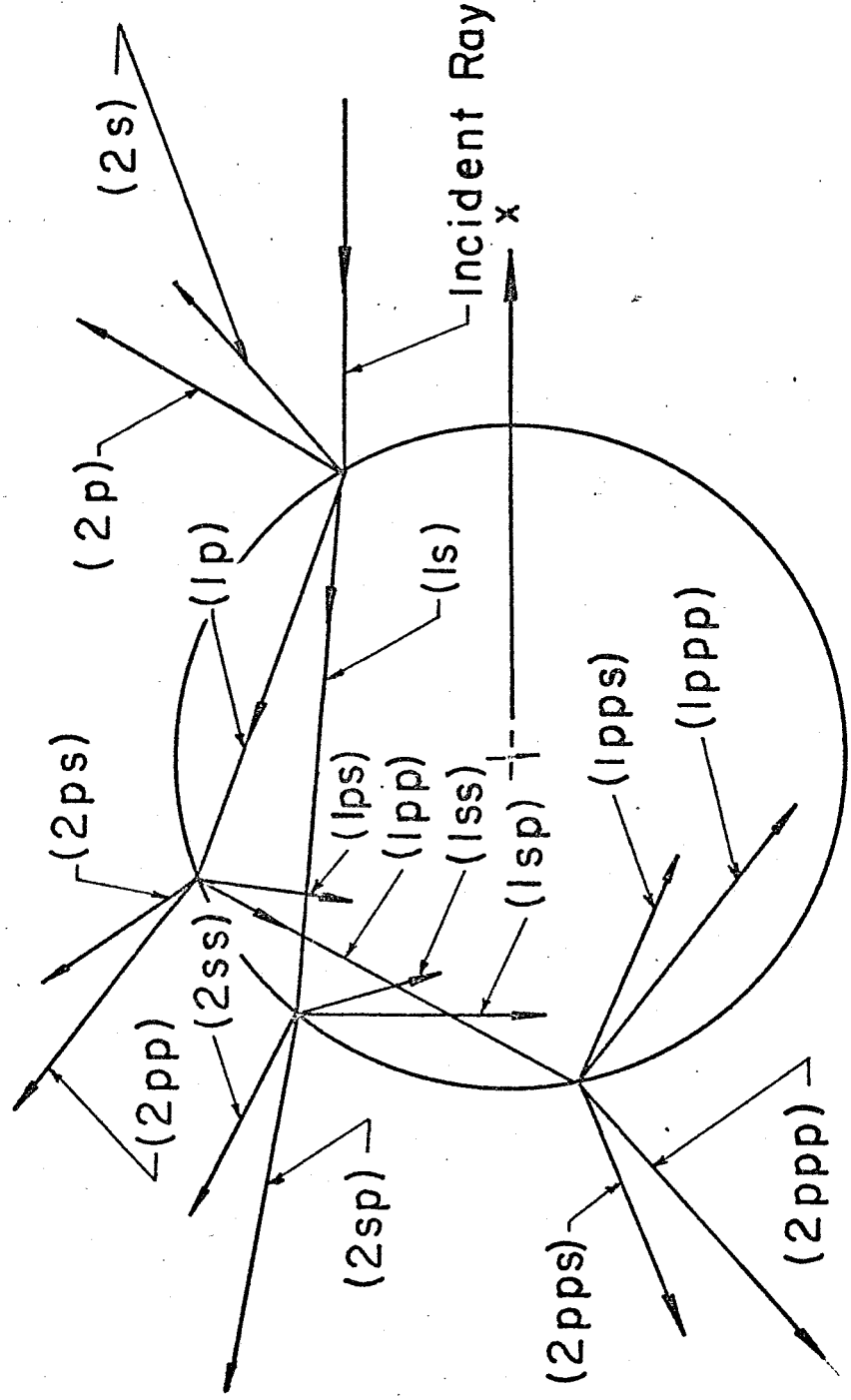


Figure 8. Refracted and Reflected Ray Notation.

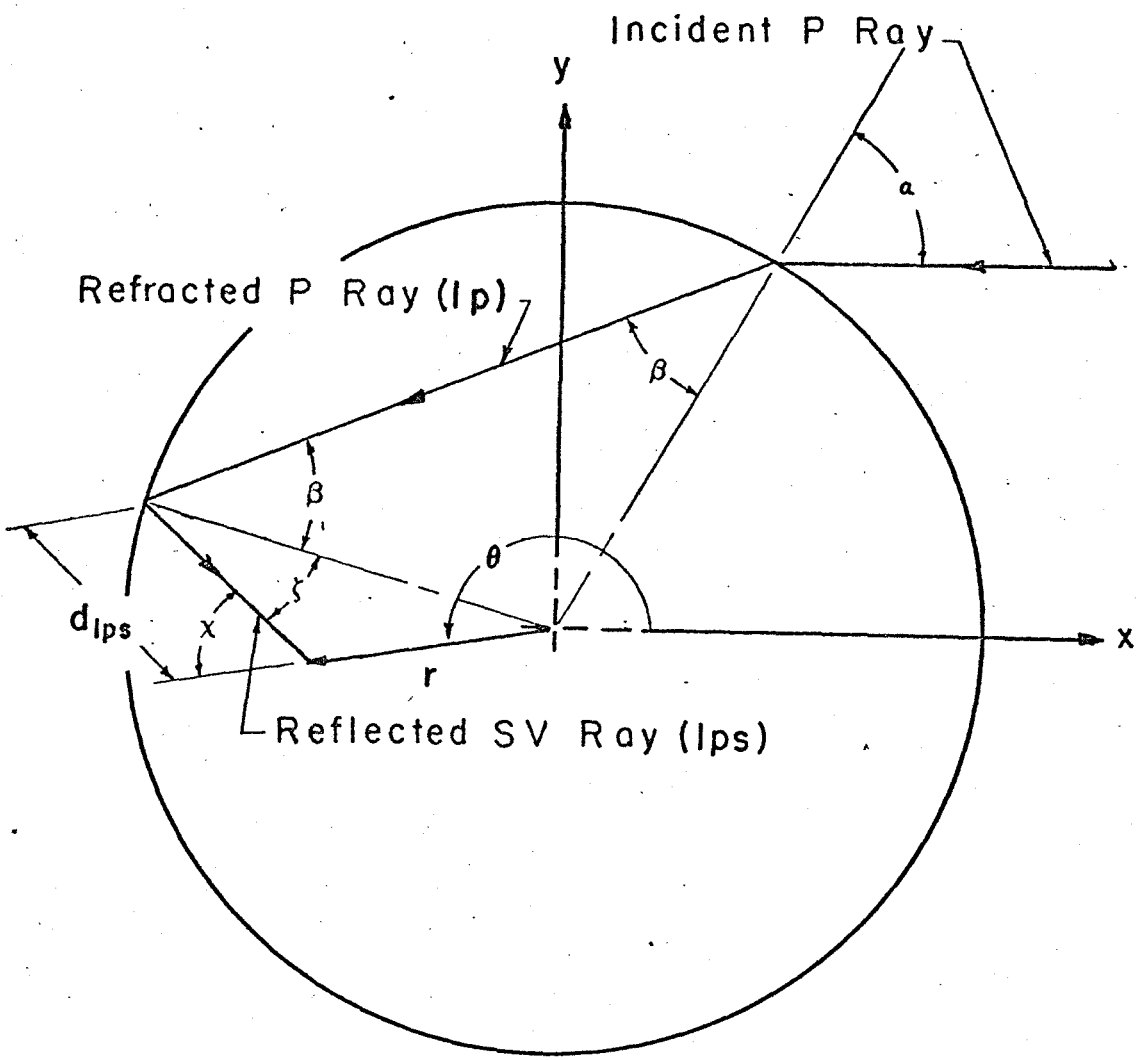


Figure 9. Refracted ($_1$p) Wave Strikes Interface and Generates a Reflected Shear ($_1$ps) Wave.

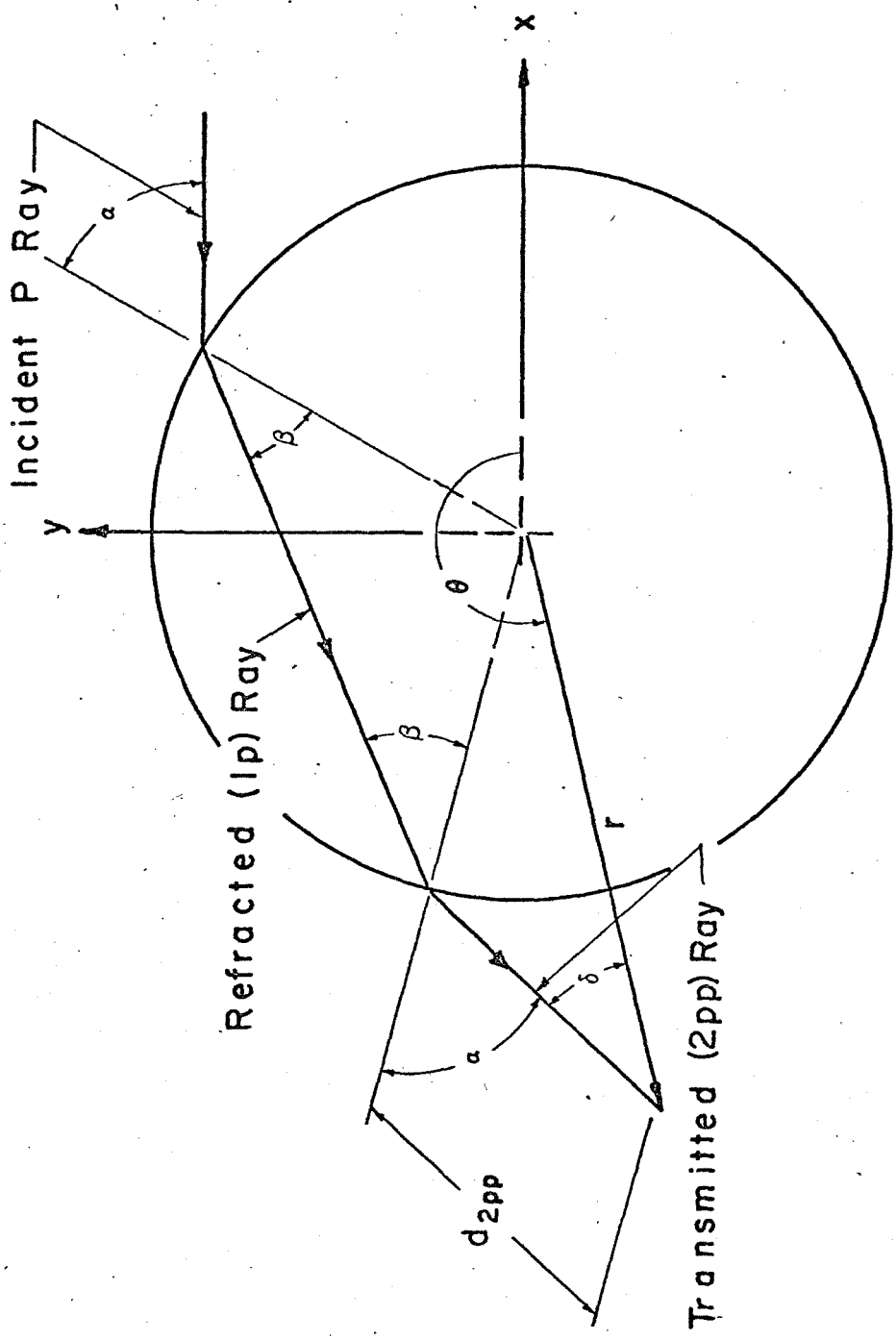


Figure 10. Refracted (1p) Wave Strikes Interface and Generates Exterior (2pp) Wave.

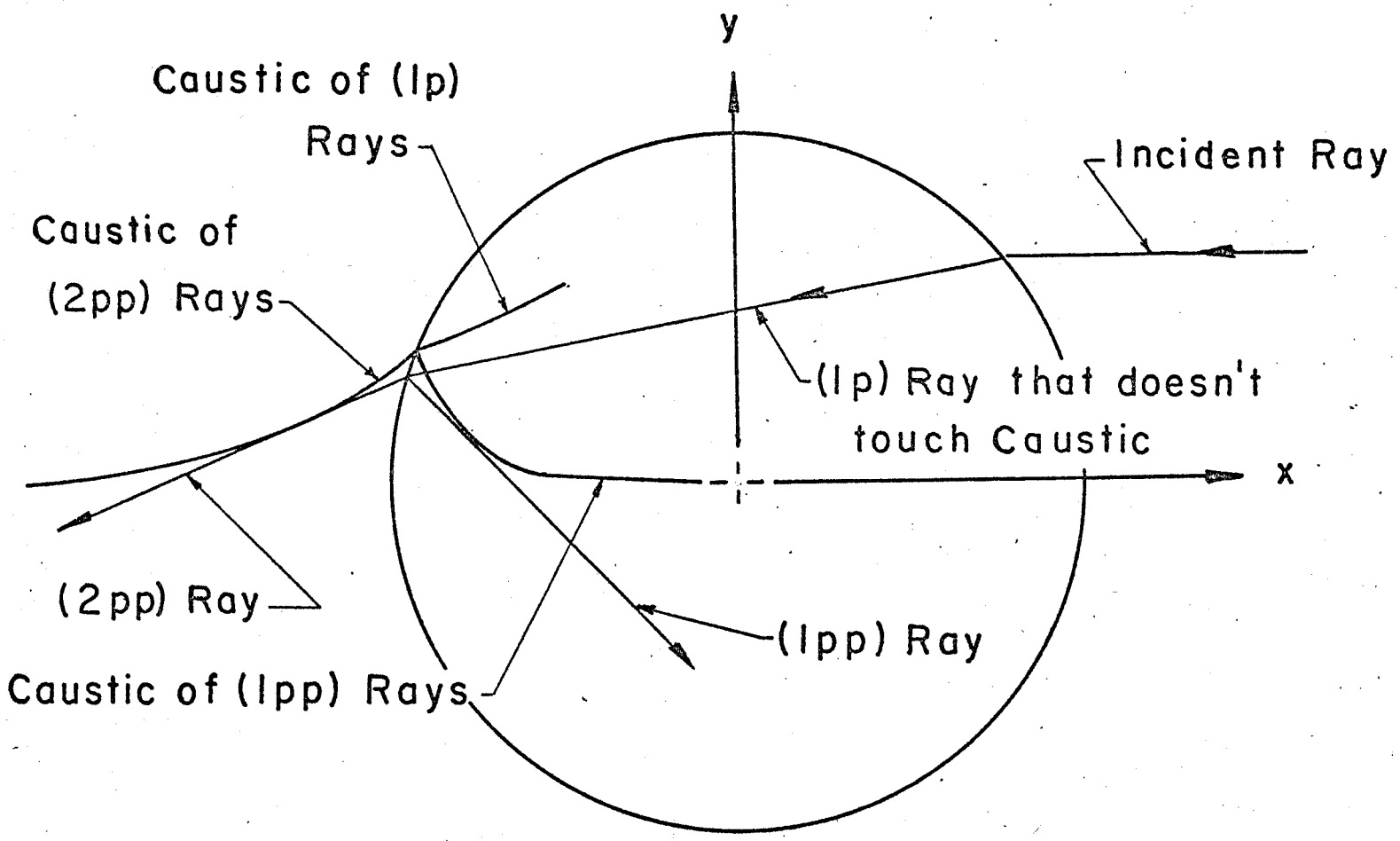


Figure 11. Caustics of ($_1$p), ($_1$pp) and ($_2$pp) Rays.

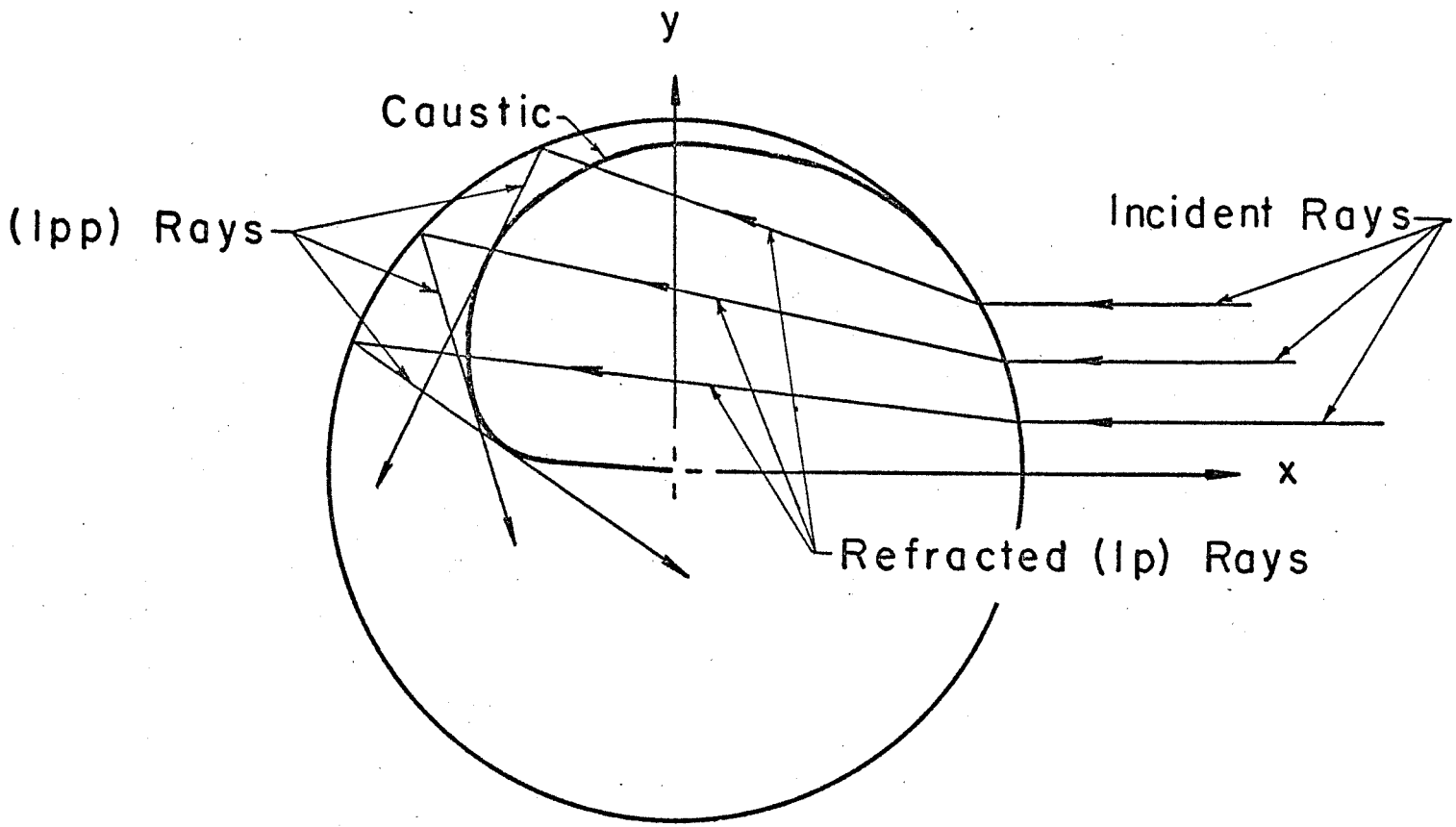


Figure 12. (ipp) Rays and Caustic For c = 1.5, $\theta > 0$.

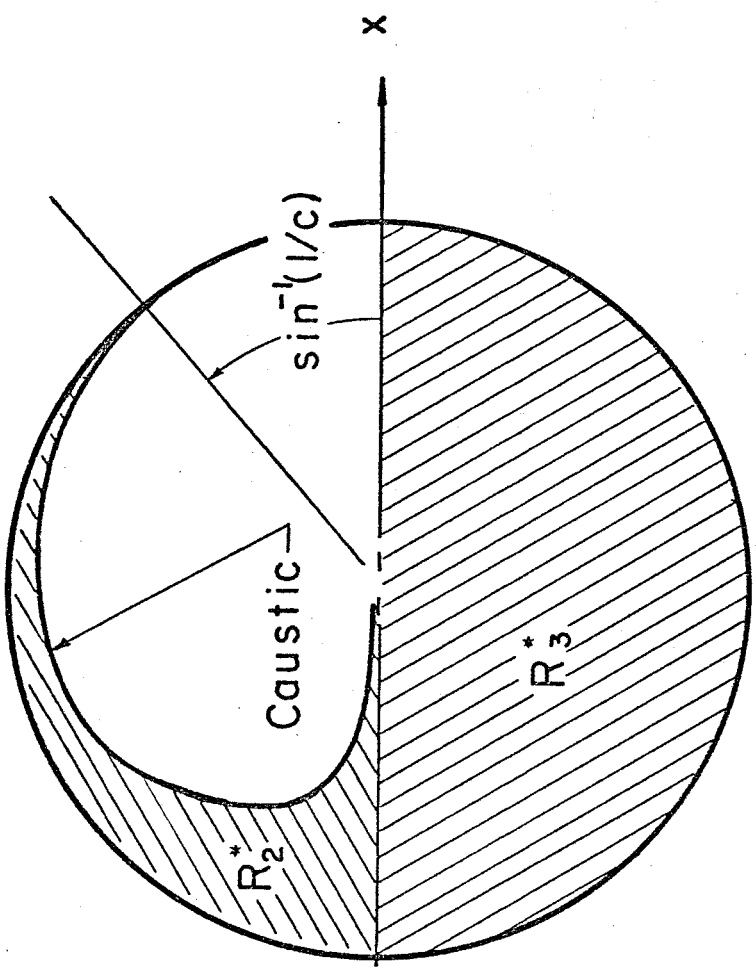


Figure 13. $R_2^*$ and $R_3^*$ For $\theta > 0$, and $c = 1.5$.

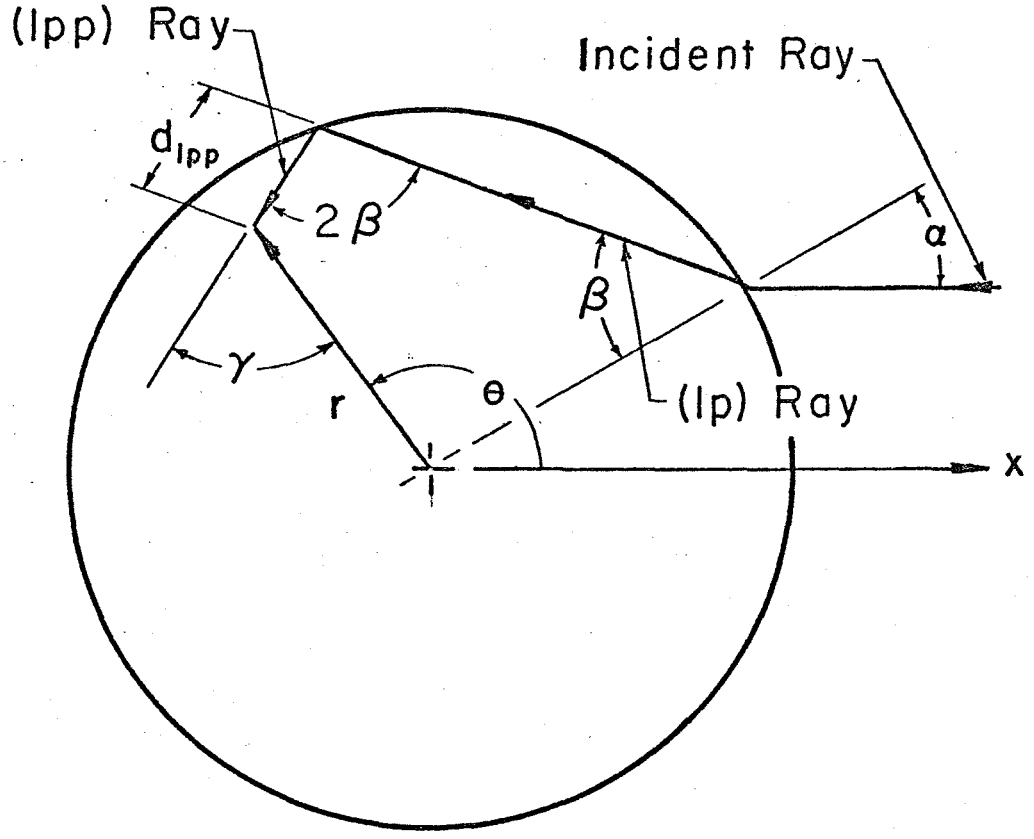


Figure 14. Geometry of (1pp) Ray for c > 1, $d_{1pp} < \cos\beta$.

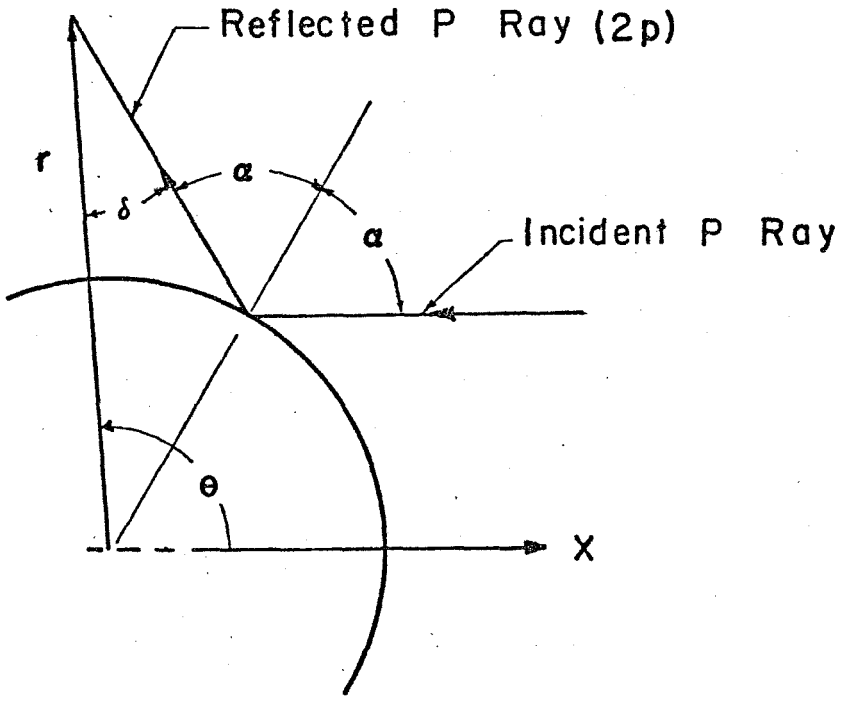


Figure 15. Ray Geometry of Reflected Dilatation ($_2$p) Ray.

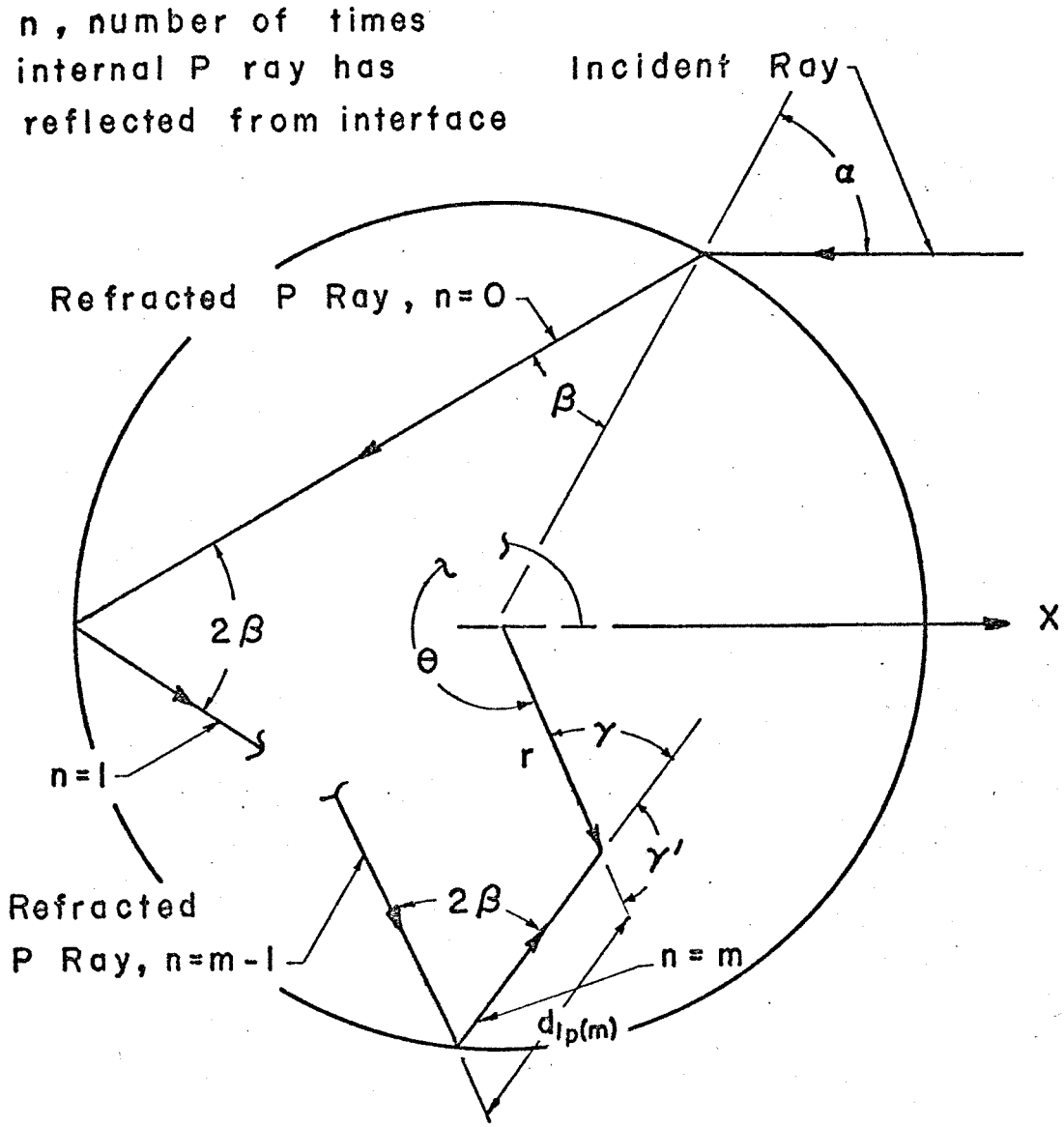


Figure 16. Ray Geometry of mth Reflected Interior Dilatation Wave.

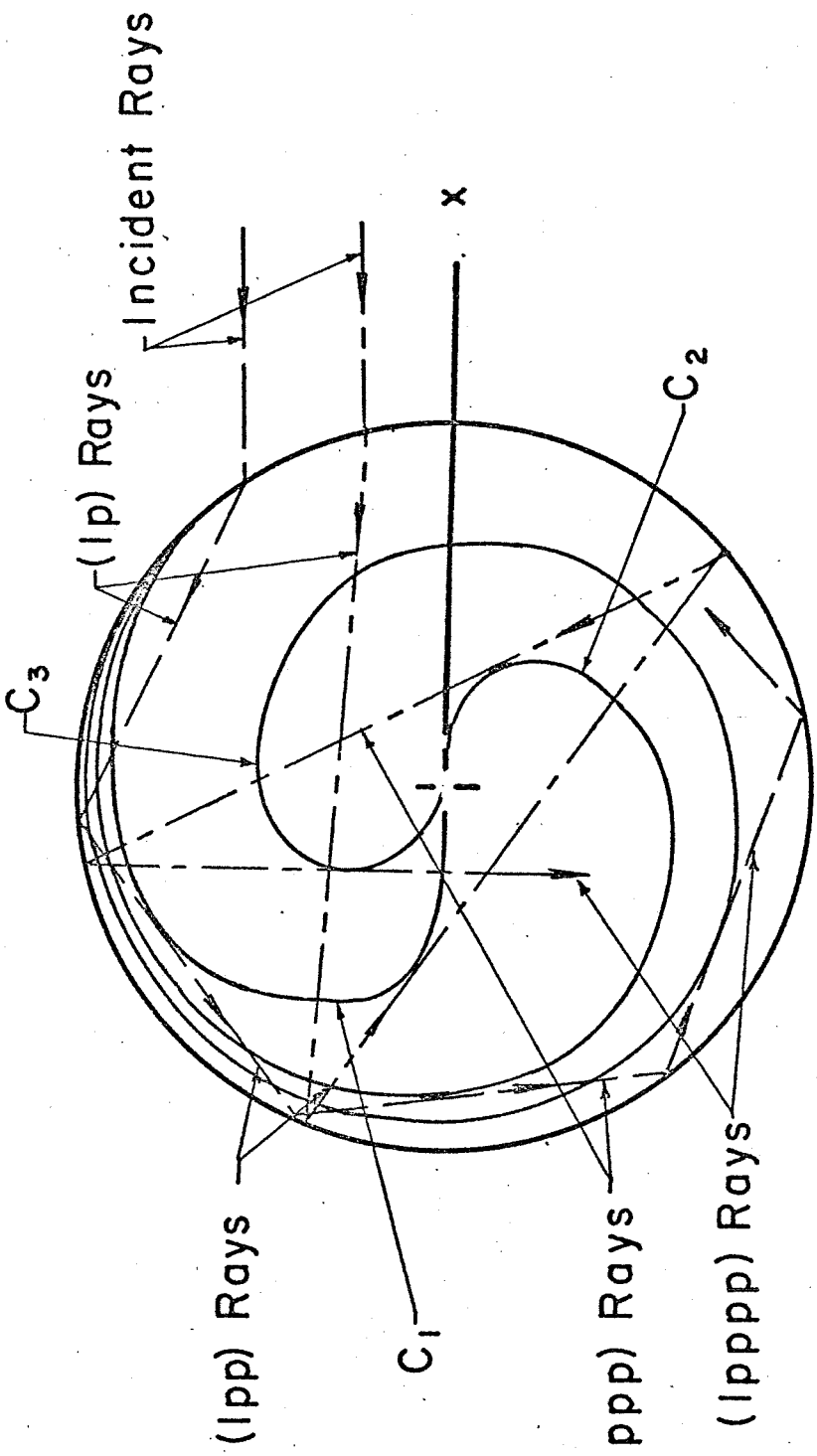


Figure 17. First Three Dilatation Caustics For $c = 1.5$, $\theta > 0$.

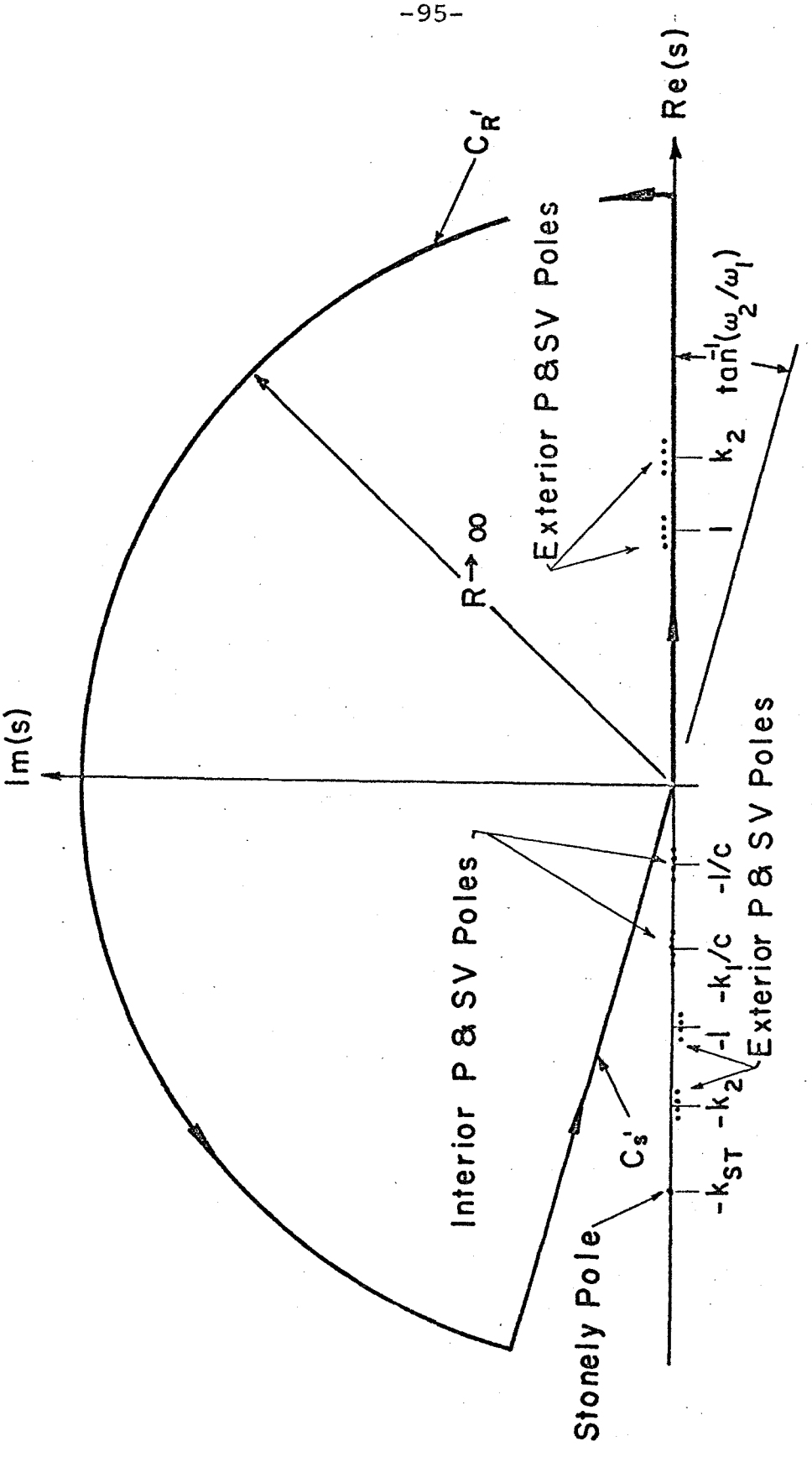


Figure 18a. Poles of $\tilde{\dot{u}}_I^*(-s\omega,\omega)$ and Contour Used in Derivation of Equation (4.5).

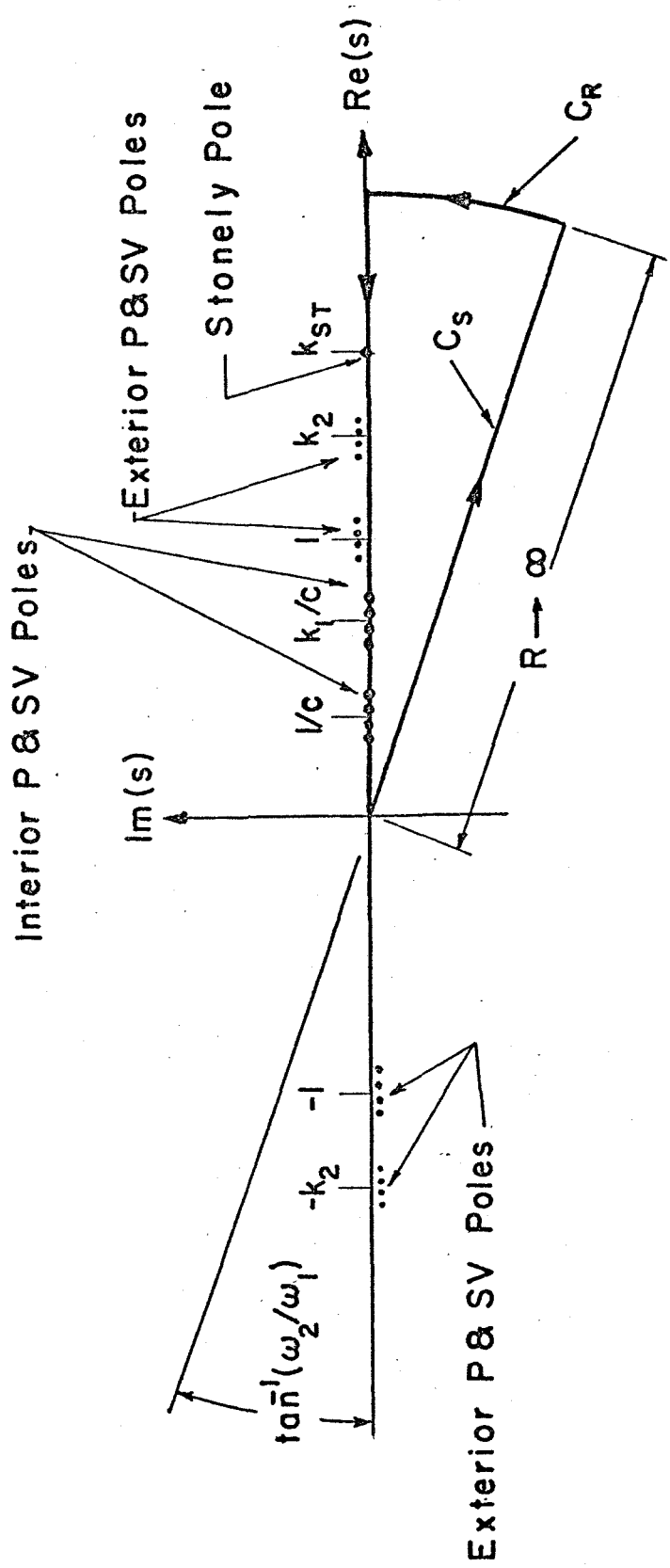


Figure 18b. Poles of $\tilde{\dot{u}}_I^*(sw,w)$ and Contour Used in Derivation of Equation (4.6).